Addis Ababa University

Addis Ababa Institute of Technology

African Railway Centre of Excellence

Optimizing Railway Energy Reliability from Wind Energy Harvesting: A case study of Addis Ababa Light Rail Transit

A Research Thesis Submitted to the School of Graduate Studies of Addis Ababa University in Partial Fulfilment of the Requirements for the Degree of Masters of Science in Railway Engineering (Traction and Train Control)

By: Tracy Hellen Nakaibaale

Thesis Advisor: Dr. Mesfin Belayneh Ageze

June/2025

Addis Ababa, Ethiopia

APPROVAL

The undersigned has examined the thesis entitled "***Optimizing Railway Energy Reliability from Wind Energy Harvesting: A case study of Addis Ababa Light Rail Transit"*** presented by Tracy Hellen Nakaibaale of registration number GSR/5390/15, in partial fulfillment of the requirements for the Degree of Master of Science in Railway Engineering (Traction and Train Control)

Submitted by:

Tracy Hellen Nakaibaale	_____	_____
(Student)	Signature	Date

Approved by:

Dr. Mesfin Belayneh	_____	_____
(Advisor)	Signature	Date
Mr. Alula Mebratu	_____	_____
(Internal Examiner)	Signature	Date
Dr. Asegid Belay Kebede	_____	_____
(External Examiner)	Signature	Date
Mr. Zewdu Moges	_____	_____
(Director of ARCE)	Signature	Date

DECLARATION

I, Tracy Hellen Nakaibaale, therefore, attest that this is my original work, researched and written by me under the supervision of Dr. Mesfin Belayneh Ageze. For this reason, all information gathered from different sources has been duly acknowledged and cited accordingly to avoid any case of breach of the universal principles of academic writing.

Signature: _____

Date: _____

Tracy Hellen Nakaibaale

ACKNOWLEDGMENT

In most special, I owe my deepest thanks to Almighty God for providing me the strength, the wisdom and the endurance to complete this process. Thanks to His guidance and blessings, this thesis would not be possible.

I would like to thank Dr. Mesfin Belayneh Ageze for agreeing to be my thesis supervisor and for providing me with constant encouragement, guidance and valuable input. It is your patience, expertise and encouragement that have helped to bring this work to becoming a reality.

I would like to express my deep appreciation to Addis Ababa Light Rail Transit(AALRT) and the National Meteorological Agency(NMA) for supplying the needed information and for their assistance in the course of this study. Your consent to provide key information has been instrumental in meeting the goals of this thesis.

I would like to thank the faculty and staff at the African Railway Centre of Excellence in Addis Ababa University for their assistance in providing resources without which this research could not have been carried out. A big thank you to any other Faculty or Staff members who assisted with technical support or provided valuable feedback.

I thank my family and my friends who stood by me throughout my endeavor and encouraged me constantly and ceaselessly. To my loving parents, Mr. Ibaale Charles Joshua and Mrs. Kaliva Zaujja, thank you for always supporting me through prayers, self-belief, and encouragement throughout this academic year.

Last, but not least, I owe my appreciation to the World Bank Group for providing the necessary funding for this study. To all those who have contributed directly or indirectly to this work, I express my gratitude.

ABSTRACT

Within the City of Addis Ababa, Ethiopia, the Addis Ababa Light Rail Transit (AALRT) contributes to crucial transportation benefits, which is a strategic connectivity of areas in Addis Ababa, however, the railway line faces a problem of frequent power outages, which undermines its energy reliability and sustainability. To address this challenge, this thesis investigates the feasibility of harnessing wind energy from moving trains along the AALRT corridor, taking into consideration the natural wind resources. Unlike large-scale grid-connected wind farms, this research explores the integration of small-scale wind turbines to supply power to railway auxiliary subsystems and employs advanced control strategies, this research aims to improve the reliability and sustainability of the railway's energy supply.

The research focuses on designing and implementing Fuzzy Logic Control (FLC) based Maximum Power Point Tracking (MPPT) to extract maximum energy from the Wind Energy Harvesting Systems(WEHS). Considering that the AALRT's average speed is 30 km/h, the opportunity lies in capturing the wind produced by the moving train, as well as natural wind in the area, for power production particularly with an emphasis on optimized energy conversion using FLC-MPPT to maximize power capture from the Wind Energy Conversion Systems(WECS) through optimizing the MPPT process i.e., the control of the Tip Speed ratio and the Pitch angle to achieve higher power output in comparison to the traditional methods.

The research concludes with practical recommendations for the deployment of integrated small-scale WECS, focusing on optimization by FLC-MPPT, along railway corridors, and power conversion to manage wind power. It also outlines future research directions to further advance wind energy harvesting technologies. The results of this thesis offer valuable insights for engineers, researchers, and industry stakeholders seeking to enhance railway energy resilience and promote sustainable transportation infrastructure, with a particular emphasis on distributed power generation through small-scale WEHS and advanced MPPT control."

Key words: Railway Transportation, Wind Energy Harvesting, MPPT, Power Electronics, Energy Reliability, AALRT.

TABLE OF CONTENTS

LIST OF TABLES

LIST OF FIGURES

ABBREVIATIONS & ACRONYMS

ACRONYM	*DEFINITION*
AALRT	*Addis Ababa Light Rail Transit*
AC	*Alternating Current*
ANN	*Artificial Neural Networks*
BDFIG	*Bipolar Doubly Fed Induction Generator.*
CFD	*Computational Fluid Dynamics*
DAB	*Dual Active Bridge*
DC	*Direct Current*
DFIG	*Doubly Fed Induction Generator*
DTC	*Direct Torque Control*
ESS	*Energy Storage Services*
FLC	*Fuzzy Logic Controller*
FOC	*Field Oriented Control*
HAWT	*Horizontal Axis Wind Turbine*
HCS	*Hill Climbing Search*
HOMER	*Hybrid Optimization Model for Electric Renewable*
HVAC	*Heating, Ventilation, and Air Conditioning*
IC	*Incremental Conductance*
LVRT	*Low Voltage Ride Through*
LRT	*Light Rail Transit*
MBD	*Model-Based Design*
MPPT	*Maximum Power Point Tracking.*
MTPA	*Maximum Torque Per Ampere*
OTC	*Optimal Torque Control*
P&O	*Perturb and Observe*
PMSG	*Permanent magnet synchronous generators*
PWM	*Pulse Width Modulation*
SCIG	*Squirrel Cage Induction Generator*
SDG	*Sustainable Development Goal*
SMC	*Sliding Mode Control*
TSR	*Tip Speed Ratio*
VAWT	*Vertical Axis Wind Turbine*
VC	*Vector Control*
VUFC	*Variable Unified Fuzzy Controller*
WECS	*Wind Energy Conversion Systems*
WEHS	*Wind Energy Harvesting Systems*
WRSG	*Wound Rotor Synchronous Generator*
WT	*Wind Turbine*

1 INTRODUCTION

This chapter presents the background, scope, and objectives of this thesis, which aims to address the energy reliability problem statement of the Addis Ababa Light Rail Transit (AALRT), establishing the relevance of the investigation to the AALRT's context, outlining the anticipated contributions to the field of sustainable transportation.

1.1. Background

Across the world, many countries are adopting sustainable energy solutions due to concerns about the environment in terms of global warming, which results in unbearable climatic disasters like very high temperatures[1]. The railway sector is one of the great beneficiaries of energy consumption globally, consisting of urban transit trains and high-speed trains responsible for transporting large numbers of passengers and freight [2]. Compared to other modes of transport, the railway has emerged to be the most efficient, but it is also recognised as one of the highest electricity consumers, hence its heavy dependence on conventional energy sources[3].

The energy harvesting methods adopted in railway systems include regenerative braking which harnesses kinetic energy from a train’s deceleration and converts the energy into electrical energy[4], solar photovoltaic panels placed in railway vicinities or on train rooftops which convert sunlight into electricity [5], piezoelectric materials which convert mechanical energy and pressure of moving trains to electrical energy[6], [7], electromagnetic induction system in which moving rails produce electrical energy through electromagnetic field[8]. Also, thermoelectric generators help transform the waste heat into electricity; hydraulic systems use pressure from trains to create energy[9], and lastly the one highlighted in this research which is wind energy harvesting which uses wind turbines in railway to harness wind created by the motion of the train or natural wind speeds and converts it to electrical power for use by the railway electrical systems[2].

Wind energy is a readily available source that doesn’t emit any dangerous gases to the environment[10], [11]. From 2017, the Netherlands is the only country whose railways run on 100% wind energy, by 2024, India will have an installed wind energy capacity of 46.4 Giga Watts, making it the world's fourth biggest, in addition, every year, the country adds over 2500 MW of wind power and electrifies approximately 2500 km of track.[12], [13]. Africa, and particularly

Ethiopia, has vast wind resource potential, namely in railway infrastructure vicinities. Thus, the increased potential for wind energy exploitation along railway routes makes it advantageous, especially given the nation's green energy direction[14]. Since wind power is a renewable resource, if wind turbines are placed in suitable positions along the railway infrastructure, wind generators can generate power even without train activity[15]. This will serve as an additional power to the utility grid, meeting the increasing energy demand.

The Addis Ababa Light Rail Transit(AALRT) railway line is a vital transportation infrastructure located in Addis Ababa, Ethiopia, that spans a distance of 17km from the city center to the south side of the city, being 34 km long as it travels in two directions. A high voltage electric grid feeds the substations with 132kV, which is stepped down to 15kV AC 50Hz at the AALRT. However, they are faced with the problem of frequent power outages, which negatively impact the power reliability and sustainability of the electrified line[16]. To address this issue, this thesis proposes a novel approach of integrating small-scale wind energy harvesting systems coupled with FLC-MPPT along the AALRT corridor through exploring the train-induced winds and ambient winds in the area. This approach aligns with Ethiopia's Sustainable Development Goals and seeks to provide a more sustainable way of powering the railway subsystems.

Unlike the conventional focus on large-scale wind farms connected to the grid, this research explores the feasibility of power generation from small-scale WEHS strategically positioned along the railway track to power auxiliary railway subsystems such as lighting, signalling, etc. MPPT control methods are used to obtain the maximum available power from the wind through a dynamic control of the wind turbine operational parameters, i.e. the pitch angle and the Tip Speed Ratio (TSR) according to the wind strength. Power electronics help in the control and conversion of the electrical energy produced by these turbines for effective power delivery[17]. This thesis aims to explore these innovative solutions for improving energy reliability in railway systems through the integration of these technologies. Since MPPT algorithms and power electronics systems are the key elements in the process of harnessing wind energy, the research aims to contribute towards the identification of the current issues with these strategies, to discover how the two elements can be adapted and optimised for enhanced use in the railway sector. The study will examine the power output of the proposed model, analysis of wind speed profiles and turbine characteristics. Through detailed analysis, this study aims to provide insights into the potential benefits and challenges of

harnessing wind energy to power the railway subsystems. This information will be essential in making informed decisions on the best approach to improve the power efficiency and reliability of the AALRT railway line while promoting sustainable development.

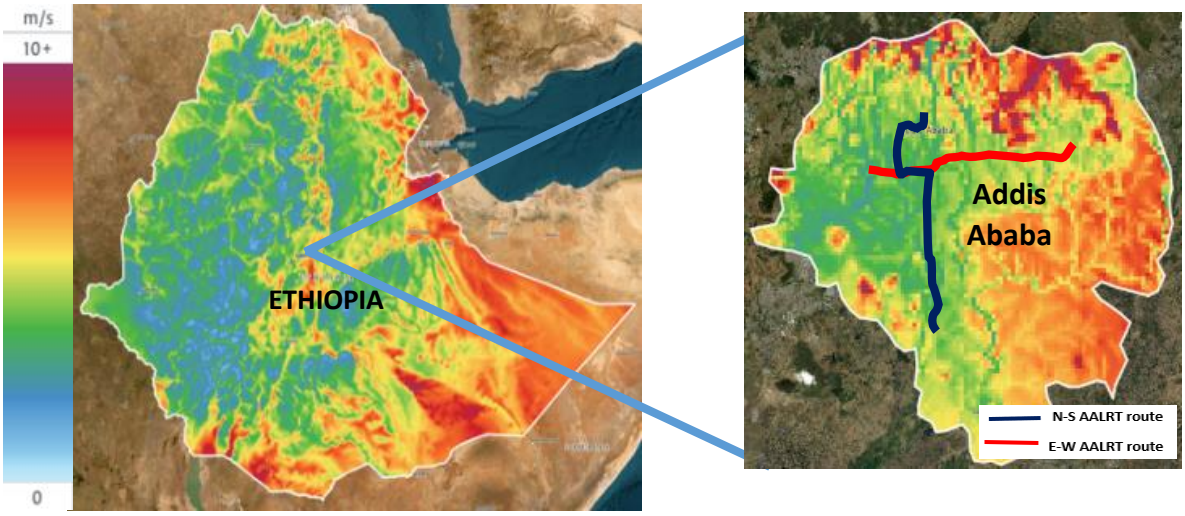

Figure 1.1: The wind map of the AALRT railway route situated in Addis Ababa, Ethiopia at 10m [18]

1.2. Statement of the problem

Ethiopia's energy consumption is roughly 40,000 GWh, out of this 4% is used by the transportation sector. The Ethiopian Railways Corporation(ERC) indicates that the Overhead Contact system(OCS) of the AALRT route uses 750V with 1050A [8], [9]. However, the AALRT railway line faces significant power sustainability challenges due to power outages, which in turn directly affect the power efficiency. According to the data retrieved from the AALRT-Kality station, cancellation of trips due to power outages undermines the railway's reliability which results into increased operational costs. To address this issue, there is a critical need to explore sustainable energy practices through the implementation of wind energy harvesting as an integrated solution to generate additional power to optimize energy extraction through the integration of the Fuzzy Logic Control MPPT algorithms along the railway infrastructure while contributing to the Addis Ababa initiative of smart city bent on adopting advanced technologies in infrastructure.

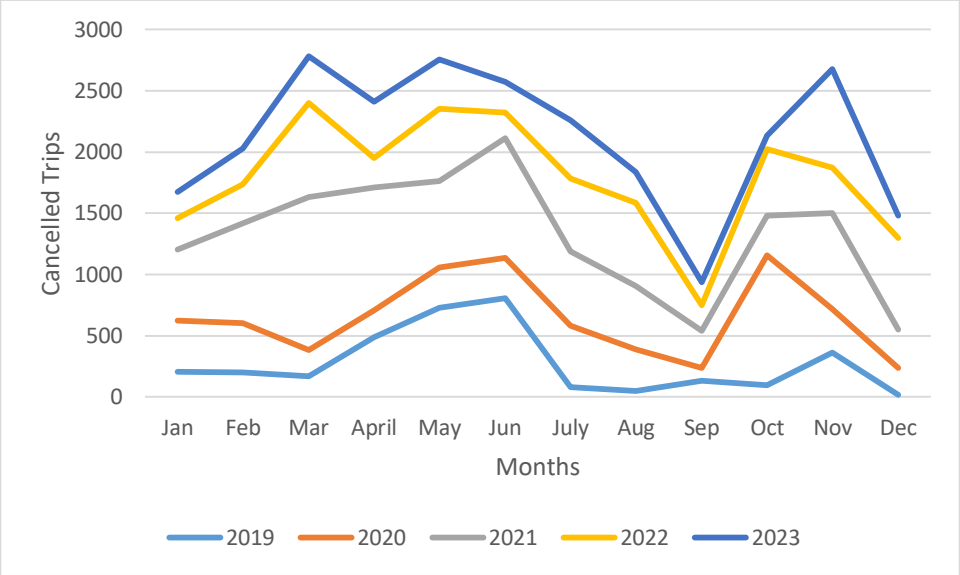

Figure 1.2: Frequency of cancelled trips due to power outage

Research questions

I. What is the technical feasibility of WEHS along LRT railway corridors, considering train gusts and natural wind?
II. How can MPPT algorithms and efficient power electronics converters contribute to the reliability of Wind energy conversion systems?
III. Which is the most suitable wind turbine for this operation?
IV. Which technical parameters directly affect the generation of wind energy from train gusts?

1.3. Objective

1.3.1. General objective

The general objective of this research is to model, design and analyze a wind energy harvesting system capturing train-induced wind and natural ambient wind placed alongside railway tracks that can be applied to LRT applications using FLC-MPPT algorithms.

1.3.2. Specific objectives

i. To perform an electrical load assessment for the Addis Ababa Light Rail Transit railway.
ii. To perform a wind resource assessment for the Addis Ababa Light Rail Transit railway.

iii. To identify the technical parameters that will determine the performance of the wind turbine operation.
iv. To develop and simulate an analytical model of the Wind Energy Conversion System(WECS).
v. To optimise the WECS using the FLC-MPPT algorithm by altering the design parameters.
vi. To validate the model.
vii. To perform the sensitivity analysis

1.4. Significance of the research

The frequent power outages undermine the operational reliability of the Addis Ababa Light Rail Transit (AALRT); therefore, this calls for the need for the railway line to put in place sustainable energy solutions. This thesis seeks to explore the feasibility of small-scale wind energy harvesting systems placed along railway tracks. Unlike large-scale grid-connected wind farms, these WEHS are designed to supply auxiliary subsystems of the railway, which require a constant power supply (e.g., lighting, signalling), thereby reducing strain on the main grid and enhancing overall energy resilience.

The key contribution of this research is the application of FLC-MPPT in small-scale WEHS for light rail transit systems operating in intermittent low-wind environments. FLC-MPPT offers a robust solution for improving energy capture and system stability under these conditions, particularly because FLC can handle the nonlinearities involved with wind energy systems. This thesis evaluates the operation of the FLC-MPPT algorithm through detailed simulations and analysis, considering factors such as wind speed profiles along the AALRT, turbine characteristics, power conversion system parameters, etc. The results will demonstrate the viability of small-scale WEHS and advanced FLC-MPPT for enhancing the power resilience and sustainability of the urban light rail transit subsystems.

Furthermore, the findings will provide valuable design guidelines and operational insights for the deployment of similar systems in other urban railway environments with low intermittent wind speed. This research contributes to the adoption of renewable energy solutions in the transportation

sector; therefore, by addressing these technical challenges, the study aims to set the way for future advancements in wind energy resilience and reliability.

1.5 Delimitation

This research has been limited to the simulation of a wind energy harvesting system from train-induced wind and the natural wind. Modeling, design and analysis of a wind energy harvesting system, employing FLC-MPPT algorithm, analyzing sensitivity for the technical parameters. However, this study will not cover the following; the economic or cost review of adopting this technology, CFD analysis, practical experimentation, and prototype development.

2 LITERATURE REVIEW

Chapter 2 discussed the literature review, which examines existing research on wind energy harvesting in railway systems, the impact of railway configurations on wind profiles. It reviews various MPPT techniques with an analysis of their limitations in the context of variable wind conditions in railway, emphasizing the FLC-MPPT and its state of the art.

2.1. Wind energy harvesting systems(WEHS)

Wind energy harvesting involves the conversion of wind energy into electricity, thereby decreasing dependence on fossil fuels[18]. A Wind Energy Conversion System is a system that converts wind energy to usable electrical energy. It is comprised of wind turbines, a control system, generators, and interconnection equipment. The energy generated is used in railway applications to run different subsystems, such as signaling, lighting, etc.[19] Related work to Wind Energy Harvesting Systems in railways is outlined in *Table 2.2*.

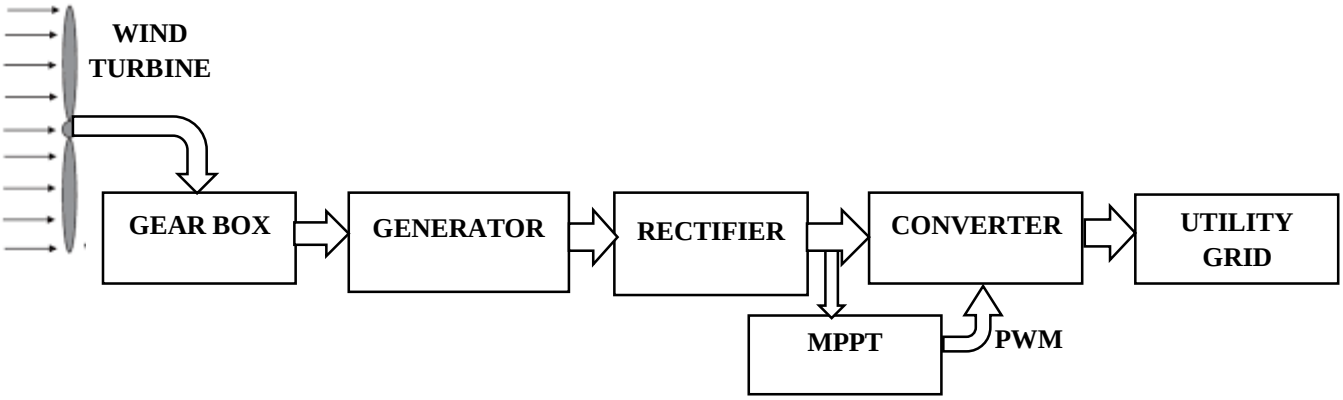

Figure 2.1: Typical block diagram of a WECS [20].

2.1.1 Wind turbines

A wind turbine is an instrument built to convert wind power to electricity, i.e., wind energy flows through its blades and then transforms the flowing wind into the generator's electricity[20]. The wind turbines employed in railway facilities are used to power the various subsystems, namely the power supply, which supplies the overhead contact system, the signaling and communication subsystem[21], etc. Wind turbines use either lift force, drag force, or both forces [22]. Wind turbines are typically grouped into Vertical Axis Wind Turbines and Horizontal Axis Wind

Turbines, as shown in *Table 2.1* these wind turbines operate either at constant or variable speeds, and it is noted that variable-speed turbines have high efficiency and low mechanical stress[23].

2.1.1.1 Principle of operation of wind turbines

Wind turbines convert wind force into mechanical force using either lift force, drag force, or

both forces. Concurrently, lift forces are the most efficient due to Bernoulli's Law principle, which states that pressure reduces as the flow of air over a given surface rises [22]

According to Bates' theory; the power output (P) of a wind turbine depends on the wind speed (V), air density (ρ), rotor swept area (A), and the power coefficient (C_p), which measures the turbine's aerodynamic efficiency. The relationship is given by[24]:

$$P = {}^{1}/_{2}\,\rho A C_p v^3 \qquad 2.1$$

The power coefficient (C_p) is a function of the TSR(λ), which is the ratio of the blade pitch angle β to the wind speed. Therefore, the typical function is[24];

$$C_p(\lambda, \beta) = 0.5176\left(\frac{116}{\lambda_1} - 0\cdot 4\beta - 5\right)\frac{-21}{\lambda_1} + 0.0068\lambda \qquad 2.2$$

where $\frac{1}{\lambda_1} = \frac{1}{\lambda + 0.08\beta} - \frac{0.0035}{1+\beta^3}$. λ Is the TSR that can be defined as $\lambda = \frac{W_m R}{v}$

The wind turbine types include;

a) Horizontal Axis Wind Turbine (HAWT)

The HAWT is a wind turbine with propellers that turn from the ground up and are set on taller structures. They start at high altitudes and advance at a steady pace to catch wind kinetic energy and turn this into rotational energy [25]. HAWTs are preferred for utility-scale wind farms and railways because their efficiency in operation depends on wind patterns and the distance between the blades [25].

b) Vertical Axis Wind Turbine (VAWT)

VAWTs are fixed at lower heights to the ground hence, they are easy to repair and maintain. They do not rely on wind direction as they do not require yaw motion to capture the energy mechanisms. However, they are faced with some challenges in the efficiency of energy, particularly in electricity generation[26]. Recent research is geared toward increasing the efficiency of VAWT turbine blades through the utilization of deflector devices[26]. There are mainly three types of VAWT, i.e., Darrieus, Savonius, and hybrid, which can be easily installed in compact spaces [27] [28].

i. Savonius VAWT

This is a drag-type VAWT turbine that is highly effective in low wind speed environments, because it can start at wind speeds as low as 1.5-3.0m/s working well with intermittent conditions compared to the Darrieus VAWT turbine[29], [30]. This has been illustrated through a case study where an experiment was conducted and yielded 4-21W of energy from a single turbine at wind speeds of 2-6 m/s[31]. Another study also aimed to design a Savonius turbine with a 60 cm diameter, and this turbine was able to produce 12.26 V at a 5.7 meter/second wind speed[32].

ii. Darrieus VAWT

This wind turbine uses aerodynamic lift to harness the wind in any direction. It is ideal for the urban and residential kind because of its new design, improved materials, and engineering[33]. This turbine works efficiently in high-speed environments, hence, it requires a higher wind speed to start. It is also complex in its design[31]. The helical-blade construction has low output torque variation and self-starting, and is specifically disadvantaged by the blade manufacturing costs[34]. The S-Darrieus wind turbine performs better than H-Darrieus when low speed of wind speeds are experienced due to its effectiveness in capturing piston wind energy from the train passing through tunnels[35].

iii. Hybrid VAWT

A hybrid VAWT wind turbine combines the Savonius and Darrieus wind turbines to increase power efficiency. Integration of a Savonius rotor with a Darrieus turbine increases self-starting properties but also intensifies vortex interactions, resulting in load fluctuations[36]. A research

study used a hybrid VAWT, which yielded a high level of performance, obtaining a 48.6% power coefficient and self-starting capability[37]

VAWTs offer advantages over HAWTs, such as lower cut-in wind speed, no wind direction control, making them good for areas with low average wind speeds of 2-5m/s and above 7 m/s peak values can capture energy from wind at low cut-in speeds [27], [38].

Table 2.1: Major classification of wind turbines [39]

	HAWT	**VAWT**
Lift type		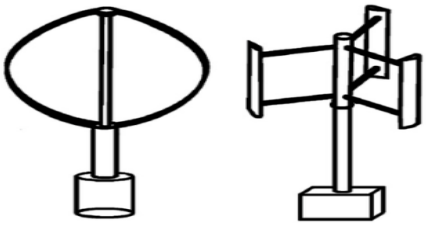
Drag type		

2.1.2 **Wind turbine placement in railway applications**

Several types of WEHS have been installed in railway infrastructure across the globe, depending on the location. Table 2.4 outlines the case studies on wind energy applications in railways, highlighting different turbine placements and power outputs under various wind speeds.

a) WEHS was placed on the train rooftop.

Train-mounted wind turbines are miniature turbines that are placed on the rooftop of the train to capture kinetic energy and transform it into electric power. These turbines are utilized to power distribution circuits in trains, and this leads to a reduction of external power usage, hence enhancing energy utilization. The benefits of this placement are that it lowers operational costs and increases autonomy, as well as possible environmental benefits [30], [40], [41].

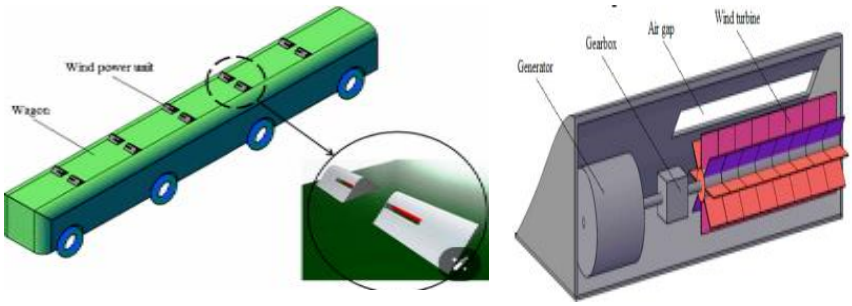

Figure 2.2: Train rooftop wind turbine placement[27]

b) Wind turbines placed alongside tracks.

These wind turbines are placed at the corridors of the railway tracks to capture wind power from natural winds as well as power from running trains. The system can be mounted at the side of the track, on top of structures forming the track, or can be installed underground [15], [29], [31].

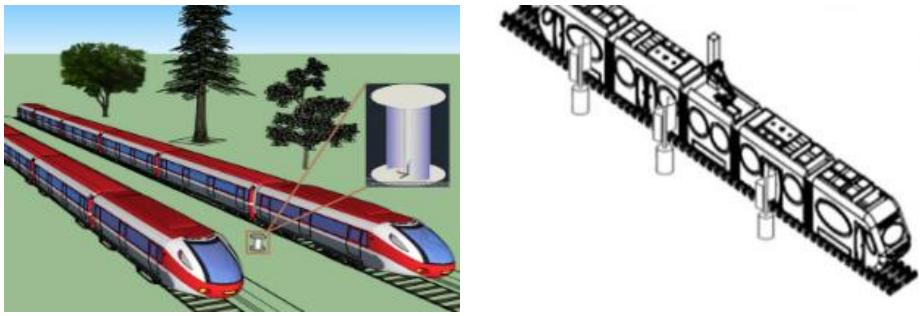

Figure 2.3: Wind turbine placement along the railway track [17]

c) Wind turbines placed in tunnels and ventilation shafts.

Tunnel & ventilation shaft turbines are wind energy systems that are placed in railway tunnels or ventilation shafts with the ability to extract kinetic energy from passing trains. These tap waste kinetic energy and generate electricity that is utilized in tunnel functions, for instance, lighting and ventilation. These turbines are installed with the minimum intrusion of the train operations at locations such as close to tunnel entrances or ventilation shafts [42], [35].

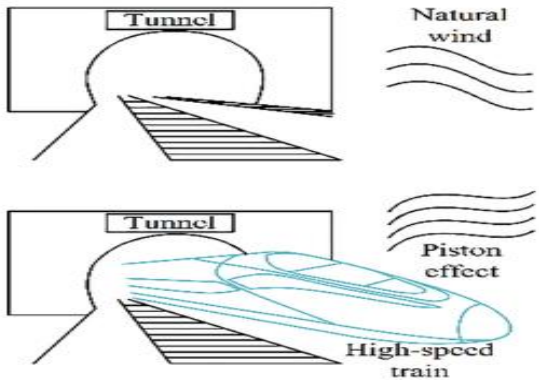

Figure 2.4: Railway Tunnel wind turbine placement [32]

d) Wind turbines installed between track sleepers.

Wind energy potential can also be tapped into by placing wind turbines on the railway track centerline to make use of the train gusts beneath speeding trains. This type of wind turbine placement is still in the conceptual stages, and very little research has been done [15].

2.1.3 **Generators**

Conventional WECS employs diverse kinds of generators which include Squirrel Cage Induction Generator, Doubly Fed Induction Generators, Wound Rotor Induction Generator, Permanent Magnet Synchronous Generators and Wound Rotor Synchronous Generators [43]. Variable-speed WECS like DFIG and PMSG are preferred over fixed-speed WECSs like SCIG because of their high dynamic performance[44]. DFIGs are the most employed generator in WECS due to the fluctuation in the operational speed and technological improvements in semiconductor switches, turbine aerodynamics, and rotor material. PMSGs present a suitable option for smaller wind turbines that demand reduced maintenance because they possess characteristics like high efficiency, dependability, high power-to-weight ratio, a gearless design, light weight, and the capacity for self-excitation [45]. DFIGs are the most employed generator in WECS due to the fluctuation in the operational speed and technological improvements in semiconductor switches, turbine aerodynamics, and rotor material [46].

Table 2.2: Summary of the literature reviews about wind energy harvesting in railway applications

Ref	Summary	Findings	Methods used	Limitations/gaps
[2]	Explores applicable power electronics approaches for making use of wind energy in railway systems	Simulations reveal that a plan utilizing ten VAWTs can generate 32.3 MWh annually, with train movement accounting for nearly 10% of energy production.	Matlab/Simulink MPPT DAB system.	What are the efficiency characteristics of the power conversion system under fluctuating wind conditions?
[25]	The paper evaluates MPPT algorithms for WECSs to improve energy extraction efficiency, classifying them based on power measurement.	MPPT algorithms combined offer many advantages over traditional methods, with their limitations.	MPPT	Need for generic smart and hybrid MPPT algorithms which don't rely on wind velocity measurement instruments for training.
[44]	The research investigates the converter's role in wind energy control and applications, highlighting the need for efficient converters in wind turbine power systems.	Advanced control systems for energy consumption forecasting and wind turbine integration are crucial. PSF is a difficult approach to apply to MPPT control.	MPPT	Future studies aim to improve converter applications for safety, affordability, sustainability, monitoring and usability.
[46]	Various MPPT algorithms have been created to optimise power from wind energy systems.	Direct power measurement techniques like TSR, OTC, and PSF are inflexible due to wind turbine characteristics, while sensorless methods like HCS and ORB are cost-effective but struggle with rapid wind fluctuations.	MPPT	Sensor-based approaches require mechanical sensors, increasing costs and reducing system reliability.
[35]	The paper presents a small-scale wind energy harvester in HSR tunnels	The harvesting system proposed demonstrated a 23.2% efficiency and electrical output of 107.76 mili Watts, hence its feasibility and effectiveness in generating electricity.	CFD	Need for experiments in the field with the proposed WEHS placed at the exit and entrance of the tunnel.
[47]	The study proposes a model for producing clean energy utilizing wind power from passing trains.	The proposed model outperforms traditional systems by producing five times more power per unit step, with each train capable of producing 13.5 KW of power.	CFD	What is the electrical grid integration process information for the power generated by wind energy?
[48]	Wind energy, a significant renewable resource, is utilised through MPPT (MPPT) techniques to optimize power output from WECSs.	HAWT are primarily used for bulk power generation, with the TSR method being efficient but less efficient than the OTC and PSF method	MPPT (P&O, IC, FLC, and mechanical MPPT-like pitch control.	Need to enhance and explore MPPT techniques for improved efficiency in WECSs.

[49]	The study categorizes MPPT algorithms into indirect, direct, and hybrid controller categories for use in WECS.	Algorithms like ORB, OTC, INC, PSF, HCS, and TSR are reliable, low-cost, efficient in memory usage and simple, but struggle with wind variations and theoretically offer better MPP tracking.	MPPT	addressing the lack of clear guidelines for selecting the optimal MPPT algorithm for different WECS installations
[50]	The paper provides an overview of P&OMPPT used in WECS.	P&O can be categorized by step sizes and tracking strategies, with hybrid step sizes and generic objective functions showing potential for enhanced algorithm performance.	Matlab	Future research should focus on robust, dynamically improved, and complex algorithms.
[51]	The paper explores MPPT strategies for a WECS using a DFIG to optimize power production under different conditions.	The study reveals that FLC outperforms traditional methods in start-ups, reducing oscillations and improving disturbance handling, ensuring good quality in both stator and rotor circuits.	Matlab/Simulink	The paper highlights the need for more adaptable control strategies due to the complexity of design, due to non-linearities and parameter variations in existing control techniques.
[52]	The research paper explores MPPT in modeling wind turbine systems with a DC-DC converter and PMSG, thereby improving energy extraction.	The MPPT algorithm optimizes the system's speed for maximum power point operation by analyzing mechanical power and rotor speed.	MATLAB	Investigating how the proposed method can scale and adapt to various wind turbine types and sizes, considering diverse operational scenarios and grid integration challenges.
[53]	The paper reviews an adaptive MPPT for WECS, combining a master-slave FLC and an approximation scheme, operating in two modes.	The proposed method efficiently determines the optimal operating point in fluctuating wind conditions without an anemometer, eliminating oscillations around the MPP and ignoring air density fluctuations.	MPPT(FLC)	Improving the reliability of MPPT techniques by utilizing FLC, which operates without previous knowledge of the system
[54]	This paper examines the latest wind turbine MPPT control methods, analyzing their performance through simulation.	The study analysed three MPPT control methods, highlighting the development of hybrid methods like PSF control and HCS for sensorless, flexible wind turbine control.	Matlab Simulink	Conventional MPPT methods face challenges in achieving MPP during rapid wind fluctuations for medium and large-inertia wind turbines.
[55]	The paper discusses the use of MPPT techniques in WECSs, highlighting their significance in improving system efficiency amidst variable wind speeds.	The study demonstrates that both the TSR and HCS methods effectively extract maximum power from wind energy systems, with simulation results indicating their performance under turbulent wind conditions.	Matlab/Simulink	This paper does not address how extreme weather conditions affect the scalability and performance of MPPT methods in larger wind energy systems.

2.2 Integration requirements

Wind power can considerably contribute to the development of railway systems regarding sustainability. However, wind power integration depends on the subsystems to benefit and the technical integration with the electrical grid or the usage of energy storage devices.

2.2.1 Railway subsystems suited for wind energy integration

Railways are made up of many sub-systems which require a constant supply of power for their proper functioning. Some of these subsystems use a lot of energy, while others, such as lighting, communication and signalling systems, need less energy; thus, they can be linked to renewable wind energy sources to cut down on the electricity costs of the company.

a) Lighting subsystems; railway lighting is very important for safety and illumination of the railway corridors, stations, tunnels, platforms, train yards, etc. Wind energy can be put to straight use for operating lighting systems while employing energy storage systems such as super capacitors and batteries that can store the energy collected during high wind times and used at low wind times to meet the energy demand [3], [56].
b) Signalling and communication systems; for the safety of the railway, these systems require a constant power supply; therefore, wind power can be integrated into such systems to power trackside signals and communication relays[2], [15].

2.2.2 Hybrid integration with the grid.

In railways, wind energy systems can be used as standalone systems or synchronised into the railway electrical grid by forming part of an integrated system.

a) Feeding into the grid; in this arrangement, the railway network takes power from the grid when wind power is limited and returns the surplus energy to the grid when generation exceeds the local consumption[57]. In some countries, feed-in directly into the grid from rail operations can be eligible for Feed-In Tariffs or other incentives, making it financially viable in the long run[58].
b) Power backup for the grid; The hybrid system also incorporates a grid-connected backup power supply where the railway systems can draw power from the main supply grid whenever there is low wind to generate electricity to meet the needs of the railway

systems[59]. Sophisticated energy control systems also use decision support such as predictive analytics, which would need to determine the right time to switch from the power grid to wind-generated electricity and vice versa to minimize disruption[60].

c) Energy storage; Highly efficient hybrid systems also consist of energy storage solutions to stabilize fluctuations of wind energy, such as battery storage solutions, super capacitors, or hydrogen storage facilities for critical loads, like lighting and signalling, must be operational and uninterrupted[3].

2.3 Effect of different railway configurations/ terrains on wind profile.

The railway configuration is a major factor in wind profiling, which affects wind turbines placement. *Table 2.3* categorizes the impact of railway configurations into three primary types: such as surface, elevated, and underground versions[61], summarizing their effect on wind profiles. These configurations affect the natural and train-generated wind differently, influencing the potential of tapping wind energy. Furthermore, the impacts of diverging and converging tracks, HSR, tunnels, and urban systems, including light rail, are also discussed.

a) Surface railways.

The rail tracks are laid on the ground oriented with limited physical obstruction [61]. They are more suitable for wind energy harnessing because they are characterised by an open area and low turbulence. VAWTs can be implemented on surface railways in regions with exposed terrains and steady and fast winds[31].

b) Converging and diverging railway tracks.

Researchers observed changes in velocity in the wind at the moment when it approached the studied models from different directions, thus describing the diverging and the converging flow. This concept can be applied to railway track configurations: in a converging configuration, there is a focus on airflow, thus increasing wind velocity, hence the Venturi effect, while in a diverging configuration, the wind disperses, thus decreasing the velocity[62].

c) Elevated tracks

These are tracks that are built above the ground level or on structures such as bridges or overpasses in urban or suburban areas[61]. It gives height access and increases wind power exposure within reach of turbines, thus enabling access to wind flow that would otherwise be interrupted by structures [63]. Elevated tracks influence wind paths by creating concentration spots or zones with higher wind velocities. They are best utilized in wind power collection, particularly in those regions that are known to experience train-induced winds caused by moving trains[64].

d) Underground tracks

Underground railways are rail systems that operate in trenches or tunnels below the ground level and are commonly located in urban centers[65]. They do not encourage the natural flow of winds, thus making the capture of wind energy rely on other sources. The Venturi effect creates substantial wind behind the train, and this can be tapped for energy production[66]. High turbulence and high-pressure changes are expected in long and straight tunnels[67].

e) High Speed Rail (HSR)

HSR is characterized by faster trains compared to traditional rail [15]. The wake generated by the HSR trains brings instabilities in terms of wind directions and thus challenges that need to be overcome in positioning turbines for wind energy harvesting[63]. The turbulent winds can be harnessed by using VAWT systems due to their resilience to withstand such winds. Research has indicated that velocities closer to high-speed trains can vary depending on certain conditions, reaching velocities as high as 15 to 20 m/s [31].

f) Light Rail and Urban Systems

Light rail is characterized by low speeds of an average of 30km/h, usually slower than HSRs located in urban areas with various structures[2] that interfere with laminar airflow, thus, it is unsuitable for large-scale wind energy extraction[40]. This makes it more feasible at sections of the railway track that are not enclosed, like elevated beams. Promising technologies include small-scale (micro) turbines and tuned turbine designs, which can be implemented to capture wind energy along the corridors of light rail[68]. Wind energy generated alongside LRT systems may be either stored in batteries or fed into urban microgrids to power subsystems as signalling [69].

g) Terrain influence on wind patterns.

Flat terrains tend to give a steadier wind pattern, which will not interfere with such factors as hills or trees. This is beneficial for the normal functioning of wind turbines since stability is always good for operations [70]. In contrast, hilly or urban areas block the wind flow, thereby forming turbulence and leading to a reduction in the efficiency of the turbines. However, the author [71] mentioned that hilly terrain can benefit wind turbine efficiency by inducing faster flow recovery compared to flat terrain. Nonetheless, VAWTs are useful in such places given that they have the capability of capturing wind from different directions[72].

Table 2.3: Impact of railway configurations on wind patterns and wind energy harvesting potential

	Surface	**Elevated (Bridges, Overpass)**	**Underground (Tunnels)**	**Wind energy harvesting potential**
HSR	Strong train-induced wind due to high speeds (250+ km/h)	Exposed to natural wind, with fewer obstructions, and high-speed train-induced wind	Strong airflow at tunnel entrances/exits due to high train speeds	High for surface and elevated; Moderate at tunnels
Light rail/urban systems	Slower speeds, turbulent wind due to nearby buildings; train-induced wind is weak	Less obstructed than the surface, but still has minimal train-induced wind	Limited airflow in enclosed underground systems	Low for surface and underground; Moderate for elevated systems
Diverging	Localized turbulence at track splits disrupts natural airflow	Increased turbulence where tracks diverge on elevated structures	Confined turbulence in tunnels disrupts airflow	Low in all cases due to wind disruption and turbulence
Converging	Airflow is disturbed where tracks merge, creating localized turbulence	Increased turbulence at merging points on elevated structures	Confined airflow variability in tunnels	Low across all cases due to the disruption of consistent wind patterns

Table 2.4: Power generated relative to wind speed/train speed

Ref.	**Application**	**Power/voltage gained**	**Wind speed (m/s)**	**Wind turbine**	**WT placement**
[73]	Harvester	48.8V/5W(470Ω)	10	HAWT	On track sleeper
		2.28V/110mW(56Ω)	10	VAWT	
[35]	Super capacitor	107.76mV/23.2% (8Ω)	11	VAWT	Tunnel
[31]	Traffic	21.508W/3.297N(TSR-0.304)	5.9	VAWT-Savonius	Along the railway track
	No traffic	3.445W/Torque-0.506N(TSR-0.301)	3.5		
[47]	Stored in pressure conduits	314W	Train@60km/h 16.7	VAWT	On the train rooftop
[30]	Onboard power for a train	121.5kWh/day-40.1MWh/year	12	VAWT	On the train rooftop
[29]	Train station	245kW	50	VAWT	Along the railway track
[2]	Catenary	11kW(peak power) 3.5kW(constant wind speed) 1.33MWh-10% (train assistance)	5	VAWT	Along the railway track
[27]	Railway monitoring sensors	57.651MWh	7	VAWT	Tunnel
		2.46W(instantaneous) 1.08W(max. av. Power)	13		
[69]	On board power	2.94kWh	16.67	HAWT	Locomotive clean room
[41]	On board power	3.17MW@10 units	27	VAWT	Wagon rooftop
		1.41MW	17.7		

2.4 Control mechanisms

In WECS (Wind Energy Conversion Systems) applied in railways, the control systems are essential in dictating most of the components' management, power produced, safety, and durability of the system. Control strategies are typically divided into two groups, i.e., electrical and mechanical control[43].

2.4.1 Mechanical control

Mechanical control is an essential function in controlling the amount of power that is generated according to wind conditions, as well as in converting wind energy to electricity, managing mechanical losses and stresses. All turbines are designed with some mechanism of control for the power to be converted. The controls include: stall control, yaw control, pitch control, and torque control[74]; they are involved in controlling the movement of the wind turbine[74]. In the pitch angle control, the pitch angle of the turbine blade can be adjusted in such a way that the speed at which the blades generate optimal energy yield. This is an important control since wind turbines harness the wind for electricity generation, and where there is strong wind turbulence, they produce excess power that may lead to mechanical breakdown[75]. This control adjustment enhances energy generation efficiency, which is desirable in the dynamic railway sector. Active pitch control may be used for an individual blade depending on the balance of the aerodynamic loads. There is the self-acting variable pitch mechanism, where the pitching moment about the blade is created through aerodynamic forces. Another way of controlling of blade pitch angle can be accomplished by gears or cam actuators[76]. Under the rated wind speeds, the angle of pitch is positioned to its optimum position, allowing the position of the blade to capture more energy by orienting the blades perpendicular to the wind path. When wind speeds exceed the rated level, the angle of the pitch is modified to cut the level of power generated and prevent spoiling of the turbine, which might lead to malfunctions within the system[77].

For stall control, when the wind speeds exceed the rated value of the turbine, the turbines use the passive stall to reduce its power intake. This involves ensuring that the turbine’s angular velocity is kept constant, the angle of the blade is adjusted to increase, and the blade is forced to stall for the required power to be produced[78]. This control minimizes the generation of excess energy,

safeguards the storage facilities utilized and lowers the mechanical stress on the turbines, which could increase the mean time between failures., the design of the rotor confines the actual rotation speed of the turbine as a result of the aerodynamic stall, brought about by high wind speeds. There are two types: passive stall, where blades are stalled at high rpm without any mechanical intervention, and active stall, which makes use of stall forces that are similar to those produced by the pitch control but do not change the angles of the blades[78]. Passive stall control is simple, low complexity, and low cost, however, its suitability reduces with the large wind turbine and becomes less efficient at low wind speeds, making passive stall a cost-effective solution for smaller wind turbines used in railway applications. Active stall control enables accurate control of the blade angle about its speed, thus controlling/tackling power spikes, but it needs a cutback of the generator rotor speed during high wind speed[79]. The yaw control is mainly used in HAWT as it assists in placing the turbine in such a way that its rotor is parallel with the wind, ensuring high efficiency of energy retrieval. Yaw control turns the rotor plane in the wind direction, thus enhancing its efficiency by reducing yaw error or the difference between the rotor plane of the wind direction[43]. Torque control determines the torque being imposed on the rotor to obtain a desired rotor speed; this improves energy efficiency under variable wind conditions[74], which aids in controlling the amount of energy used when the wind conditions change along the railway track.

2.4.2 **Electrical control**

Electrical control is very crucial in railway-integrated wind energy systems as it regulates the generator, power electronics, energy storage systems and the grid interface. These control strategies are concerned with the enhancement of the performance efficiencies of these systems as well as with the design standards that are ideal for railway use to offer both functional efficiency and security.

a) Generator control

WECSs use generators to ensure smooth running and maximum power generation. Two primary methods are Direct Torque Control (DTC) and Vector Control. DTC controls torque and magnetic flux directly, offers a quick dynamic response, and provides stability during wind variation. Vector Control, also called Field-Oriented Control(FOC), provides a clear separation of the generator's flux and torque components and works with high efficiency and with a very high degree of

control[80]. Such controls are especially important for railway systems where the power load changes according to the train schedules and the wind conditions, which differ as the train passes.

b) Grid integration

Grid integration is important in controlling the relationship between wind power systems and electrical networks to achieve quality electricity. It comprises voltage, frequency, and reactive power control, all of which are maintained by power electronic converters [72]. Reactive power assists in the management of voltage in weak networks and long-distance transmission to maintain the dependability and integration of wind energy into the grid [73]. The GSC and MSC are the basic parts of the power electronic conversion system used in WT systems. Both have very different yet equally important functions in terms of the efficiency of energy conversion and their integration into the electrical network.

i. Grid Side Converter(GSC)

In WECS, the GSC regulates the DC-linked voltage and the power. It controls the stator current direct and quadrature axis components to provide only the real power at the unity power factor. The control strategies used for GSC are the Vector Oriented Control(VOC) and the Direct Power Control(DPC). DPC makes algorithms easy to implement and removes uncertainties, while VOC improves power quality and minimizes the issue of harmonics[79]. Concerning irregularities of wind energy, GSC has proficiency in maintaining the level of voltage at the DC link[44], [81].

ii. Machine Side Converter(MSC)

The Machine Side Converter (MSC) is particularly important in wind turbine systems for variable frequency control and improved performance[82]. It regulates the speed of the rotor of the wind generator through the application of Field Oriented Control(FOC) and Direct Torque Control(DTC)[79]. It also regulates the voltage at the DC bus, low harmonic, power factor correction, and nearly sinusoidal current waveforms. The MSC also functions to control the rotor speed when there is a variation in the wind[44].

2.4.3 **Maximum power point tracking (MPPT) algorithms**

MPPT is crucial in managing the output power from the wind turbines in railway infrastructure as it enables the turbine to be adjusted depending on the wind conditions. MPPT ensures maximal power extraction from available wind sources, thereby enhancing the reliability of WEHS systems[83]. In wind systems, MPPT techniques are divided into direct and indirect control methods. Indirect methods, i.e., Power Signal Feedback and Optimal Torque Control and these methods include an element of the wind turbine characteristics needed for efficient working, while the direct control methods, such as Hill Climbing Search(HCS), Fuzzy Logic Control(FLC), Perturb and Observe(P&O), are not dependent on wind turbine characteristics[84], making them suitable for railway systems. The Optimal Torque Control(OTC) method ensures extracting maximum energy from the wind, where it regulates the difference between the intended value and its present position and feeds it to the controller. It controls generator torque to obtain the optimum torque reference curve for the highest power output of a wind turbine at a specific wind speed. This reference torque is used as a reference for the MPPT controller, which subtracts the actual torque to minimize the difference between the two[48],[85]. The PSF method depends on the maximum power curve data and a power reference for maximum power operating conditions. However, PSF and OTC control methods suffer some limitations in tracing MPP, especially when wind speed is low, particularly in large-inertia wind turbines. They depend upon accurate specifications of factors related to wind turbines[83]. P&O method is a mathematical algorithm employed in wind energy systems to locate maximum points along the curve. It involves adjusting a control parameter and observing the variations in the target function until the slope reaches zero. In case the operating point is on the left part of the characteristic curve, the controller must shift it to a position marked by MPP [48]. FLC is a computational paradigm for controlling processes based on fuzzy sets and variables instead of Boolean values of typical digital systems. Due to its abilities of robustness to uncertainty, nonlinear control, and easy implementation, it is suitable for systems with uncertainties and nonlinearities[86]. This control is also accurate and uncomplicated and does not depend on an understanding of the system's mathematical equations. A Fuzzy Logic Control system consists of mainly fuzzification, Inference engine, and defuzzification[84]. FLC is adopted and further discussed for this research due to its strengths listed in *Table 2.5* showing the FLC comparison to the other traditional methods, discovering its potential improvement in wind

variability handling and system performance whereas *Table 2.6* gives a summary of the Maximum power point tracking algorithms employed in railway applications.

Table 2.5: Comparison of the performance of MPPT techniques [25], [46], [48], [50], [79], [83]

MPPT technique	**Complexity**	**Robust**	**Adaptability**	**Wind speed measurement using sensors**	**Prior knowledge**	**Efficiency**	**Perf. Varying wind speeds**
FLC	High	Robust	Excellent	Depends	Required	Superior	High
P&O	Depends	Robust	Good	Depends	Not required	Very high	High
TSR	Easy	Not robust	Average	Required	Not required	High	Moderate
PSF	Minimal	Relatively robust	Average	Required	Required	Moderate	Moderate
HCS	Easy	Not robust	Good	Not required	Not required	Minimal	Moderate
OTC	Minimal	Relatively robust	Average	Not required	Required	High	Moderate
IC	Easy	Relatively robust	Average	Not required	Not required	Minimal	Moderate

2.4.4 **Fuzzy logic control (FLC) algorithm**

FLC is an MPPT algorithm used to enhance the speed and power of WEHS, especially in intermittent wind conditions. It enhances attributes, e.g., pitch angle, power quality, and generator torque, to get the best out of wind turbines with minimal stress on the mechanical system.[86]. The summary of FLC-MPPT in *Table 2.7* reveals the advantages of the FLC in the wind energy extraction process, where some of the difficulties of the method include computation intensity and sensitivity to the quality of the input data.

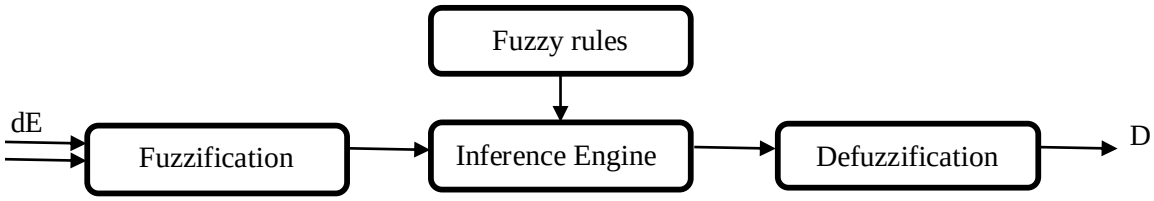

Figure 2.5: Block diagram of FLC MPPT[26]

Key components of FLC

a) Fuzzification: This stage requires changing the input variables into fuzzy sets. This is a vague set whose elements qualify for membership based on membership functions [87].
b) Inference Engine: The control action is computed inside the FLC core, and the inference engine maps the fuzzy rules over the input variables. These rules are normally in the form of IF-THEN [88].

c) Defuzzification: This is the last stage where the output of the inference engine is a crisp control signal. This control signal is used to modify one of the parameters of operation of the turbine to allow the turbine to make the required power output[89].

FLCs are important for enhancing wind energy conversion systems since functions such as pitch angle control, power electronics, and generator torque are significant, and their enhancement would significantly lift efficiency. FLC operates in response to this variability of wind power by continuously optimizing the amount of energy captured as well as minimizing mechanical stress.

A. Pitch Angle Control using FLC

Fuzzy logic control systems are used for controlling the pitch angles to maximize energy capture as well as for safety considerations at high velocities of wind[90]. Fuzzy controllers are superior in response flexibility and real-time optimality as compared to the other controllers, which makes them more suitable to respond to wind direction changes along the railway track[91].

B. FLC in power electronics in WEHS

Fuzzy logic is incorporated into WEHS power electronics for converters and inverters, which convert fluctuating AC power from wind turbines into constant DC power for rail-grid applications or battery energy storage. These converters regulate the output voltage with a lower ripple value than the comparative conventional controllers[92]. In the railway grids, Fuzzy logic controllers facilitate harmonics and power quality control, according to the changes in loads and wind conditions[93].

C. Generator Torque Control with FLC:

To ensure a stable power supply for railway networks, balancing the electromagnetic torque of the machine with the mechanical torque of the turbine is essential for the stability power supply of railway networks. FLC optimises the generator torque and makes corrections from the set power and the rotor speed, hence enhancing the efficiency of energy conversion and minimizing the fluctuation of torque[89].

Table 2.6: Overview and Summary of MPPT Strategies in Wind Energy Systems

MPPT	Ref.	Summary	Findings
P&O	[50]	The article explores different perturbation step sizes in wind turbines, including fixed, variable, adaptive, hybrid, and multivariable, and their impact on turbine performance, complexity, and power generation.	P&O algorithm adopts a fixed step size, which can negatively impact wind turbines' dynamic performance, while adaptive and hybrid approaches enhance tracking speed and performance.
	[94]	The P&O method is common in WECS, adjusting system operating points based on observed power output.	The study introduces the integration of FLC and P&O method, enhancing the conventional Perturb &Observe approach, achieving 36.38% power capture and faster response times in fluctuating wind conditions.
	[95]	The P&O MPPT optimizes WEHS power output without requiring wind speed sensors or aerodynamic characteristics knowledge.	P&O is effective in tracking maximum power points, but can lead to inefficiencies in high and medium-power wind systems
TSR	[83]	The TSR MPPT algorithm is another tool that controls the wind mechanical power by changing the rotor speed.	TSR MPPT algorithm, despite its superior efficiency and cost-effectiveness, requires a wind speed sensor, posing challenges in practical applications due to its reliance on sensors.
	[48]	The TSR method is an adaptive MPPT algorithm that optimizes wind turbine rotational speed for optimal energy conversion under varying wind conditions.	The TSR method optimizes generator speed and MPPT performance, enhancing efficiency under fluctuating wind conditions, but may increase system costs due to constant wind speed measurement.
	[25]	The TSR MPPT algorithm optimizes power output from WECS by regulating rotor speed based on wind speed measurements. It uses mechanical sensors and wind speed estimation without sensors.	Effective in various environments, the TSR method has limitations like higher costs and reduced reliability due to mechanical sensors. Wind speed estimation algorithms can improve energy tracking and harvesting accuracy.
PSF	[83]	The PSF MPPT algorithm, a part of the Indirect Power Control (IPC) category, is renowned for its speed and simplicity in maximizing mechanical wind power capture.	The PSF algorithm, a cost-effective solution for maximizing mechanical power, faces limitations in optimizing electrical output due to its need for a wind speed sensor and variations in wind velocity measurements, making it less effective in real-time applications.
	[50]	The PSF MPPT algorithm uses optimal power lookup tables for wind turbines, estimating power based on changes in DC-link current and voltage.	The PSF, while robust and cost-effective, struggles with low wind speeds, particularly for large-inertia turbines. The PSF MPPT algorithm's reliance on lookup tables may hinder its efficiency.
	[25]	The PSF MPPT algorithm optimizes power extraction from WECS, requiring speed sensors and turbine parameter knowledge, and uses lookup tables for optimal power generation.	The PSF algorithm, a cost-effective method for tracking wind turbine maximum power point, faces challenges in performance during fluctuating wind conditions, inefficiency in power extraction, and exhibits oscillations around the MPP.
HCS	[48]	The HCS method is an MPPT technique that optimizes wind turbine operating points by observing speed changes and adjusting energy output.	The HCS method, when combined with P&O, improves performance and costs by tracking maximum power points, but may increase costs and require more complex setups.

	[49]	The HCS MPPT is also commonly adopted in WECS for locating the MPP by perturbing a control variable.	The HCS algorithm, effective in tracking MPP, struggles with wind variations, but a modified version improves speed and efficiency by adjusting step sizes and reducing oscillations around the MPP.
	[45]	The HCS control method is a popular MPPT technique in WECS due to its simplicity and effectiveness, eliminating the need for wind speed measurements.	HCS control is a two-stage algorithm that enhances energy capture efficiency by quickly adapting to wind speed changes. Despite its limitations, it's preferred for its simplicity, and future research aims to improve its applicability in larger systems.
OTC	[83]	The OTC MPPT is simple and efficient, enabling fast tracking of maximum power points without direct wind speed measurements, improving operational speed and responsiveness.	The OTC algorithm, while efficient, may not accurately reflect changes in wind conditions, which can hinder its performance in fluctuating wind environments.
	[84]	The OTC method adjusts the torque of the PMSG based on wind speeds, requiring knowledge of optimal turbine characteristics like power coefficient and TSR.	OTC optimizes wind energy system power output but requires slower response time, energy loss, and turbine characteristics, hindering effectiveness under changing wind conditions.
	[96]	The OTC MPPT algorithm optimizes turbine rotation speed in a hybrid wind-solar energy system, maximizing energy capture from varying wind conditions.	The OTC MPPT algorithm is superior in power extraction efficiency compared to TSR, enhancing the system performance, but it faces challenges like environmental sensitivity and potential oscillations.
IC	[83]	The INC method is an MPPT algorithm that improves wind energy conversion efficiency by eliminating the need for previous knowledge about wind turbine parameters and measurement instruments.	The INC method improves wind energy conversion system tracking efficiency by calculating power variations and slopes. However, its performance is limited by generator parameters and implementation complexity. The adaptive INC control method refines dynamic performance and convergence speed.
	[97]	The IC method is a widely used technique for MPPT that compares incremental conductance with instantaneous conductance to determine the MPP.	IC is more accurate and stable than P&O but struggles with rapidly changing atmospheric conditions. Despite its advantages, IC can be slow and inaccurate under changing conditions, requiring low tracking speeds.
	[98]	The IC method is an MPPT technique used to optimize power generation under different weather conditions by adjusting the system voltage based on current-voltage relationships.	The IC method is a stable, precise control technique that enhances energy output, especially in rapid atmospheric changes, achieving around 380V (DC). It can be integrated with other MPPT techniques for higher voltage generation, but may pose challenges in implementation.

D. Multi-Input Fuzzy Controllers

Newer versions of Fuzzy Logic Controllers enhance decision-making in railway-integrated wind energy systems since they have more than one input variable. These help to provide improved insight into the wind turbine's operational state, which can be used effectively to precisely regulate rotor speed and angle of the blades[99]. These controllers improve the efficiency of WEHS and perform well in fluctuating wind conditions and, as such, are preferred in large wind farms[100].

E. Advanced FLC MPPT techniques.

Adaptive Fuzzy Logic Controllers (FLCs) and Neuro-Fuzzy Systems are computational intelligent systems utilized in wind energy systems. Their adaptive FLCs can modify rules and membership functions, enhancing wind energy capture efficiency in railway applications[101]. Neuro-fuzzy systems use the integration of FLC and ANN to enhance flexibility and learning aspects[74], [79]. These hybrid systems improve power tracking accuracy at variable wind speed conditions[99].

F. FLC in small-scale WEHS

FLCs are a basic, low-cost, and efficient solution for micro and Pico turbines in small wind power stations. They complement power acquisition without incurring extra hardware expenses and perform energy storage, battery recharging, and constant voltage in isolated railway networks[102]. They regulate wind availability and storage capacity, control load, and protect against over-discharge to minimize the impact on the lifespan of the railway operational system[94].

G. Hardware implementation of FLC

Recent advances in the hardware domain, especially Digital Signal Processors (DSPs) and microcontrollers, facilitate real-time FLCs in integrated WEHS for railway systems. DSPs offer high-speed data processing and optimal control tuning for fuzzy control systems. It is a low-cost, single-chip solution for wind turbine control[103]. These controllers are faster and less power-consuming, and ideal for small and distributed wind power systems[104]. However, questions and issues such as computational complexity and system scaling are still in place.

Table 2.7: Fuzzy Logic Control performance and limitations

Article	Summary	Findings	Limitations
[44]	The document suggests integrating FLC techniques with ANN for a more advanced control strategy, enhancing wind turbine performance and efficiency.	FLC optimizes wind energy extraction, enhances efficiency, and allows optimal wind speed tracking in wind turbine systems, reducing mechanical stress, improving operational life, and enhancing energy generation reliability.	FLC design and implementation can be complex, requiring computational resources and affecting system cost, while performance is sensitive to input data accuracy, affecting control strategy effectiveness.
[45]	The paper discusses wind energy conversion systems using FLC methods, including PMSG and BDFIG generators, focusing on power output, efficiency, and robust speed control using a Takagi-Sugeno-Kang fuzzy model.	FLC MPPT control methods improve WECS efficiency by handling noisy signals, while FLC methods track MPP and optimize performance under varying conditions.	Traditional control methods struggle with turbines with large inertia, causing issues in maintaining optimal power output under changing wind conditions. Improved methods address mechanical stress and system response times.
[83]	The study compares FLC with other MPPT algorithms for optimizing WECS, focusing on VSWT and SCIGs for power extraction and reliability.	FLC demonstrated superior stability, rapid tracking, and time response, outperforming TSR and PSF, with higher efficiency and less oscillation compared to Hill Climb Search.	Some algorithms, like ORB, require significant memory for storing optimal relation curves, while PI controllers struggle with tracking maximum power due to system nonlinearity.
[48]	FLC techniques in WECS, such as MPPT, adaptive controllers, VUFC, and SMC, improve power extraction, manage system non-linearity, and enhance performance.	The FLC has been found to enhance power output, response time, reliability, and energy extraction efficiency in wind energy systems, outperforming traditional controllers in complex environments, and can be combined with genetic algorithms.	FLC faces challenges like implementation complexity, noise sensitivity, computational demand, accurate measurements dependence, and calibration issues, hindering system responsiveness and time-consuming optimization using genetic algorithms.
[50]	The article examines P&O and FLC algorithms, noting that Fuzzy Logic Control is a better strategy. (DFIG, PMSG, HAWT)	The FLC optimizes control variables for optimal power production from wind turbines, adapting to fluctuating wind conditions. The P&O is simple and effective. FLC-based MPPT algorithms show high efficiency, reaching 98.04% in some implementations.	FLC algorithms face challenges due to prior knowledge of wind turbine characteristics and environmental conditions, and may require tuning for optimal performance under different wind conditions.
[87]	The paper discusses an FLC_MPPT to optimize energy extraction, enhancing system reliability and cost reduction.	The simulation results reveal that FLC significantly improves WECS efficiency by precise maximum power point tracking, eliminating the need for mechanical sensors, and enhancing reliability in wind energy systems.	Traditional MPPT techniques often rely on inaccurate wind speed measurements, and while fuzzy logic can address challenges, wind variability consistently makes achieving the maximum power point challenging.
[95]	The study explores the use of MPPT techniques in WEHS, focusing on FLC to improve turbine efficiency.	FLC outperforms other MPPT methods for stable output with 121 V maximum voltage and 28 V minimum variation, enhancing wind turbine energy	The study highlights the limitations of FLC, including inverter side control, pitch angle control, and input parameter tuning, suggesting the need

		conversion capabilities and efficiency under changing operational conditions.	for additional control strategies for real-world applications.
[90]	The study explores the use of FLC in enhancing the frequency regulation capacity of VSWTs under varying wind speed conditions, integrating FLC methods into inertia control loops and frequency control of the pitch angle.	The FLC-based method demonstrated superior frequency regulation performance, indicating its potential to optimize wind energy systems, leading to more reliable and efficient systems.	The proposed FLC method overcomes the limitations of previous methods by offering adaptive control responses.
[93]	The study evaluates three MPPT techniques (PI control, P&O method, and FLC) in extracting optimal power from a PMSG under varying wind speed conditions.	The FLC method outperformed the Proportional Integral and P&O methods in tracking maximum power, providing a steady power output of 5112 W and a voltage output of 500V. It effectively tracked wind speed changes, improving efficiency and stability, especially under variable wind conditions.	FLC, a rule-based decision-making system, requires prior system knowledge, critical fuzzy rule design, and complex implementation, posing challenges compared to simpler methods like PI and P&O.
[99]	The study explores the use of FLC in wind turbines/generators, highlighting the crucial role of control systems in optimizing wind energy performance.	The study analyzed performance indicators like power output and energy conversion efficiency, revealing improvements in FLC implementation compared to traditional control methods.	The study addresses technical issues like computational complexity and scope limitations, suggesting potential areas for future research and real-world applications.
[101]	The paper presents an adaptive fuzzy logic-based MPPT control for a PMSG-based variable speed WECS, enabling online updates of scaling factors at high convergence speed.	The proposed FLC enhances WECS performance by maintaining optimal power coefficient under wind speeds, achieving a total harmonic distortion of 2.2% in grid current and 22.1% in load current.	The study suggests that classical FLC may not be adequate for uncertain non-linear systems, with challenges in parameter tuning, implementation complexity, and performance under extreme wind conditions.
[105]	The FLC tracks maximum power point using error and rate of change of error, adjusting the buck converter duty cycle with an HCS algorithm for optimal power extraction. (stand-alone WECS with a battery storage system)	The FLC enhances system efficiency by tracking MPP under changing wind conditions, is simple and robust, requiring no detailed knowledge of wind turbine characteristics.	Designing an FLC involves complex membership functions and rules, and its performance relies heavily on error accuracy and rate of change.
[106]	The study investigates the use of Four FLCs in a WECS, focusing on regulating active power extraction and maintaining reactive power, aiming for static precision and robustness.	The FLC outperforms traditional PI controllers in stability, precision, and robustness, effectively managing rotor currents and DC-link voltage, and maintaining good dynamic performance during parameter variations.	Tuning the fuzzy rules and membership functions to optimize performance under varying conditions.
[51]	The study uses a DFIG for a WECS and uses FLC for pitch angle control and MPPT, without wind speed measurement.	The FLC, when combined with the P&O algorithm and fuzzy control, significantly improves the maximum power tracking in WECS, outperforming conventional controllers.	The paper acknowledges system modelling challenges due to non-linearities and parametric variations, but the FLC's ability to function without precise system parameters mitigates some of these issues.

3 METHODOLOGY

This chapter outlines the systematic approach undertaken in this research. It details the research design, encompassing the selection and description of the case study, data collection, parameters and configurations of the WECS model, and general frameworks undertaken for the FLC-WECS.

3.1. General framework

The general framework of the methodology for the thesis is represented as depicted in *Figure 3.1.*

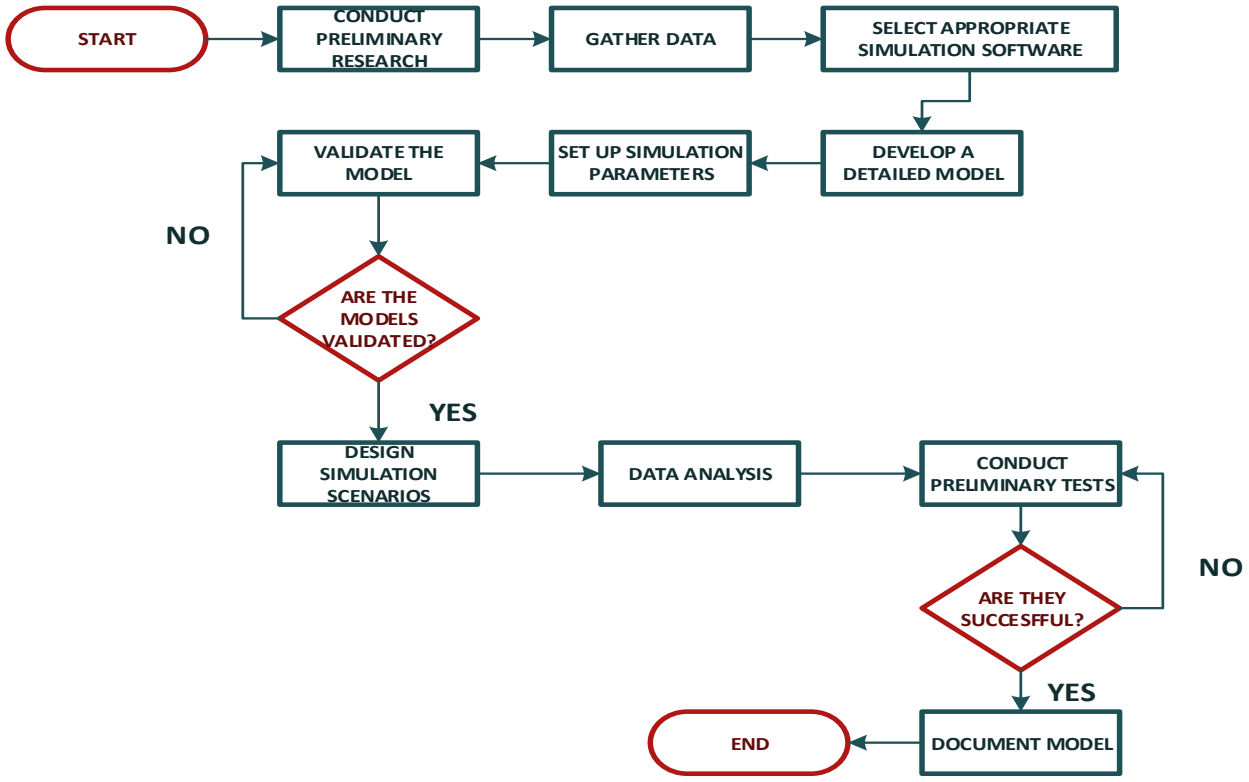

Figure 3.1: Flowchart for the general methodology

A. Conducting Preliminary Research

This is the initial phase of the research, which involves gathering the necessary information about Wind energy harvesting, MPPT algorithms, turbine configurations, and electrical power controls. This foundational research informed the selection of suitable technologies for optimizing energy reliability in AALRT. Key areas of focus included the study of existing wind energy harvesting

systems and their applications in railway environments, as well as the analysis of the various MPPT strategies with emphasis on the Fuzzy Logic Control(FLC).

B. Gathering and analyzing data

The data collected is categorized into primary and secondary data.

a) Primary data: The primary data generated for this research was derived directly from the Simulink simulations, designed to model the WECS and the FLC control system within a light railway environment. They directly address the research objective of evaluating the FLC's performance in controlling the WECS under dynamic conditions, and thus constitute primary data central to the analysis and conclusions presented in this study."

b) Secondary data: Complementing the primary data generated from the simulations, secondary data played a crucial role in validating and contextualizing the research findings. Specifically, the validation paper, which provided a pre-existing Savonius VAWT model, served as a key source of secondary data. Furthermore, to ensure the simulation's environmental parameters accurately reflected the Addis Ababa context, wind speed data were obtained from the Ethiopian Meteorological Agency. This data provided historical wind patterns and average wind speeds relevant to the region, informing the selection of our base wind speed and wind variability parameters. Additionally, data from the Global Wind Atlas(GWA) was collected to gain a broader understanding of wind resource potential in the geographical area surrounding the AALRT. This resource provided valuable insights into regional wind characteristics and potential energy yields. Finally, operational data from the Addis Ababa Light Rail Transit itself, including train schedules and power consumption patterns, was used to inform the development of a realistic load profile.

C. Operational feasibility.

To assess the feasibility of incorporating WEHS alongside the AALRT railway line, we used wind speed data obtained from the National Meteorological Agency and the Global Wind Atlas. In this case, the average wind speed recorded was 2.5m/s cut which is necessary for the function of the VAWT, whose cut in wind speed is 1.5-2m/s making it suitable for areas with

low wind speed[3]. These results indicated that 70% of the time, wind speed was above 2 m/s, which is necessary for the effectiveness of VAWTs. The highest values of wind speed of more than 2.47 m/s at 10m height from the ground were identified in the afternoon and evening. Seasonal analysis showed that January to April, as well as October to November, recorded wind speeds of around 2.5m/s. This established that there was an opportunity for wind energy in the enhancement of the energy efficiency of railways.

D. Select appropriate simulation software.

This is a critical step as the selected software should be capable of handling the complexity of the models, and one such software is MATLAB/Simulink, chosen for its capabilities in modelling wind energy systems and control algorithms, enabling dynamic analysis of the system's performance. Origin software is selected for data analysis, which involves plotting graphs and analyzing scientific data. Visio is selected for the creation of schematic diagrams and flowcharts.

E. Develop a detailed model.

The development of the model included the Wind turbine specifications, electrical power controls, and MPPT algorithm, which in this case is the Fuzzy Logic Controller (FLC). Two models are developed, one without the FLC-MPPT control and the second one with the FLC-MPPT control. The key parameters, such as the wind turbine dimensions, generator characteristics, pitch angle ranges, and DC-DC boost converter specifications, were established based on literature reviews and validated models[107].

F. Set up simulation parameters.

Process of defining constants, variables, and initial conditions, as well as giving limits/scopes of the problem. It sets the level of realism, coverage, and applicability of the simulation, which affects all the other stages of the research process. Setting parameters correctly means that the conditions most likely the real-physical system or the phenomena under analysis are presented, and the model gives a proper basis for analyzing and making decisions. The simulation parameters chosen for the Fuzzy Logic Controller outputs are the pitch angle and the TSR, while the inputs are the Rotor speed and the Power output.

G. Validation of the model.

Validation is a fundamental step in simulation based research, important to establish accuracy, reliability and trustworthiness of the developed numerical model and its generated results. The validation of the WECS model, comparing the results of the simulation model with theoretical or empirical findings. It helps to guarantee that the given model corresponds to the studied phenomenon and provides correct and credible simulation results.

H. Prepare Data Collection and Analysis.

This involves setting up data collection mechanisms and deciding on which performance metric, which in this case is power output and performance of the WECS, and how they will be analyzed. Optimization of turbine settings using the FLC-MPPT algorithms and performing a sensitivity analysis of the technical parameters. The selected performance metric for this analysis is the power output of the WECS, which will be evaluated under different operating scenarios. The analysis aims to show how different factors affect the power generation.

a) Sensitivity analysis; this is an important part of the methodology, showing how variations in key parameters affect the performance of the WECS. In this research, the sensitivity analyses were carried out in regards to the wind speed ranges, i.e., 2.66m/s – 7.6m/s, reflecting the common operational conditions for the WECS. This range allows the assessment of the turbine performance under the lower and higher wind conditions, identifying thresholds where the system operates optimally. The effect of resistance loads will also be taken into consideration, ranging from 0Ω to 300Ω. This analysis aims to show how the turbine's power output is influenced by the electrical load. The pitch angle and TSR ranges for the WECS without FLC range from 0^0 to 30^0 [108]and 0.2 to 1.0 [109], respectively, were considered. These parameters are vital for optimizing the performance of the turbine. This analysis helps to identify the optimal points that maximise power generation. Conducting Preliminary tests.

Preliminary tests were conducted to evaluate the reliability and validity of the model. This involved assessing the external and internal parameters that influence the model simulation outcomes, data inputs, and operation of the algorithms. Safeguard all elements that are correctly implemented,

engage according to plan, return correct values, and appropriately configure the simulation. The tests focused on verifying wind speed calibrations and operational integrity of the FLC-MPPT algorithm used in the simulations.

I. Document the model.

Finally, documenting the model and the setup process is an important process in research studies, particularly in simulation studies for replicability and knowledge sharing. This documentation included a detailed description of the simulation environment, settings, parameters and conclusions drawn from the research. It provides a reference point for future work, makes a study replicable, and is an avenue for disseminating research findings to a broader audience.

3.2 Description of the study area

For this study, the Addis Ababa Light Rail Transit railway is selected. It has a track of 17km in length from the industrial area to the southern side of the city. It has two routes, i.e. the East to West line running from Ayat to Torhailoch, and the North to South line running from Menellik II square to Kaliti. These two lines intersect at a common track, which is elevated thereby chosen as the site of study. There are 4 route sections at elevation along the common track, i.e., from St.Lideta to Tegbared, Tegbared to Mexico, Mexico to Leghar and Leghar to Stadium, where the common section is a 2.7 km section of the double-track north-south and east-west routes of the AALRT, where trains have an average velocity of 20km/hr. Considering one mast location along this elevated section, the VAWT wind turbine is suggested to be installed between the double railway tracks to utilize train-induced wind from either direction. The power generated is to be collected and stored in batteries to power the railway subsystems. Wind speeds for this area, with an average ambient wind speed ranging between 2.47m/s and to 2.66m/s, depending on the elevation of the track above the ground, which is sufficient for VAWT whose cut-in wind speed is as low as 1.5m/s. The turbines are to be placed along the track between the double tracks in addition to the train-induced wind when a train passes every 10 minutes at an average speed of 20-30 km/h. These factors influence the power availability from the VAWTs, given their dependence on the wind speed profile, and must be considered in meeting these loads. This analysis includes the power requirements for various components in the Addis Ababa Light Rail Transit backup

generator load system. The study [110] mentions that measurements for the average auxiliary load are 15 kW in AALRT.

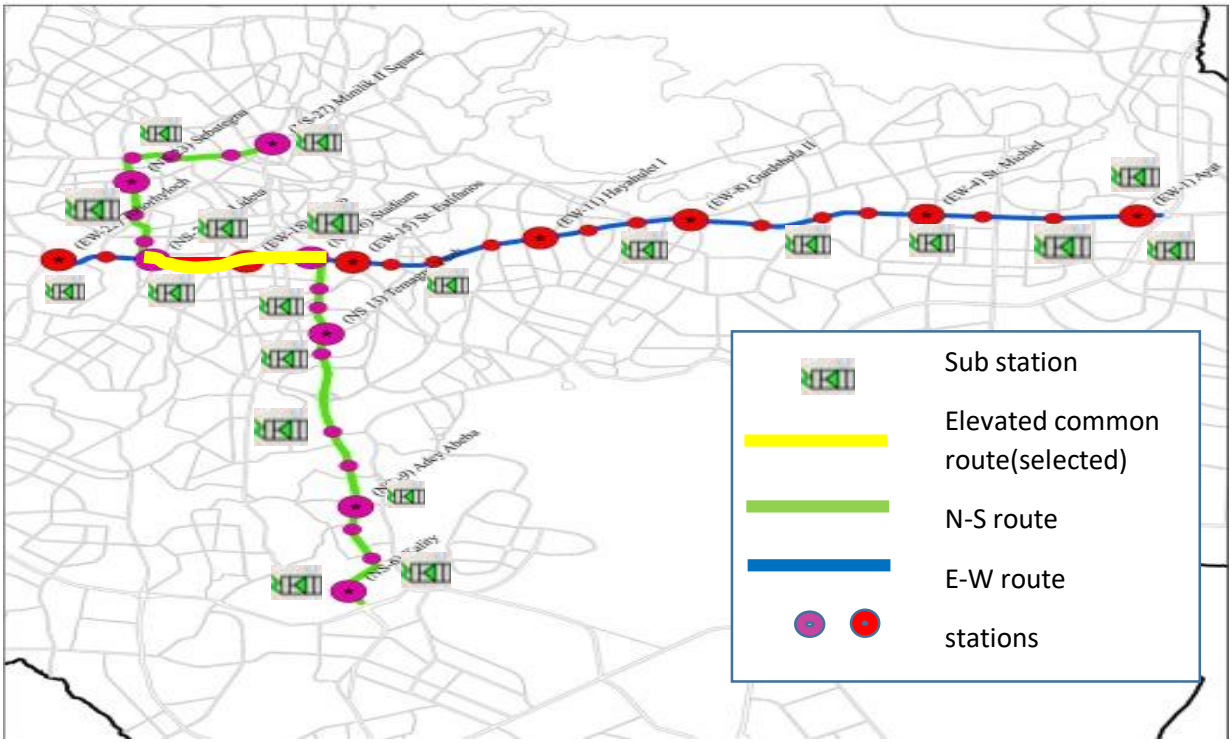

Figure 3.2: The AALRT route showing the selected section for this study

3.3 Data collection and analysis

3.3.1 The electrical load assessment

This load assessment report evaluates the electrical loads that the proposed Savonius-Vertical Axis Wind Turbines (VAWTs) may help support within the railway infrastructure system. By harnessing wind energy along the tracks, the aim is to reduce power dependency on the primary grid which is particularly relevant for the AALRT railway line, where energy reliability is a key challenge. By supplementing power from traditional sources with renewable wind energy, we aim to achieve better sustainability and operational efficiency. This assessment considers the subsystem loads such as signaling systems, emergency lighting, communication equipment, etc. The railway infrastructure comprises multiple high-priority loads essential for operational safety, communication, and station functionality. The report provides the required power capacity for each load to determine how much can feasibly be supported by energy harvested from the

WECS. *Table 3.1* shows some of the AALRT subsystem components, with their power requirements as collected from [111] and AALRT-Kality offices.

Table 3.1: Power requirements of the auxiliary loads of the AALRT railway line

Equipment	**Power requirement**
Axle counter	0.020 kW
Level Crossing	0.110 kW (220V 0.5A)
Signal interlocking	4.3976 kW
Signal power for crossing	0.25208 kW
Power for communication	0.7489 kW
Platform light and basement safety light	36W lamps
Substation Lighting	1.1408kW
Power Supply for Substation Service	1.6376kW
Point Machine(comm. Equipment)	380 - 400V

3.3.2 **Wind resource assessment**

Wind resource assessment is the rational and coordinated process of quantifying the wind power prospects of a specific site or region. It encompasses gathering and processing information on the condition of the wind to assess the viability of projects on wind energy. It is important because of the technical and economic feasibility of wind energy systems[112].

3.3.2.1 KPIs considered in wind resource assessment

The key performance indicators used in the wind resource assessment are measurable quantities that measure the success and viability of wind energy projects. Such indicators assist the stakeholders in evaluating the effectiveness of energy production, the economic feasibility of the site and its efficiency. Below are the primary KPIs:

a) Wind shear coefficient(α); this describes how wind speed changes with height above ground.

where: V_z = Wind speed at height Z
V_{ref} = Wind speed at reference height Z_{ref}
α = wind shear exponent

$$V_z = V_{ref}\left(\frac{Z}{Z_{ref}}\right)^{\alpha} \quad \textbf{3.1}$$

b) Cut-in and cut-out wind speeds. The cut-in speed is the lowest wind speed at which the turbine begins producing power, and the cut-out wind speed is the highest wind speed at which the turbine stops operating to ensure safety. When calculating wind power, the wind speed is the primary factor that affects how much electricity the wind turbine can generate. It is divided into three categories: cut-in, Vrated, and cut-out wind speed, where Avg is calculated as the average wind speed[113].

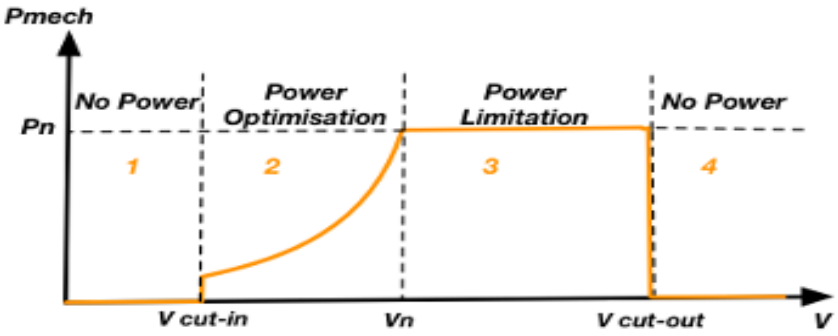

Figure 3.3: The ideal wind turbine power curve and its operating zones[3]

To calculate the cut-in, cut-out and rated-wind speed, the following equations are used as stated below[114]:

$$V_{cut-in} = 0.5V_{avg} \quad \textbf{3.2a}$$

$$V_{rated} = 1.5V_{avg} \quad \textbf{3.2b}$$

$$V_{cut-out} = 3.0V_{avg} \quad \textbf{3.2c}$$

Assuming that the wind speeds are equally divided over the 30 seconds when the train is passing a specific position.

$$Average\ wind\ speed = \frac{\sum_{i=1}^{n} V_i}{n} \quad \textbf{3.3}$$

Where $\sum_{i=1}^{n} V_i$ is the V_i is the sum of all the wind speed values, and n is the number of wind speed values.

$$Av.Wind\ speed(Train\ induced) = \frac{7.6 + 7.28 + 6.67 + 5.22 + 4.39 + 4.16 + 2.66}{7}$$

$$= 5.71m/s$$

Total r = time for one cycle = 690+30 = 720seconds

Total time for one cycle = 690 + 30 = 720 seconds

$$Weighted\ Average = \frac{\sum_{i=1}^{n}(w_i \,.\, x_i)}{\sum_{i=1}^{n} w_i} \quad \textbf{3.4}$$

Where n is the number of data points, w_i is the weight of the i-th data point, and x_i is the value of the i-th element.

Weighted average Wind speed $= \frac{(690\ X\ 2.66)+(30\ X\ 5.71)}{720} = 2.82$m/s

$$V_{cut-in} = 1.41m/s$$

$$V_{rated} = 4.23m/s$$

$$V_{cut-out} = 8.46m/s$$

c) Wind power density(W/m^2)

It measures the amount of power present within the area of the wind per unit. It depends on the formula below;

$$P = \frac{1}{2}\rho V^3 \quad \textbf{3.5}$$

Where: P = Wind power density, ρ= Air density, and V= wind speed

d) Capacity Factor (%); This is the proportion of actual energy produced compared to the maximum potential energy within a specified timeframe.

$$CF = \frac{Actual\ Energy\ Output}{Rated\ Energy\ Output} x\ 100 \quad \textbf{3.6}$$

Where:

CF = Capacity factor

AEO = Actual Energy Output

REO = Rated Energy Output

e) Turbulence Intensity (%); this represents wind speed fluctuations at the site.

$$Turbulence\ Intensity = \frac{\sigma}{V} \quad \textbf{3.7}$$

Where σ is the Standard deviation of wind speed and V is the mean wind speed

This wind resource assessment evaluates the potential wind speeds that can be captured by the VAWTs, considering both ambient wind conditions and the additional wind speed generated by train activity on the tracks along the Addis Ababa Light Rail route, emphasizing the elevated tracks. The assessment focuses on calculating the wind speed variation at the optimal VAWT location, taking into account two key factors: Ambient Wind Speed: The natural wind speed in the area without the influence of train activity, which is 2.47m/s average.

i. Train-induced Wind Speed: The additional wind speed generated when a train passes in this instance taking into consideration the double tracks at a distance of 1.350m with the presence of the train on both tracks creating ample space for the installation of a 0.125m rotor diameter, a clearance height of 0.25m and the height of the wind turbine being 3.75m hence a total wind turbine height of 4m from the ground on elevated track.

Wind measurements for the area show an average ambient wind speed of 2.47 m/s. The speed of the trains on the track is assumed to be 20 km/h (5.56 m/s). These values are used to determine the

resulting wind speed at the VAWT, assuming that the train is travelling in the same direction as the ambient wind.

a) Train Headway: Trains pass at intervals of 12 minutes travelling at an average speed of 20 km/h (5.56 m/s).
b) Track Configuration: The VAWT is placed between double tracks (with potential activity on both tracks). The wind speed will increase with train activity on either track.
c) Track Type: The Savonius wind turbine is located on an elevated section of the varying pier heights of 8.55m, 8.25m, 9.4m, 9.25m, 9.05m, 9.55m and 8.9m above the ground. The diameter is 0.125m, the height of the turbine is 25cm(0.25m), clearance of up to 3.75m, hence 4m from the ground to ensure that the turbines capture wind also above the height of the train (which is 3.65 meters). This also contributes to a greater height for wind capture at the different elevations stated above, i.e., 12.55m, 12.25m, 13.4m, 13.25m, 13.05m, 13.55m and 12.9m, respectively. The diameter is small to ensure adequate placement of the VAWT between the double tracks.

V_{ref} = 2.5 m/s at Z_{ref} = 10m

k_r = 0.24; shear coefficient (reference from the Ethiopian Building Code standard for loading[115])

The power law formula is:

$$V_z = V_{ref}\left(\frac{Z}{Z_{ref}}\right)^{k_r} \quad \textbf{3.8}$$

$$V_{12} \approx 2.61\text{m/s}$$

Table 3.2: Ambient Wind speed at varying elevation points across the railway track

Elevated track height(m)	Wind speed(m/s)
10	2.47
12	2.58
12.25	2.60
12.55	2.61
12.9	2.63
13.05	2.64
13.25	2.68
13.4	2.65
13.55	2.66

d) Circulation of wind around the Train.

When a train is in motion, it creates three separate flow zones along the track path. At the front, the train nose(inviscid) itself pushes air forward and outward as what is known as a bow compression wave, in which a high-pressure zone moves alongside the train nose, then a low-pressure zone follows after it[116]. Along the sides of the train, a boundary layer forms due to air viscosity, creating a strong velocity gradient between the train surface and the surrounding air. At the rear, the wake region comprises turbulent vortex flows, with a low-pressure zone near the train's tail transitioning to a high-pressure zone immediately behind it. These aerodynamic effects result from the train's interaction with the surrounding air and railway structures, producing varying airflow dynamics[117].

The airflow patterns caused by trains are influenced by the distance from the train, duration of its passage and the speed of the train. The highest velocities are observed adjacent to the train, with the velocity rapidly decreasing as distance from the train grows[118], and the velocity rapidly drops within 30 seconds to 1 minute. Observations indicate that at a height of 2.8 m from the train surface, the wind speeds are approximately 62% less than those at a height of 0.8 m[119]. The inverse square law explains this behaviour, as wind speed decreases with the square of the distance from the source due to the spreading of airflow over an increasing area[120]. Although the elevation does appear to have an impact on the train-induced wind speed, the results are by magnitude relatively small in comparison to the key parameters (train speed, distance from the train, and the train head/tail shape)After 10 feet the induced airflow stops rising so the induced airflow is significantly less at greater distances[121].

$$Ws \propto V^2 \qquad \textbf{3.9}$$

Where Ws is the wind speed and V is the train speed

The induced wind speed Ws is directly proportional to the square of the speed at which the train is running, and hence, the higher the running speed of the train, the stronger the airflow[120]. Other factors related to train-induced wind include the train's nose and tail shapes influencing the currents and other aerodynamic factors, and how the zones of airflow interfere with the environment [121].

These dynamics are important for the analysis of impacts/train-induced wind on structures, as well as for enhanced integration of railway networks.

e) Formula to estimate the induced winds from the moving trains.

The Federal Railroad Administration(FRA) -computed model shows that train-induced air flow decreases significantly beyond 10 feet as the airflow tends to plateau. The maximum wind velocity around an object near a train can be calculated using the equation[118], [121]

$$u = (1.2319)^{0.072v-4} x\,(0.4575d^2 - 3.5496d + 9.1545) \quad \textbf{3.10}$$

Where:

u = maximum wind velocity around a body/object near the train(mph)

v = train running speed(mph)

d = human-train distance (feet)

f) Calculation of Wind Speed with Train Activity

The total wind speed at the location is determined by adding the ambient wind speed and the train-induced wind speed. By utilizing the principle of superposition which states that [122], we can determine the wind speed experienced at a point near the train. This approach ensures that all contributing factors, such as the induced wind from the train and the existing ambient wind, are accounted for accurately. Recent studies have introduced momentum-conserving wake superposition methods that accurately predict wind turbine wake effects, which can be comparable to train induced winds[122]. It outlines the validity of combining induced and ambient wind speeds to derive a comprehensive understanding of the aerodynamic environment, which is crucial for safety assessments, design considerations, and operational strategies. The study [123] demonstrated that aerodynamic forces on vehicles encountering trains at different wind speeds can be obtained by superposing the aerodynamic variation caused by the moving train and the forces in its traveling state.

The principle of superposition calculation is as follows:

$$V_T = V_{train} + V_{amb} \quad \textbf{3.11}$$

Where V_T is the actual/total wind speed, V_{train} is the train-induced wind speed, and V_{amb} is the ambient wind speed.

By combining ambient wind speed with the induced wind speed from the train, this study seeks to offer a holistic perspective on the total wind conditions experienced in the vicinity of the train. This holistic understanding is crucial for accurately analyzing the effects of wind on various systems, from infrastructure to energy generation. Accounting for both ambient and induced wind speeds will lead to more accurate predictions of energy output. Understanding the total wind speed allows for optimization of turbine placement and operational strategies, ultimately enhancing energy capture.

Table 3.3: Train-induced wind speeds

Train distance from the VAWT(ft)	**Induced wind speed(m/s)**	**Combined wind speed(2.66m/s_13.55m) ambient wind speed(m/s)**
0.5	4.94	7.6
0.66	4.62	7.28
1	4	6.67
2	2.56	5.22
3	1.73	4.39
4	1.50	4.16

g) Factors determining the location of the wind turbine.

i. Train speed; when the train moves at high speeds, the wind speed increases as well.

ii. Train frequency; with many trains passing the location, the chances of harvesting high wind energy volumes also increase.

iii. Number of train tracks. Placing VAWTs between double tracks could allow for capturing wind from trains passing in both directions, potentially increasing energy output.

iv. Adequate space for the VAWT installation

v. Elevated and above-ground track, the higher the elevation from the ground, the greater the wind speed, the higher the electric power generated.

vi. Distance to stations to power up the auxiliary loads, hence reducing the dependence on the main grid

vii. Wind speed profile at the wind turbine location; The wind speed will fluctuate over time as the trains pass by. *Table 3.2* shows how the wind speed changes at different track elevation points based on train activity.

viii. Wind Resource for Energy Generation; The total energy available for capture relies on the wind speed that the turbine experiences at the moment of the train's passage.

By calculating the total wind speed at different times during train passage, the prospects of wind power production can be estimated. The use of VAWTs is promising as the turbines can harness wind energy even under fluctuating conditions caused by moving trains, making this an innovative solution for energy generation along railway tracks.

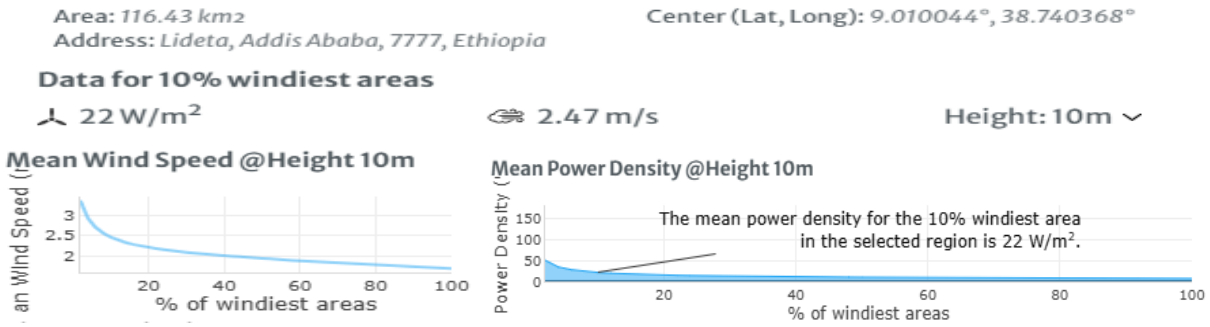

Figure 3.4: Wind information from the GWA of the selected region along AALRT route[124]

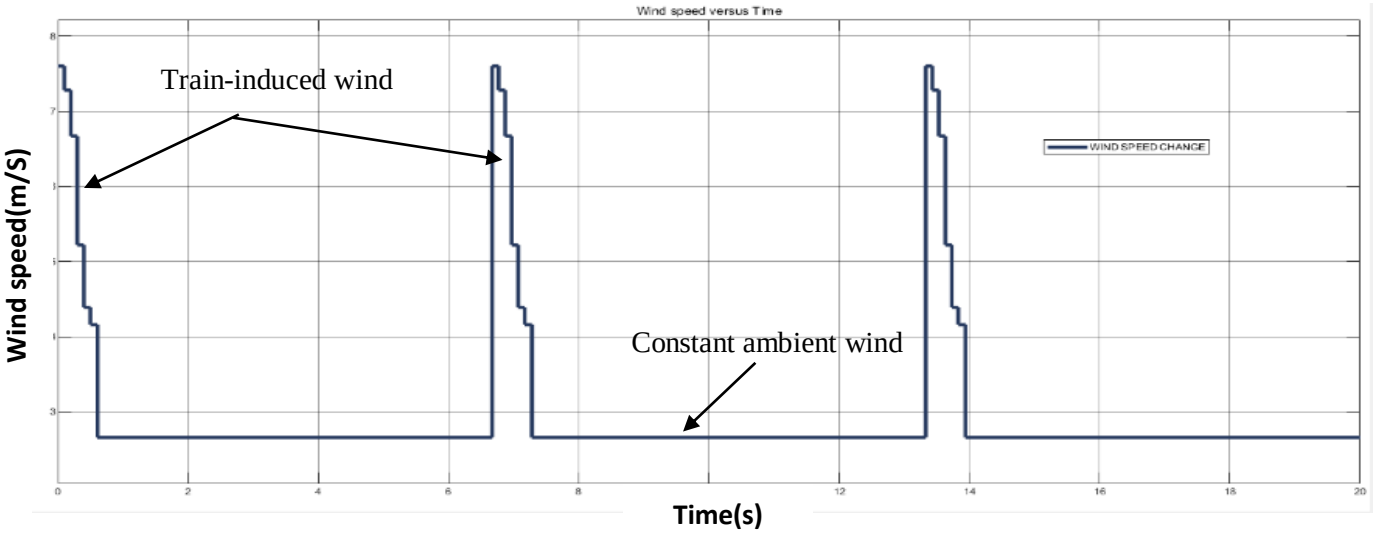

Figure 3.5: Variation of Wind Speed Over Time: Train-Induced Wind and Constant Ambient Wind

Considering double tracks (one track for each direction), there are 4 route sections at elevation along the AALRT railway line, i.e., from St.Lideta to Tegbared, Tegbared to Mexico, Mexico to Leghar and Leghar to Stadium. The Lideta common section is a 2.7 km section of the double-track north-south and east-west routes of the AALRT system. The common section that is elevated from Lideta to Stadium is divided into North-South(Menilik II square to Kality) and East-West(Ayat to Hailoch), the N-S routes have an average of 90 trips/day where 16 trips are dedicated to the common section whereas the E-W route has an average of 76 trips/day and 14 trips go through the common section daily making that a total of 30 trips hence an increase in the train frequency provides a greater chance for higher power generation from the VAWTs installed along this route.

The gathered data is divided into primary and secondary:-

Primary data

The primary data generated for this research was derived directly from the Simulink simulations, designed to model the WECS and the FLC control system within a light railway environment. They directly address the research objective of evaluating the FLC's performance in controlling the WECS under dynamic conditions, and thus constitute primary data central to the analysis and conclusions presented in this study."

1. Secondary data

Secondary data consists of the research findings from the validation paper, which provided the Savonius VAWT model turbine and the PMSG specifications, which served as one of the sources of secondary data. Furthermore, the wind speed information was sourced from the NMA, providing historical wind patterns and average wind speeds relevant to the region and data from the Global Wind Atlas(GWA) for the geographical area surrounding the AALRT. Finally, operational data from the AALRT Kality offices, which included train schedules and power consumption patterns used to inform the development of a realistic electrical load profile.

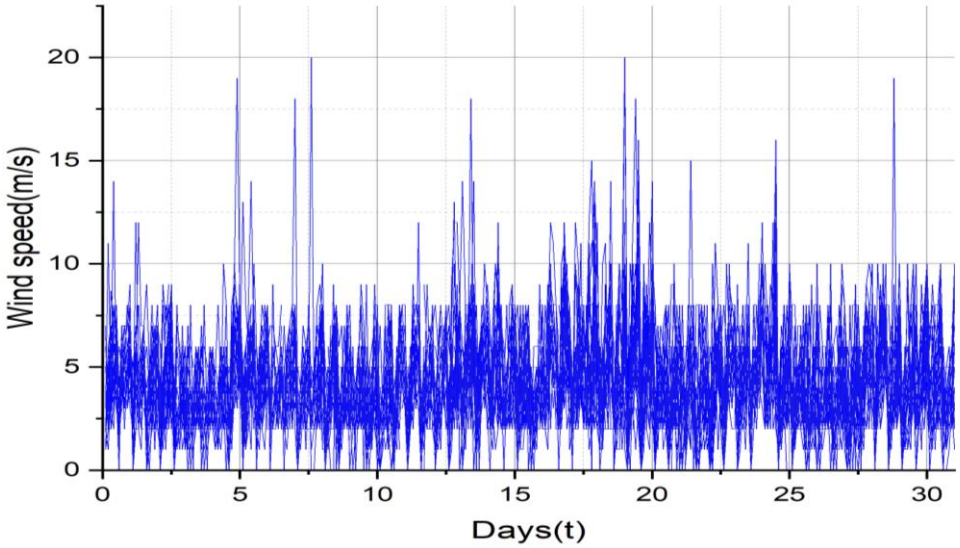

Figure 3.6: Yearly ambient wind speed data from National Meteorological Agency(NMA)

3.4 Model validation

The validation was based on the Savonius wind turbine specifications and generator parameters adopted from the previous study published in [107]. This study investigated small-scale wind energy systems using a P&O-MPPT method. This research controlled different parameters from the ones controlled in the validation paper which controlled the voltage output using current input and boost converter duty cycle whereas the controlled parameters in my research are pitch angle and TSR with an input of the rotor speed and power output for the FLC-MPPT because controlling these parameters enables the system to operate at a closer MPP under varying wind conditions. The range of the pitch angles used is 0^0 to 30^0 was chosen based on literature reviews on Savonius VAWT[108]. Savonius VAWTs typically operate at relatively low TSR values, and previous literature gave a good indication of the TSR value range, i.e. 0.2 to 1.1[109]. The rotor speed and power output were considered as the FLC inputs due to their ability to reflect the turbine's operating state under changes in wind conditions. The wind speed conditions used for validation were characterized as intermittent, with 10% of the time at 2 m/s and 5 m/s, and the remaining 5% of the time exceeding 8 m/s. The maximum power coefficient of 0.102 attained in the reference study[107]. [125]

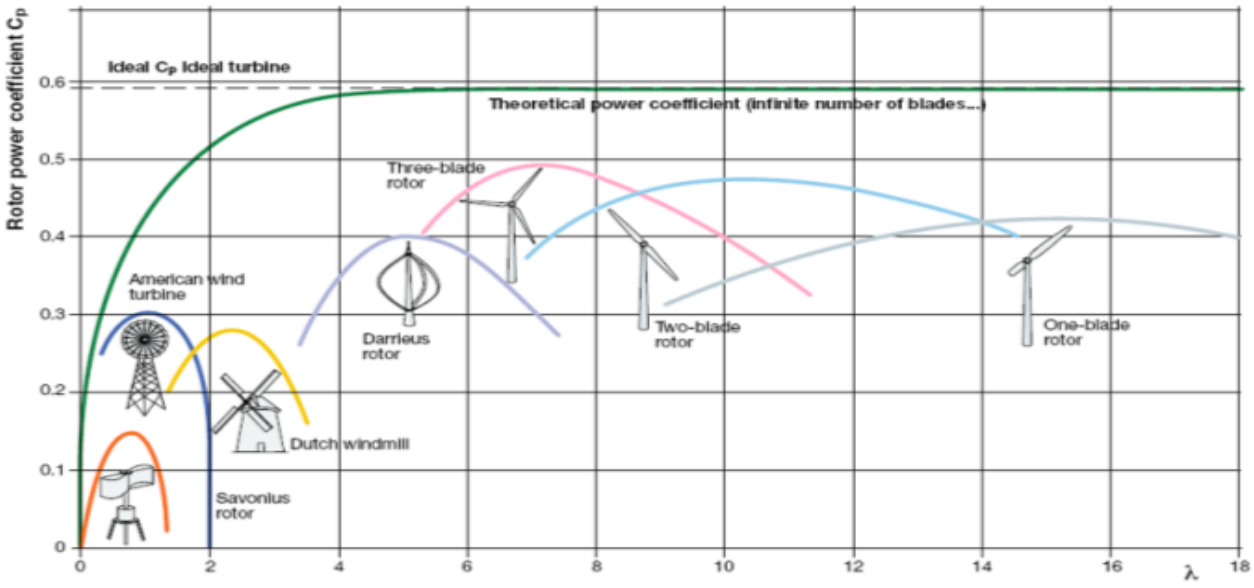

Figure 3.7: The wind turbine design power coefficients relative to the tip speed ratio [124]

3.5 Fuzzy logic control methodology framework

The fuzzy logic control system follows a systematic framework, as shown in *Figure 3.8*, which is an essential maximum power point tracking algorithm in wind energy harvesting systems. The FLC-MPPT is beneficial for environments that experience variable wind conditions because it adapts quickly to these conditions while maximizing power output.

A. Detect wind speed change; this triggers the FLC-MPPT algorithm only when necessary, preventing unnecessary processing and control actions during periods of stable wind speeds.
B. Measure rotor speed(ω) and Power output(P); if a wind speed is detected, the system measures the current rotor speed(ω) and power output(P) of the wind turbine. These measurements are the inputs to the FLC, and if no significant wind speed change is detected, the system maintains the current pitch angle and TSR of the wind turbine. This ensures stable operation during periods of constant wind speed. If MPP has not been reached, the system repeats the measurements and control process, starting with measuring the rotor speed and power output.

C. Detect wind speed change; this triggers the FLC-MPPT algorithm only when necessary, preventing unnecessary processing and control actions during periods of stable wind speeds.

D. Measure rotor speed(ω) and Power output(P); if a wind speed is detected, the system measures the current rotor speed(ω) and power output(P) of the wind turbine. These measurements are the inputs to the FLC, and if no significant wind speed change is detected, the system maintains the current pitch angle and TSR of the wind turbine. This ensures stable operation during periods of constant wind speed. If MPP has not been reached, the system repeats the measurements and control process, starting with measuring the rotor speed and power output.

E. Fuzzification; this stage converts the measured rotor speed(ω) and power input(P) into fuzzy sets. The fuzzy sets represent linguistic variables (e.g., low, medium, high) and allow the FLC to handle uncertainty and imprecise data.

F. Fuzzy rule evaluation(inference); this step applies the fuzzy rules defined in the FLC's rule base. The fuzzy rules determine the appropriate control actions based on the fuzzified inputs. This is where the intelligence of the FLC resides, as it mimics human-like decision-making based on Fuzzy logic.

G. Defuzzification: This step converts the fuzzy outputs from the rule evaluation into crisp (numerical) values. These crisp values represent the changes that need to be made to the pitch angle and Tip speed ratio.

H. Calculate Pitch and TSR; the system calculates the specific changes required to the pitch angle(β) and TSR(λ) based on the defuzzified outputs.

I. Update Pitch angle and TSR; The system adjusts the pitch angle and TSR of the wind turbine according to the calculated changes.

J. Monitor power output(P); The system continuously monitors the power output(P) to examine the performance of the control actions. Check if the maximum power point(MPP) is reached; this is another decision point where the system checks if the MPP has been reached. This could involve monitoring the rate of change of power output or comparing the current power output to a target value.

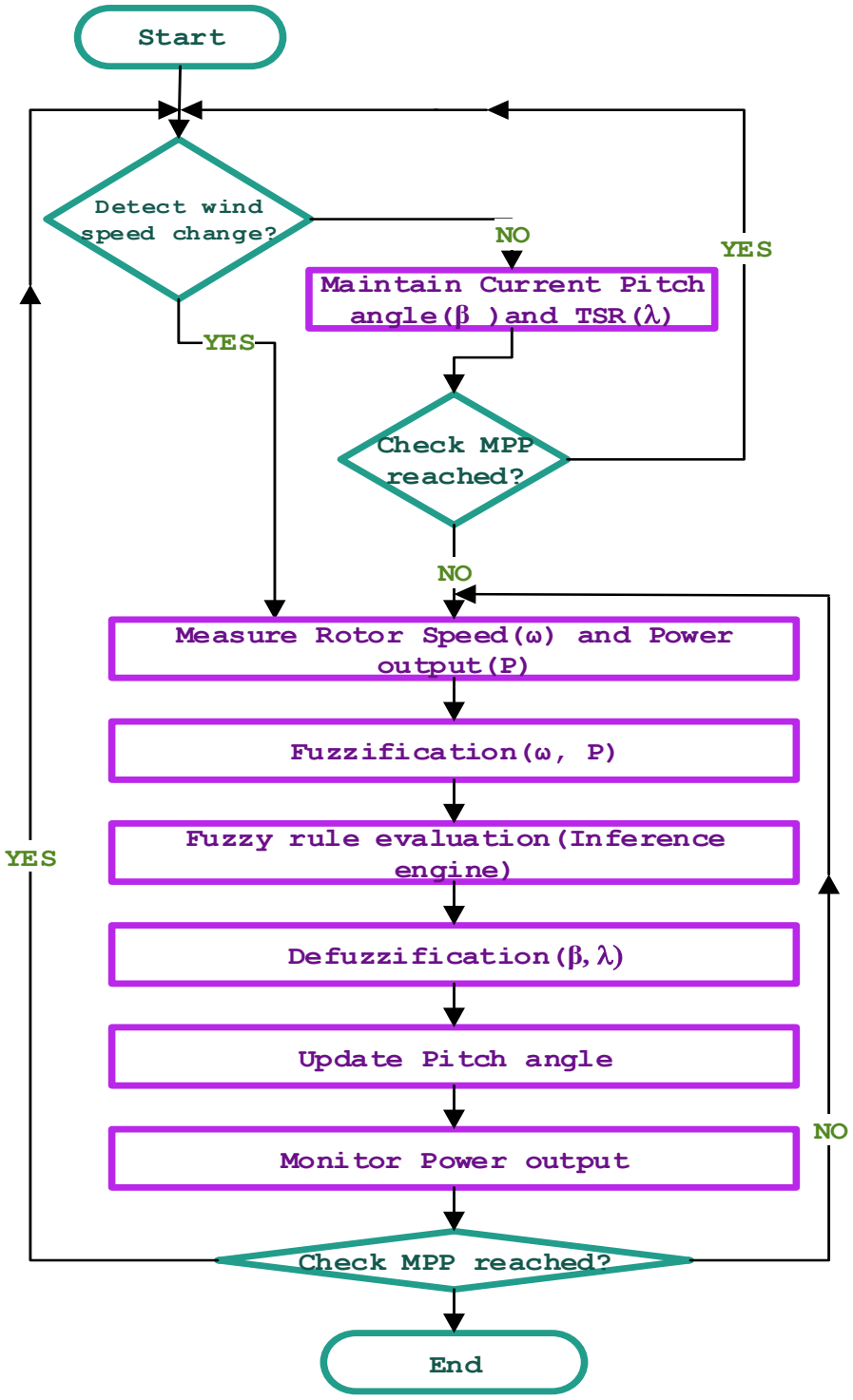

Figure 3.8: Fuzzy Logic Control MPPT methodology flow chart

Analytical models of the wind energy conversion system.

This system primarily comprises of the wind turbine designed to convert the wind kinetic energy from the wind into mechanical energy as illustrated in *Figure 3.9*. The turbine is equipped with a Permanent Magnet Synchronous Generator(PMSG) which converts the mechanical energy into AC electrical energy. This is then rectified to DC by the rectifier diode. The DC output is stepped up by the DC-DC boost converter to meet the specific demands of the connected load(see *Figure 3.11*). Additionally, the FLC is integrated into the system as show in *Figure 3.10* to optimize the wind energy conversion system. This is done by adjusting operational control parameters in real time based on fluctuating wind conditions and load requirements. This smart control mechanism enhances the overall reliability of the system, ensuring that the maximum amount of available wind energy is effectively optimized.

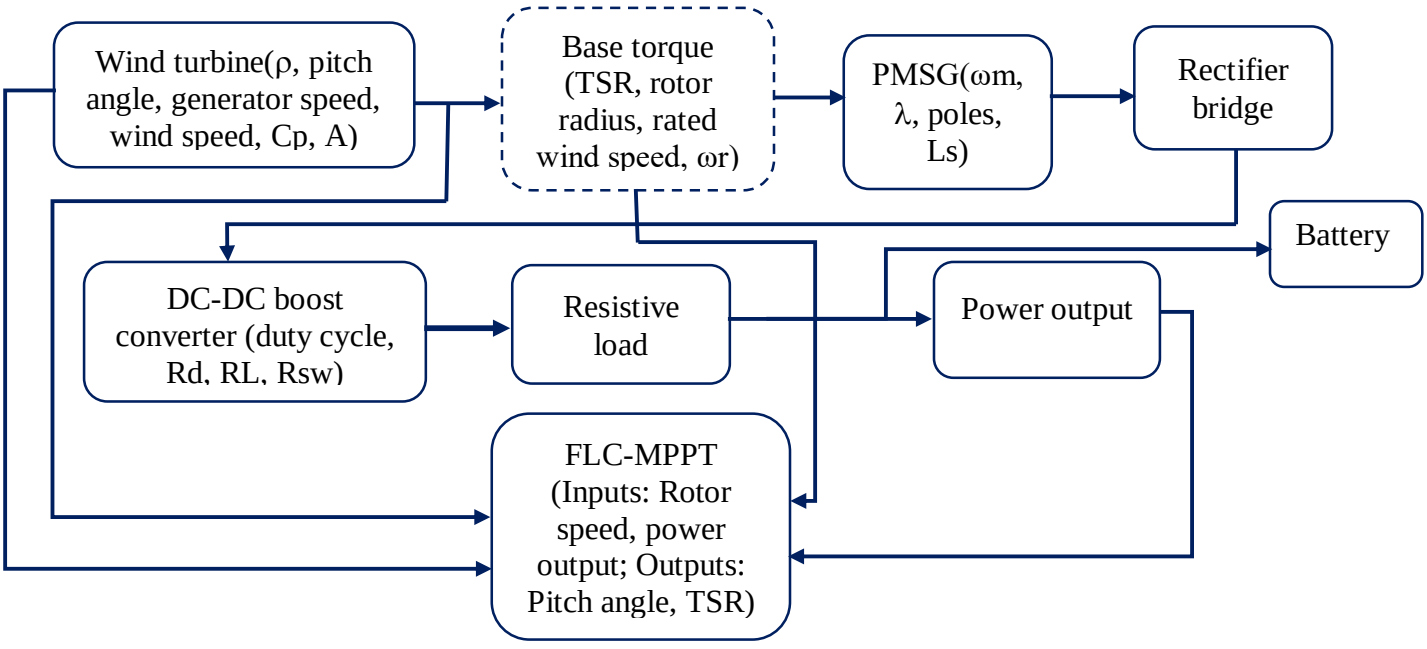

Figure 3.9: Block diagram of the wind energy conversion system

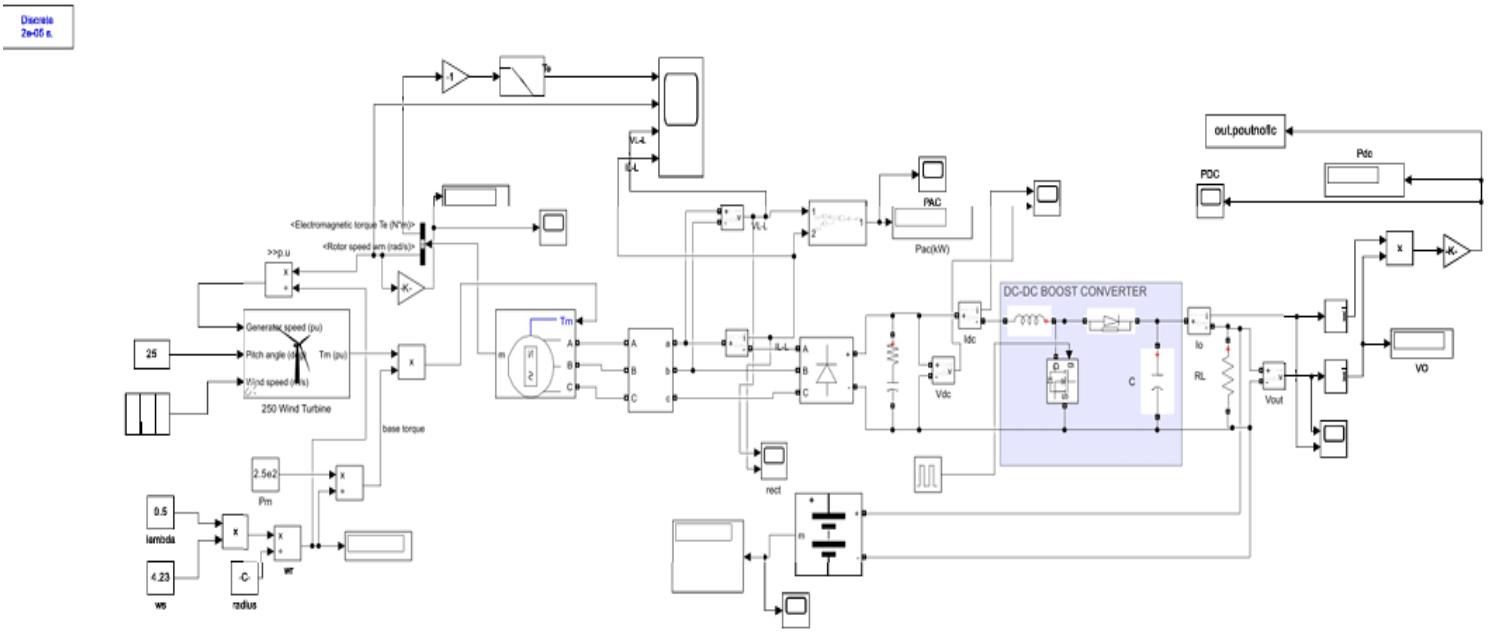

Figure 3.10: Analytical model of the WECS without MPPT

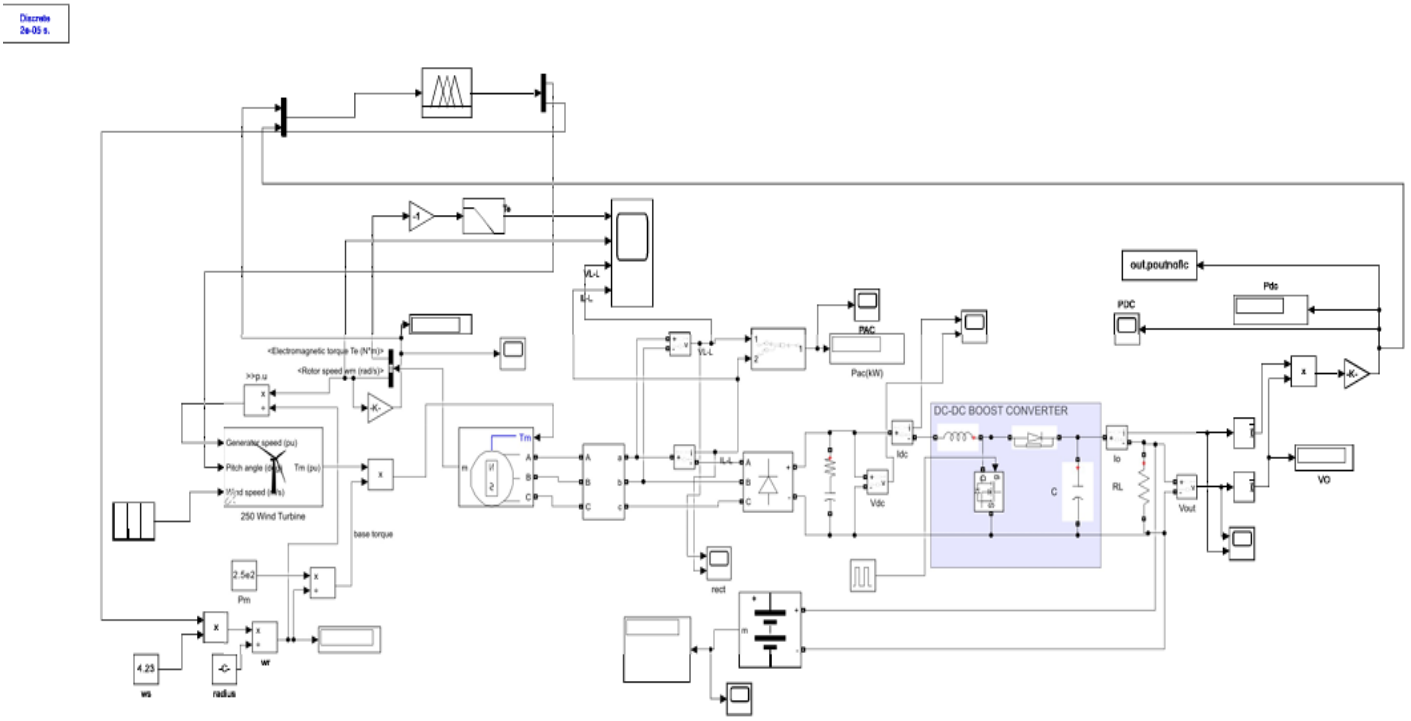

Figure 3.11: Analytical model of the WECS with MPPT

4 RESULTS AND DISCUSSION

This chapter shares the findings from the simulation and validation of the proposed Wind Energy Conversion System (WECS) for small-scale applications along the Addis Ababa Light Rail Transit (AALRT). The results are analyzed to evaluate the system's performance in terms of power generation and adaptability under varying wind conditions. Key insights are discussed, highlighting the effectiveness of the FLC-MPPT algorithm and the feasibility of integrating Savonius Vertical Axis Wind Turbines into urban railway infrastructure by installing them along railway tracks.

4.1 Wind energy conversion system without fuzzy logic control system

4.1.1 The power coefficient of the wind turbine

The power coefficient indicates a wind turbine's effectiveness in transforming the wind's kinetic energy into mechanical energy. It is noted that the power coefficient of a small-scale Savonius VAWT wind turbine ranges between 0.1 to 0.3 theoretically implying that the wind turbine can only convert between 20% to 30% of available wind to power[126][127], a high positive pitch angle is beneficial at lower TSRs and also improves performance at lower wind speeds this is to maximize the lift to maintain a high lift/drag ratio thereby enhancing blade torque efficiency[128], however in the simulation at TSR, $\lambda = 0.5$, and pitch angle 25^0 the maximum Cp attained is 0.1966 indicating that only 19.66% of the available wind is converted to power as represented in *Figure*

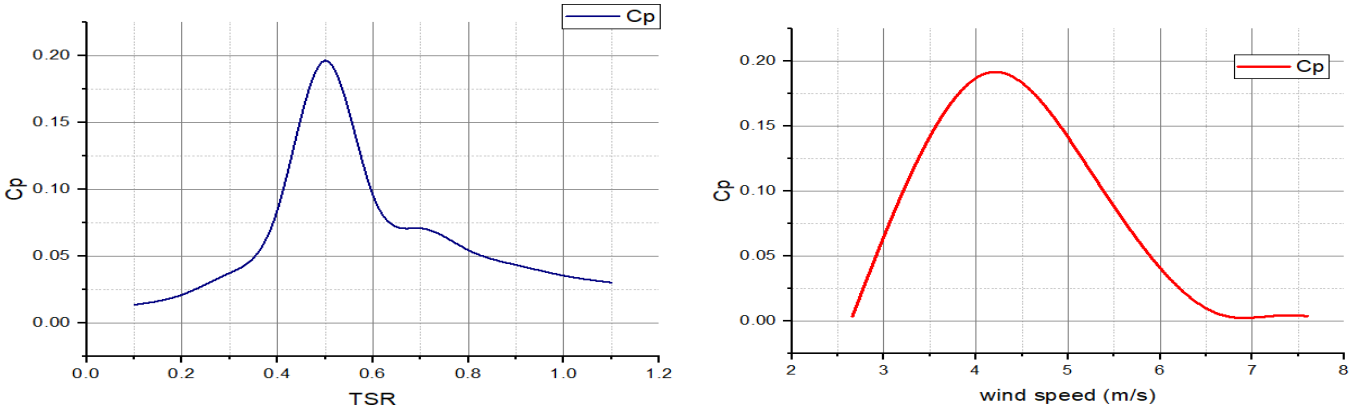

Figure 4.1: (a) Power coefficient(Cp) relative to Tip speed ratio(TSR) and (b) Power coefficient(Cp) versus the wind speed variation

4.1(a). It is also shown in *Figure 4.1(b)* that the power coefficient rises with increasing wind speed, peaking at a specific wind speed (around 4m/s in this case) before it gradually declines as wind speed continues to increase.

Figure 4.2 clearly shows how a small-scale Savonius WECS performs across various load resistances and wind speeds. The observed trends demonstrate a clear relationship between load and power output, highlighting that power generation initially increases with load resistance until reaching an optimal point after which it begins to decline. This behaviour underscores the importance of selecting an appropriate load to maximize energy capture from the available wind. The distinct curves for each wind speed indicate the turbine's enhanced capability to generate power under higher conditions, with maximum outputs significantly greater at speeds such as 7.6m/s compared to lower speeds like 2.66m/s. These findings reinforce the Savonius turbine's potential for effective generation in environments with variable and intermittent wind patterns, like alongside railway lines, particularly favouring low to moderate wind speeds.

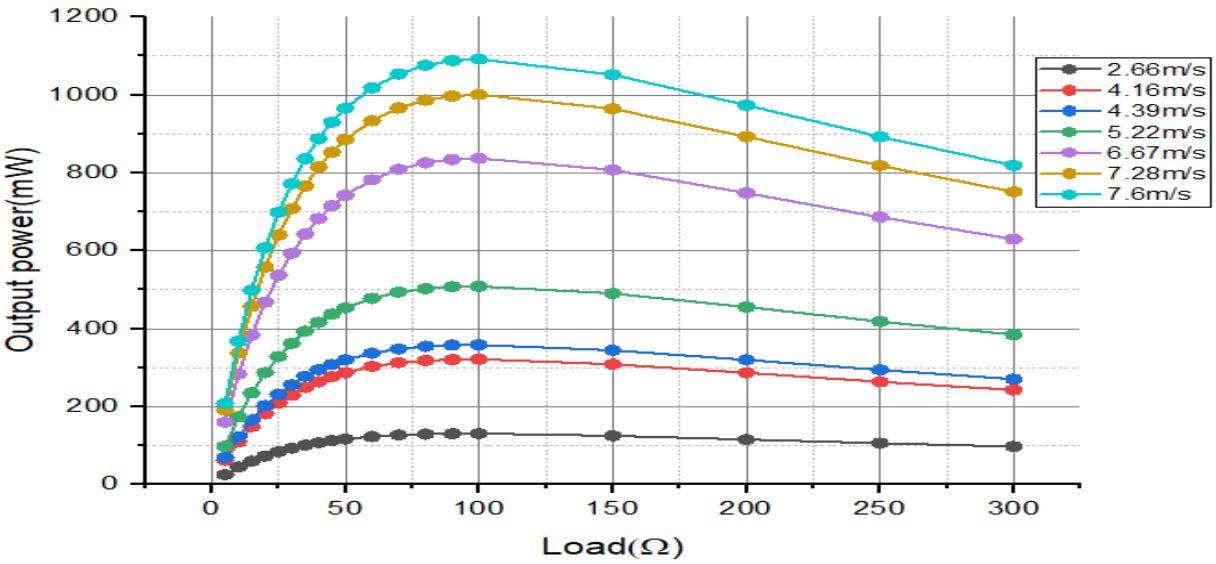

Figure 4.2: Power output as a function of resistive loads

Figure 4.3 illustrates the output power relationship regarding the output voltage for a small-scale Savonius WECS, effectively demonstrating the turbine's effectiveness across different wind speeds. The graph clearly shows that as wind speed increases, electrical power significantly increases. This aligns with how Savonius wind turbines are expected to behave as they efficiently capture energy when wind speeds are low to moderate. Notably, the rapid increase in output power

at lower voltages suggests that the turbine operates optimally within these conditions, making it ideal for environments where the most power is generated before reaching a plateau.

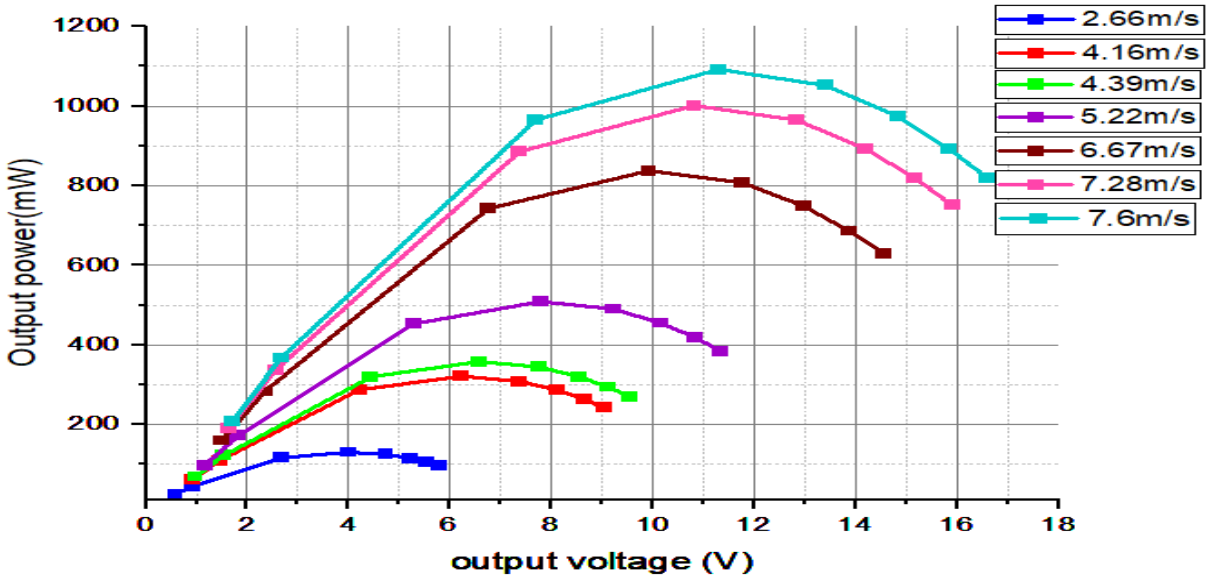

Figure 4.3: Output power as a function of output voltage

4.1.2 **DC-DC boost converter**

When the load resistance is low, the load requires more current. If the current demand exceeds the converter's ability to supply power, the output voltage can drop below the input voltage. A higher load resistance leads to a greater need for current. In this case, the boost converter operates more efficiently, allowing it to increase the output voltage above the input voltage. This behaviour is expected as the converter is designed to boost voltage under normal operating conditions. *Figure 4.4* illustrates how the efficiency of the DC-DC boost converter varies with output voltage across different wind speeds, which is determined by the converter's power output relative to its power input. From the simulations, it is noted that for lower wind speeds (e.g., 2.66 m/s and 4.16 m/s), the efficiency starts relatively high but tends to drop off significantly as the output voltage increases. This suggests that, at lower wind speeds, the system might not be generating enough power to maintain high efficiency at higher output voltages. As wind speed increases, the efficiency curves generally rise, indicating that the converter performs better with higher input power, achieving efficiencies above 90% in many cases.

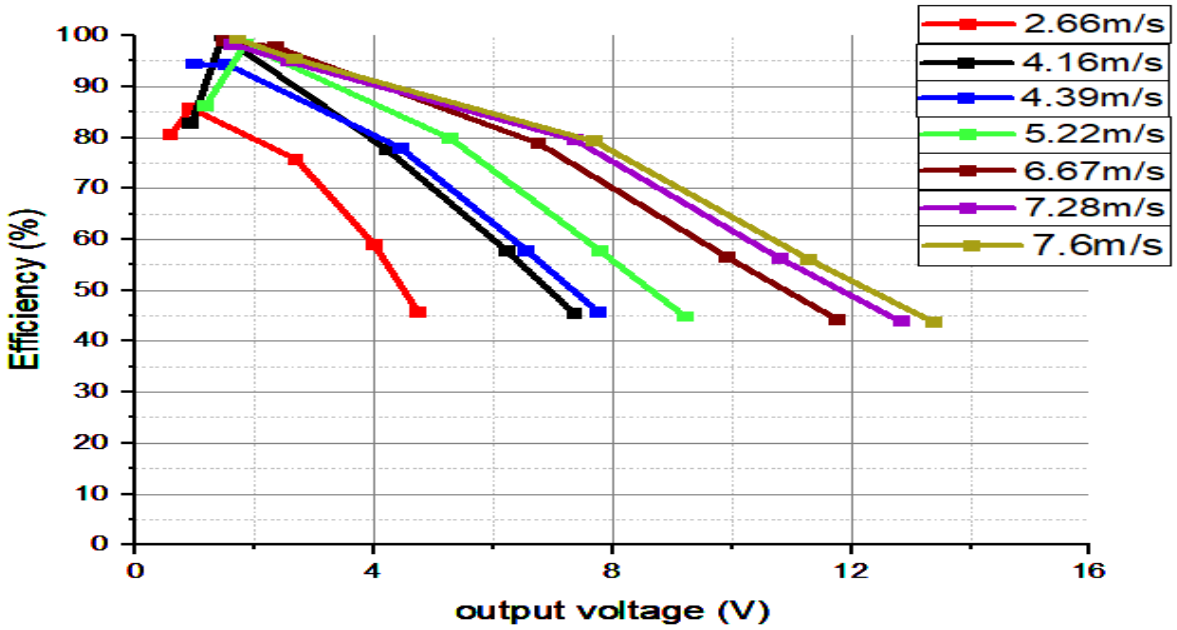

Figure 4.4: Efficiency of the DC-DC boost converter

The peak efficiency occurs at specific voltage levels, typically between 1V to 3V, depending on the wind speed. Beyond this range, the efficiency begins to decline, likely due to increased losses from switching, conduction, and other inherent inefficiencies in the circuit components. The curves demonstrate that the boost converter's performance depends on the input power supplied by the wind turbine. As wind speed increases, more power becomes available, allowing the converter to operate more efficiently.

4.1.3 **Battery connection**

In Wind Energy Conversion Systems, battery connection is very crucial especially while dealing with railway subsystems. The batteries store energy generated by the wind energy harvesting system. Some of the batteries employed in previous studies involving the feasibility of small-scale WECS are Lithium-ion, Nickel Metal Hydride, and Nickel Cadmium among others, due to their various advantages. From the simulation of WECS without FLC implementation as summarized in Table 4.1, it was noted that at pitch angles (0^0 – 15^0), at low wind speeds($\leq$5.22m/s), the battery remains discharging across all wind speeds due to insufficient turbine power output. At Pitch angle (20^0), the battery begins charging only at higher wind speeds($\geq$6.67m/s), indicating that turbine power output becomes sufficient to overcome losses. At pitch angle (25^0), the WECS demonstrates optimal performance with effective charging across all wind speeds. At high wind speeds(7.22m/s-

7.6m/s), the SOC reaches its peak value of 61%, suggesting maximum energy capture and storage efficiency. While at the pitch angles (>25^0), wind speeds show a drop in SOC, indicating inefficiencies in turbine power output at excessively high pitch angles. These results highlight that a pitch angle of 25^0 is optimal for maximizing energy capture and storage for this WECS configuration. A dynamic pitch control system implemented adjusts the blade's angles in real-time wind conditions to optimize battery charging rates.

Table 4.1: Impact of pitch angle and wind speed on battery state of Charge (SOC)

Pitch angle (degree)	**Low wind speeds**	**High wind speed**	**Optimal range**
0	Discharging	Discharging	Never changes
15	Discharging	Discharging	Never changes
20	Discharging	Charging	Charges only at WS ≥ 6.67m/s
25	Charging	Charging	Charges at all WS
30	Charging	Charging	Inefficient at high WS

The graph shown in *Figure 4.5* illustrates the impact of wind turbine pitch angle(β) on the state of charge (SOC) at varying wind speeds. Given an initial SOC of 50%, hence below 50% shows a discharging cycle and above 50 indicates a charging cycle of the battery. Pitch angles > 15^0 are at 49.99%, indicating a discharge at all wind speeds. Pitch angles ≤ 20^0, the SOC begins to increase significantly for wind speeds ≥ 6.67m/s. For lower wind speeds ≤ 5.22m/s, show discharging cycles until the pitch angle is 25^0 after which all wind speeds show effective battery charging indicating a higher turbine power output. The peak SOC generally occurs around a pitch angle of 25^0 for the high wind speeds, with the highest wind speed at 7.6m/s achieving the maximum SOC at approximately 61%. However, beyond 25^0, some wind speeds show a drop in SOC, suggesting an optimal pitch range for maximizing energy capture and storage for this WECS configuration.

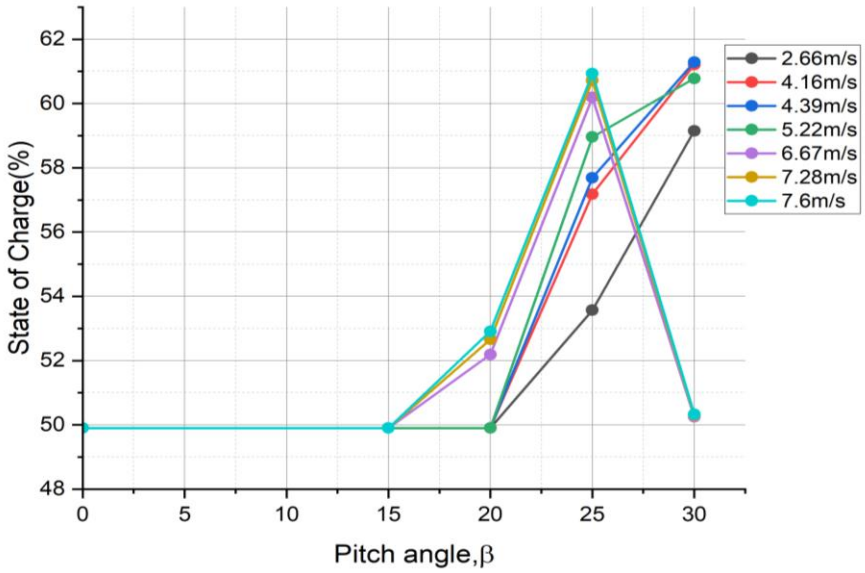

Figure 4.5: Relationship between SOC and Pitch angle

The graph *Figure 4.6* illustrates how adjusting the pitch angle affects the power flow into or out of a battery at different wind speeds. Negative battery current indicates charging while positive indicates discharging therefore we use the fundamental equation P = V*I to obtain the battery power. At 0^0 to 15^0 pitch angles, the battery discharges across all wind speeds. However, as the pitch angle increases, the battery starts charging. For lower wind speeds, the battery initially discharges slightly before charging at higher pitch angles (25^0 – 30^0). In contrast, higher wind speeds lead to significant battery charging with increasing pitch angles, generally peaking at 25^0. Beyond this optimal pitch for higher winds, the charging rate decreases, suggesting that for each wind speed, there is an ideal pitch angle that maximizes the power directed into the battery for charging. The graph highlights the potential for a pitch control system to dynamically adjust the blade angle based on the current wind speed to optimize the battery's charging rate in the WECS for the AALRT subsystem.

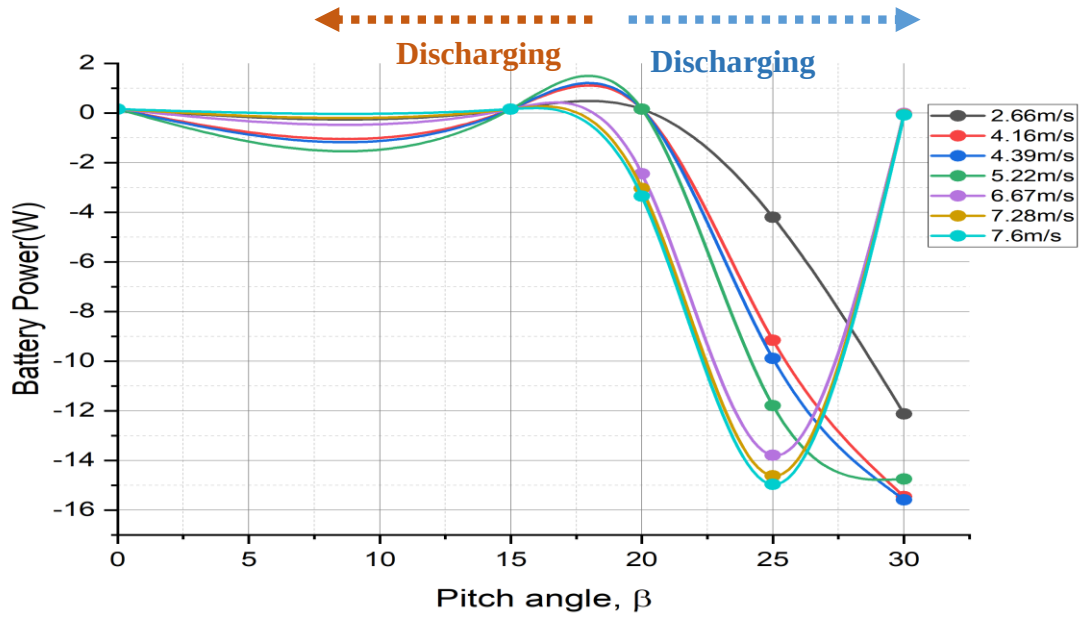

Figure 4.6: Battery power as a function of wind turbine pitch angle and wind speed

Figure 4.7 Illustrates the power generated by the turbine(in watts) about the wind turbine's pitch angle(β) at different wind speeds. At a pitch angle of 0^0, the turbine power output is close to zero across all wind speeds, indicating a near-idle state with minimal power exchange. As the pitch angle increases, the power output begins to increase significantly based on the wind speed.

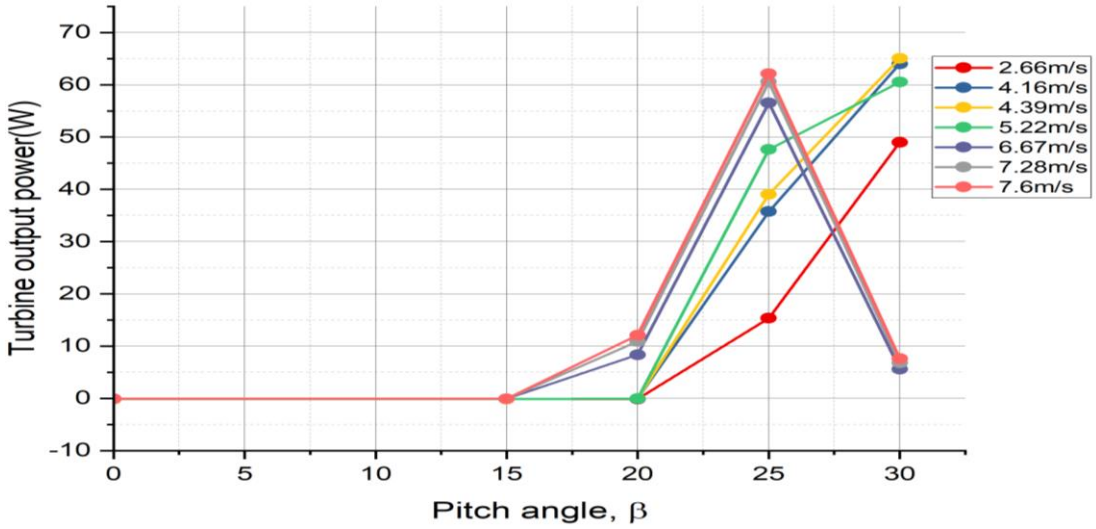

Figure 4.7: Turbine power output as a function of pitch angle

4.1.3.1 Comparative analysis between the Lithium-ion battery, Nickel-Metal Hydride battery and Nickel-cadmium battery.

This analysis is based on simulated data under the same wind speeds, TSR (0.5) and pitch angle (25^0) focusing on the State of Charge(SOC), current and voltage characteristics.

Table 4.2: Battery charge efficiency

Battery model	**SOC@2.66m/s(%)**	**SOC@7.6m/s(%)**	**ΔSOC(%)**
Li-ion (3.7V nominal, 2.3Ah capacity)	53.6	60.9	+7.3
NiCd (3.6V nominal(3S), 2.3Ah capacity)	53.1	59.6	+6.5
NiMH(3.6V nominal(3S), 2.3Ah capacity)	53.3	60.1	+6.8

Li-ion achieves the highest SOC gain due to higher charge efficiency (95% vs 80% for NiCd/NiMH). NiMH slightly outperforms NiCd, attributed to its absence of memory effect, also noting that there is consistency with empirical studies, i.e., Li-ion stores energy more efficiently per watt hour.

Table 4.3: Voltage and Current characteristics of the batteries

Battery	**Voltage range (V)**	**Charging Current range (A)**
Li-ion	4.24 – 4.84	0.99 to 3.09
NiCd	4.38 – 5.37	0.99 to 3.08
NiMH	4.43 – 5.36	0.99 to 3.08

NiCd/NiMH exhibits wider voltage fluctuations peaking at ~5.4V which exceeds safe limits in real systems. The expected values are NiCd ≤ 4.65V, NiMH ≤ 4.50V (for 3S configuration) and the result of the deviation in the results could result from the fact that Simulink's model may not enforce voltage damping hence a need to integrate a charge controller to damp voltages at safe limits. The Li-ion remains within stable limits of 4.24 – 4.84V reflecting its flat discharge curve. *Table 4.4* shows the comparison between the three batteries i.e. Li-ion, NiMH and NiCd batteries.

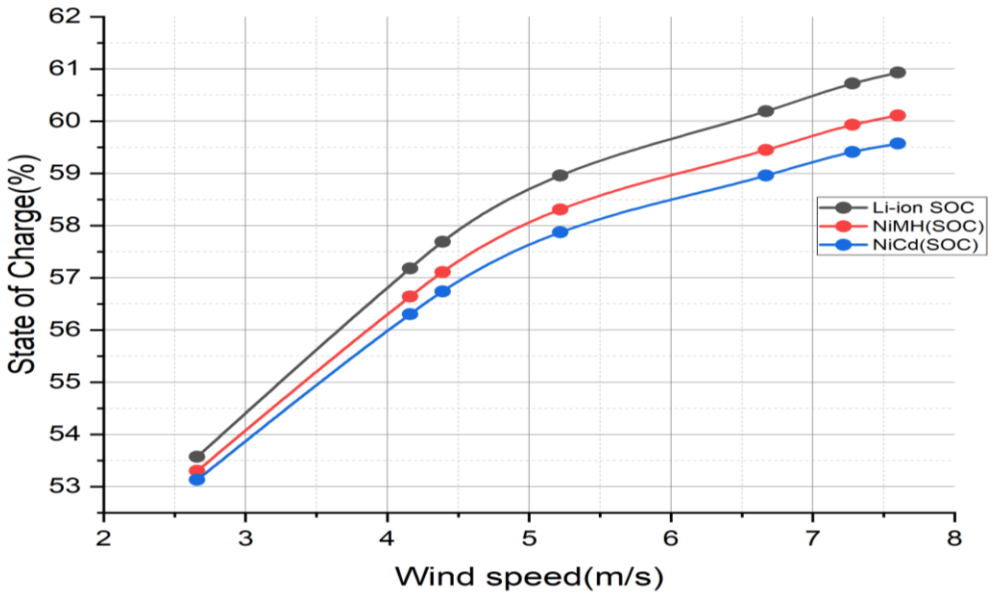

Figure 4.8: Comparative analysis of the state of Charge of Li-ion, NiCd and NiMH batteries at varying wind speeds

Table 4.4: Function distinctions between the Li-ion, NiMH and NiCd batteries[129]

Li-ion battery	NiMH	NiCd
▪ Function through the movement of lithium ions between electrodes. ▪ During discharge: Li+ ions flow from the negative electrodes (anode to the cathode. ▪ During charging, the process reverses ▪ No physical charge in electrodes ▪ Typical cell voltage: 3.6V-3.7V ▪ No memory effect ▪ Self-discharge rate (2-3%) ▪ Requires precise voltage control	▪ Function through hydrogen absorption/desorption reactions. ▪ Positive electrode contains Nickel oxide hydroxide. ▪ Negative electrode contains hydrogen-absorbing metal alloy. ▪ During discharge, Metal hydride releases hydrogen ions that combine with hydroxide ▪ Typical Cell voltage: 1.2V ▪ Minimal memory effect ▪ Self-discharge rate (15-30%) ▪ Uses delta-V or temp detection to terminate charging ▪ It provides a good balance of cost, performance and environmental considerations for small-scale WECS.	▪ Similar chemistry to NiMH but uses cadmium at the negative electrodes ▪ During discharge, the cadmium oxidizes to cadmium hydroxide ▪ Typical cell voltage is 1.2V ▪ Significant memory effect ▪ Self-discharge rate (10-20%) ▪ More tolerant of overcharging

4.2 Optimization of the WECS with fuzzy logic control-MPPT

The FLC-MPPT in this research is a Mamdani-type fuzzy inference system designed with two inputs and two outputs managed by a rule base of 20 fuzzy rules. The inputs of the FLC include RS (Rotor speed) and PO (Output power). 'RS' is fuzzified into four membership functions: 'VL' (very low), 'L'(Low), 'M'(Medium) and 'H'(High) using trapezoidal and triangular membership functions. The input 'PO' is fuzzified into five membership functions: 'VL' (Very Low), 'L'(Low), 'M'(Medium), 'H'(High) and 'VH' (Very High), also using trapezoidal and triangular membership functions. The fuzzy inference employs the 'min' operator for the AND method, 'max' for the OR method, 'min' for the implication method and 'max' for the aggregation method. Finally, the defuzzification process, which converts the fuzzy outputs into crisp control signals, uses the 'centroid' method. This FLC system dynamically adjusts two output variables i.e., 'PA' (Pitch angle) and the 'TSR'(Tip Speed Ratio) based on fuzzy rules consisting of IF-THEN statements that define how the system should respond to different input combinations aiming to optimize energy capture by the wind turbine across varying operating condition. The rules make certain that the turbine runs near its optimal Tip speed ratio. It is observed that there is better performance and higher output at low wind speeds after implementing an FLC-MPPT in the WECS.

4.2.1 Performance enhancements with FLC-MPPT

As observed in *Figure 4.9,* there is optimised electricity generation during low wind conditions, i.e., the FLC-MPPT is effectively optimising the turbine's operation at lower wind speeds, allowing it to extract additional energy from the wind compared to the non-FLC system. The possible mechanisms include intelligent adjustment to blade pitch to maximise the lift-to-drag ratio and real-time tracking of the optimal TSR for efficient power conversion. It is also noted that there is the highest power output across different wind speeds, i.e., the FLC-MPPT WECS delivers significantly higher power output at all wind speeds, demonstrating superior energy extraction. The controller's adaptive logic ensures stable operation even under fluctuating wind conditions, making it ideal for railway-side WEHS installations where wind patterns are intermittent. The fuzzy logic control system may be better suited to adapt to the variable conditions present at lower wind speeds, allowing for more efficient power extraction.

Figure 4.9 illustrates the impact of implementing Fuzzy Logic Controller MPPT on the power output of the small-scale Savonius WECS at different wind speeds. With FLC-MPPT, the power output is significantly higher across all wind speeds compared to the system without FLC-MPPT. This demonstrates the effectiveness of FLC-MPPT in optimising power extraction from the wind, leading to improved efficiency and better utilisation of wind energy. The consistent increase in power output with FLC-MPPT highlights its capability to adjust to fluctuating wind conditions and maintain optimal performance, making it a valuable enhancement for small-scale wind energy systems. The increased power output with the FLC-MPPT is supported by the study [130] which achieved efficiencies greater than 90% with the implementation of the FLC-MPPT.

4.2.2 **Dynamic pitch angle and TSR control**

In Figure 4.10, Plot (a) shows that the pitch angle stabilises at 30^0 for the ambient wind speed and at lesser degrees for the higher wind speeds due to the train activity working closely to the pitch angle before FLC-MPPT implementation. The FLC proactively decreases the pitch angle during these higher wind speed events, a typical strategy to maximise power extraction by optimizing the pitch angle relative to increased wind speed. (Plot b) shows that the TSR, which is a crucial parameter for WECS efficiency, stabilizes at around 0.45. This initial rise corresponds to the turbine accelerating under the influence of the wind. The TSR remains relatively stable at this value for the majority of the simulation, suggesting the FLC is effectively maintaining a near-optimal TSR for the ambient wind speed. The graphs demonstrate the FLC's ability to dynamically adjust the pitch angle according to variations in wind speed caused by train movements, aiming to optimize energy capture. The relatively stable TSR indicates that the FLC is also working to maintain efficient operation by managing the correlation between the rotor speed and the wind speed, even during transient wind events. The FLC's proactive reduction of pitch angle during wind spikes and its subsequent return to a steady state highlight its adaptive control strategy for maximizing power extraction under the combined influence of ambient and train-induced wind.

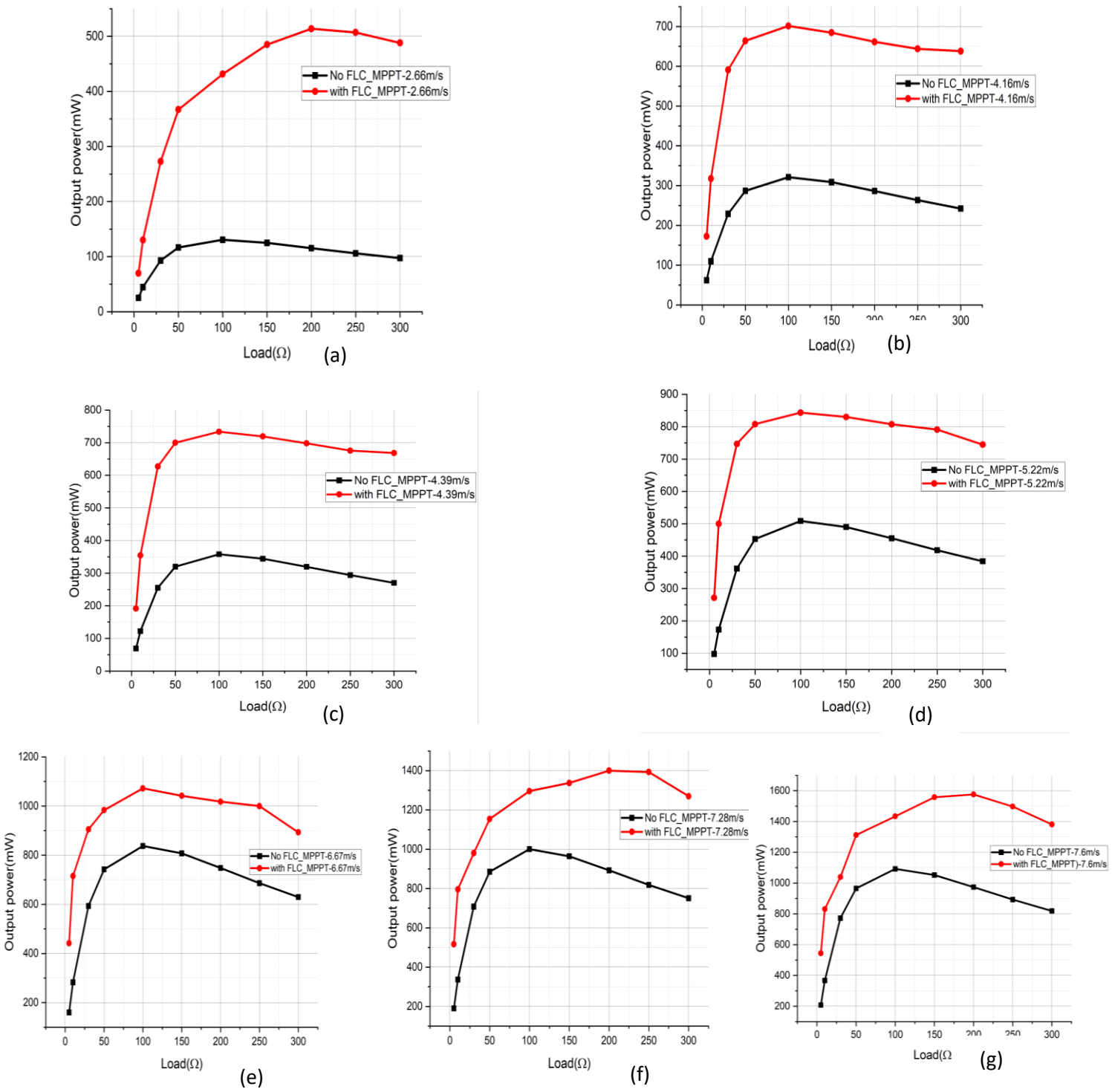

Figure 4.9: Output power as a function of the resistive loads at the different wind speeds comparing FLC-MPPT system(red) against operation without FLC-MPPT(black), (a) 2.66m/s, (b) 4.16m/s, (c) 4.39m/s, (d) 5.22m/s, (e) 6.67m/s, (f) 7.28m/s and (g) 7.6m/s

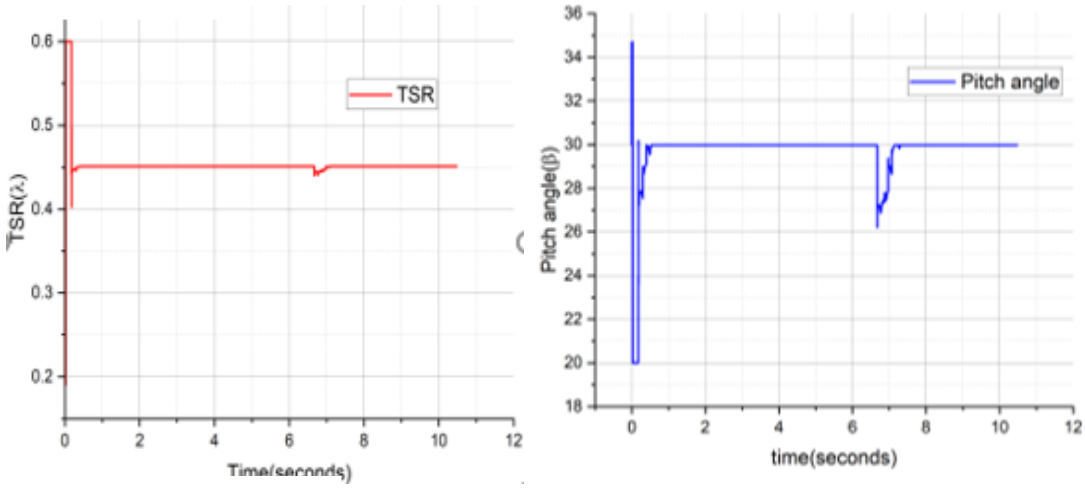

(a) (b)

Figure 4.10: (a) Tip Speed Ration(TSR) profile under the FLC and (b) Pitch angle adjustments controlled by FLC-MPPT

4.2.3 **FLC-MPPT behaviour after battery integration using the Lithium-ion battery.**

The comparison in *Figure 4.11* reveals the effect of battery implementation on the output power delivery characteristics of the FLC-MPPT system. Before battery implementation (a), the power output directly follows the intermittent nature of the wind, with high peaks during gusts and a low baseline during ambient wind. This suggests that the load experiences significant fluctuations in power availability. After battery implementation (b), the power output delivered to the load is more stable and generally higher during the periods between wind gusts. This indicates that the battery is acting as a buffer, smoothing out the power supply by discharging stored energy during periods of lower instantaneous power generation. In essence, the battery implementation, in conjunction with the FLC-MPPT, improves the reliability and stability of the WECS by storing excess energy and releasing it to provide additional power during periods of lower production. This leads to a more consistent and potentially higher average power delivery to the load.

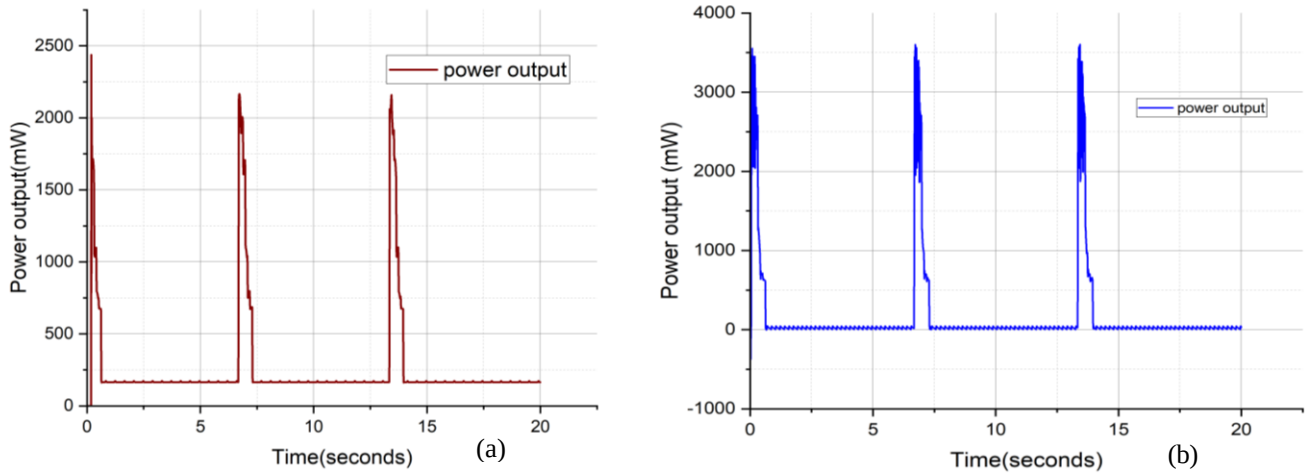

Figure 4.11: (a) Power output of the FLC-MPPT system @ before battery implementation and (b) after battery implementation

4.3 Model validation

One of the major objectives of this study is to validate the numerical methods. This was achieved by adopting a Savonius wind turbine system previously published in [107], where the design specifications of the Savonius rotor and generator parameters were also taken from, which investigated small-scale wind energy for monitoring systems using P&O-MPPT. In their study, the wind speed is intermittent, with 10% of the time at 5 m/s and 2 m/s, and the remaining 5% of the time, the wind speed is more than 8 m/s and the maximum power coefficient (Cp) achieved is 0.102. The design specifications used for the Savonius VAWT system, adopted from [107], are summarized in *Table 4.5*.

The validation of the WECS model and the FLC-MPPT system was approached through a combination of methods, focusing on comparing the simulation results with established theoretical principles, published literature, and the experimental results presented in [107]. This comparison aims to establish the credibility and accuracy of the constructed model. The power output characteristics of the simulated Savonius VAWT were compared against theoretical power curves derived from the Betz limit and generalized performance curves for similar VAWT designs. This comparison ensured that the model accurately reflects the fundamental correlation between wind speed and the achievable output power of a Savonius turbine. The simulated graphs/plots were

also compared to the experimental power curves presented in *Figure 8[107]* which show the relationship of the power coefficient relative to wind speed showing that the savonius attained a Cp of 0.102 and *figure 9 [107]* shows the output power as a function of the resistive loads. While the specific control parameters of P&O MPPT in their experiment differ from this study, the general trend and shape of the power curves were compared to ensure that the Simulink model exhibits a similar response to changes in wind speed. This comparison focused on matching the overall behaviour and trends observed in the experimental data, as suggested by the referred article, rather than achieving a perfect numerical match. For example, the overall pattern of power rising with wind speed and the presence of a peak power point were evaluated against the experimental curves. The Simulink model's ability to replicate this fundamental behaviour, as seen in *Figure 4.2* where power increases with wind speed, supports its validity in representing the Savonius VAWT's response to wind. The Permanent Magnet Synchronous Generator (PMSG) model's performance was also adopted as described in Table 1 of [107]. The electrical components of the system design, including the DC-DC boost converter, Schottky diode, capacitor, MOSFET switches, and load, were validated by ensuring that they adhere to fundamental circuit laws and power flow principles. The component specifications from *Table 4.5* were used to model these components. The Simulink model's representation of the electrical system, the model's ability to represent power flow from the generator to the load, with and without battery implementation (as shown in *Figure 4.11*), was compared to the general principles of power transfer in electrical circuits. The behaviour of the DC-DC boost converter is validated by comparing its input-output voltage and current relationships to *Figure 12* provided in the referred paper[107]. The FLC-MPPT system focused on assessing its ability to effectively track the MPP in differing wind speeds, and comparing its performance characteristics to the general behaviour of MPPT controllers, for instance, the P&O algorithm used in [107]. The power output achieved by the FLC-MPPT system was compared against the theoretical maximum power curves for the simulated Savonius VAWT. This comparison assessed the FLC-MPPT's efficiency in extracting the highest power across different wind speeds. The closeness of simulated power output relative to theoretical maximum indicated the FLC-MPPT's effectiveness. The improvement in power output with FLC-MPPT, as shown in *Figure 4.9*, demonstrates the FLC-MPPT's ability to approach the MPP.

Table 4.5: Specifications of the WECS using the Savonius VAWT turbine

Parameters	**Specifications**
Blade radius(r)	0.065m
Blade diameter(d)	0.125m
Pitch angle range	0 to 30^0
Height	25cm
Blades	2
Mechanical power	250 Watts
Wind speed range	2.66m/s to 7.6m/s
Optimum TSR range	0.5 to 1
Cut in wind speed	1.41m/s
DC-DC boost converter	
Inductance(L)	2e-3H
Schottky diode(IN5818)	0.001Ω, 0.26V, C=2.5e-7F Rs=500Ω
Capacitor(C)	1.6e-04F
Converter switches_MOSFET	
Ron	0.012Ω
Lon	0.1e-07H
Rd	0.01Ω
Vf	0.8
Duty cycle	40-60%
Switching frequency(fsw)	10kHz
Load	5Ω
Battery	Lithium-ion - 3.7V
Generator(PMSG)	
Number of turns(N)	135
Magnetic flux density, Bm	0.226T
Air gap(a-g)	3mm
The radius of the coil(r)	4.86cm
Number of coils	9
Stator resistance(ohms)	0.05
Stator inductances(H)	0.000635
DC bus capacitor(C)	100µF
Magnetic flux linkage	0.087
Number of poles	12
Converters switches	MOSFET-diode
Rotor type	Salient pole
Switching frequency(fsw)	10kHz

4.3.1 Wind turbine

The equations below are derived for the highest power extracted by a wind turbine [131]

Where A represents the area swept by the turbine blades (m^2), V is the wind speed (m/s), P_0 denotes maximum energy yield from the wind, Cp is the wind turbine's power coefficient, and ρ is the air density (usually 1.25 kg/m3). The highest achievable power coefficient is physically limited to 59.3% as imposed by the Betz limit.

$$P_T = C_P P_0 = \frac{1}{2} C_P \rho A V^3 \quad \textbf{4.1}$$

Here, T denotes aerodynamic torque, and ω_m is angular velocity(rad/s) for the wind turbine determined as the ratio of the turbine's shaft power relative to the wind's available power. One way to express the power coefficient about the TSR is as below:

$$C_p = \frac{\omega_m T}{P_0} \quad \textbf{4.2}$$

$$\lambda = \frac{\omega_m R}{v} \quad \textbf{4.3}$$

Where R represents the turbine rotor's radius. The Savonius VAWT has a 12.5cm diameter and 25 cm height[107].

4.3.2 Generator dynamics

The three-phase(3-ϕ) PMSG parameters and model were also adopted, which is linked to the wind turbine to convert kinetic energy into mechanical energy. The low on-state voltage drop Schottky rectifier diode rectifies the AC to DC.

The generator equation is given by[107].

$$\left.\begin{aligned} v_a &= L_S\frac{di_a}{dt} + R_s i_a - E_a \\ v_b &= L_S\frac{di_b}{dt} + R_s i_b - E_b \\ v_c &= L_S\frac{di_c}{dt} + R_s i_c - E_c \end{aligned}\right\} \quad \textbf{4.4}$$

Where Ls represents the synchronous inductance per phase, phase resistance (Rs), and E denotes the maximum induced voltage calculated by;

$$E_{max} = \frac{4\omega_e k_s N B_m l r}{poles} \quad \textbf{4.5}$$

$$\omega_e = \omega_m poles/2 \quad \textbf{4.6}$$

Where: Ks – coil winding coefficient, poles - count of poles, N - number of stator winding turns (per phase), B_m - peak flux density(T), *l* – rotor's axial length (m), and r - radius to the air-gap (m).

$$\frac{d\omega_m}{dt} = \frac{T_v - T_e - b\omega_m}{J} \quad \textbf{4.7}$$

$$T_v = PT/\omega_m$$

The 3.16 is the dynamic equation that controls the turbine/generator's angular motion where; J – moment of inertia, b –coefficient of friction, T_e – electric torque and T_v – mechanical torque (N.m) where V is RMS phase voltage (V_{rms}), F_p is the power factor and I is the RMS phase current.

$$T_e = \frac{3IVF_P}{\omega_m} \quad \textbf{4.8}$$

4.3.3 **Rectification and conversion**

The rectified DC is stepped up by the DC-DC voltage booster to an elevated and stable voltage required by the batteries. This also ensures efficient energy transfer and maximum power extraction[107]. The inductor, L, with a resistance RL and a capacitor ideal capacitor C, is series-connected with RC. The Schottky diode used has a forward resistance Rd and a low on-state

voltage drop V_d. The MOSFET is regulated by the PWM, given that the maximum value for the Duty cycle is 80%. The MOSFET has an internal resistance of R_{sw}, and its on-state voltage drop is V_{sw}. The load Ro, preferably a resistor or a battery, receives energy from the converter. The load voltage and the load current of the boost converter are given as;

$$V_0 = \frac{V_s}{1-D} \quad \textbf{4.9}$$

$$I_0 = (1-D)I_L$$

where: D is the duty cycle, I_L is the coil's current, and. The expressions for inductance and capacitance are $L = V_s D/\Delta I_L f$ and $C = V_0 D/R_0 \Delta V_0 f$, respectively, where the variable f denotes the converter's switching frequency, Vo is the load voltage, ΔV_0 is the capacitor voltage variation, and ΔI_L is the coil current fluctuation. Considering coil's inductance, 2 mH if Vs = 1 V and f = 10 kHz. With a 10% V_o, the capacitance is 160 μF for the lowest load of 5Ω[107].

The converter's dynamic behaviour is determined by the Laplace transform.

$$I_L = \frac{1}{sL}[V_s - (1-\gamma)V_d - (\frac{R_0 R_c}{R+R_c}(1-\gamma) + R_L)I_L - \frac{R_0}{R_0 R_c}V_c(1-\gamma)]i_0 = (1-D)i_L \quad \textbf{4.10}$$

$$V_C = \frac{R_0 I_L (1-\gamma) - V_C}{sCR_0 + R_c} \quad \textbf{4.11}$$

The switch state(on/off) is indicated by γ, and voltage drop(V_d) of the diode, which is significant for small-scale systems.

4.3.4 **Tip speed ratio (λ)**

The TSR of the Savonius wind turbine was not provided in the available data. An optimal TSR of 0.5 was obtained in this study. This is justified by references to works such as [125], [126], and [127], which report an optimal TSR range of 0.5 to 1.1 for Savonius turbines, also indicating that Savonius wind turbines have greater efficiency at low Tip Speed Ratio values.

4.4 Sensitivity analysis and the effect of the control parameters

The analysis of sensitivity evaluates the way variations in key parameters impact the operation of the WECS. The speed of wind, which is the primary driver for power generation, was tested under a constant ambient wind speed of 2.66m/s and variations in the train-induced wind speed ranging between 4.16m/s and 7.6m/s. At 7.6m/s, the power output increased greatly compared to the ambient wind speed(2.66m/s). The system's cut-in wind speed(1.41m/s) was validated with no power generation below this threshold. The blade pitch angle ranges between 0^0 to $30^{0,}$ observing that the optimal range was $20^0 – 25^0$ for all wind speeds. Beyond $25^{0,}$ the efficiency for the high wind speeds (6.67m/s – 7.6m/s) is due to excessive drag. For the electrical load resistance, the optimal load (100Ω) maximized power transfer, while higher loads(>150Ω) reduced current flow and power production. Overall, the sensitivity analysis emphasizes the importance of managing wind speed, pitch angle and load resistance to optimise the energy efficiency of the WECS.

1. Tip Speed Ratio (λ)

The TSR is defined by ωR/v, where ω is the rotor speed and R is the rotor radius. The optimal range: 0.5 – 1.0 for Savonius VAWT, where below 0.5, it was observed that low rotor speed and low power output, while above 0.8, there was excessive drag due to mechanical stress. The FLC maintained $\lambda \approx 0.45$ under ambient wind(*Figure 4.10*).

2. The pitch angle(β)

The role is to balance the lift/drag forces to maximise Cp (power coefficient). After FLC implementation, at low wind speed(2.66m/s), $\beta = 25^0$ to enhance lift, at high wind speeds (5.22m/s – 7.6m/s) reduced β to 20^0 to mitigate drag (*Figure 4.10*). the Pitch Angle's impact on battery charging is that at $\beta = 25^0$, the battery charged at all wind speeds and at $\beta = 30^0$, charging efficiency dropped by 15% during stronger winds.

The Fuzzy Logic Control effectively optimizes operational parameters regarding the Wind Energy Conversion System, resulting in enhanced energy capture and system stability. By dynamically adjusting the pitch and TSR, the FLC enhances the turbine's ability to adapt to variable wind conditions, thereby maximizing power extraction and improving overall system efficiency.

Electrical loads for the signaling and communication equipment at AALRT

a) Signal lights

Signal lights in railway systems(*Figure 4.12*) are visual indicators to the train drivers on how to proceed safely. The colors used are Green(Proceed), Yellow (Caution/ prepare to stop), Red(stop), controlling the train's movement and ensuring safety. Other signals include a double yellow for preliminary caution, white signal at the shunting yard. These operate at 220V[111].

Figure 4.12: Signal light at the Kality depot AALRT

b) Level crossing gate

This is a barrier placed at intersections of the railway line and the road/pedestrian path designed to stop vehicles and pedestrians from crossing the railway when a train is approaching to ensure safety, as seen in *Figure 4.13*. This crossing operates at 220V AC and uses 110 Watts, drawing a peak current of 0.5 Amps[111].

Figure 4.13: Level crossing at AALRT Kality

c) Balise

This is a transponder that is mounted on the track for communication with the onboard equipment for the transmission of information like speed limits, signal aspects, location, hence ensuring safety due to the automatic train control and protection systems(see *Figure 4.14*).

Figure 4.14: Balise placed on a track

d) Station led lights

These are modern lighting systems that illuminate the platforms. LEDs are preferred due to their low energy consumption, durability and brightness. *Figure 4.15* shows the LED lights found at the passenger platforms at the AALRT railway.

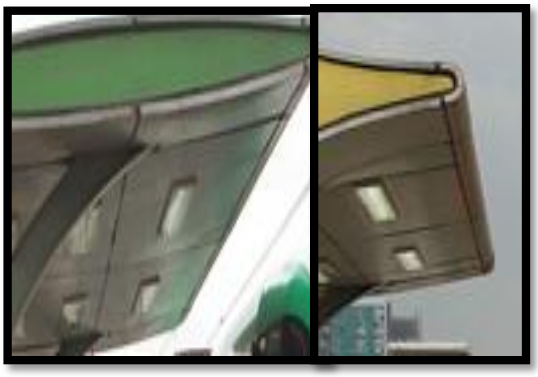

Figure 4.15: Station lights at the AALRT passenger platform

e) Point machine

This device is placed at the railway trackside used to lock the railway switches into position. This enables trains to switch from one track to another, ensuring proper alignment of the rails at the junctions.

Figure 4.16: Point machine at Kality depot AALRT

f) Axle counter

The axle counter is a sensor that tracks the axle count, i.e., those that leave and enter the track section, to determine whether the section is free or occupied, functioning as a traditional track circuit for detecting the train. Every axle counter uses 20 Watts, 24V ± 5% DC.

Figure 4.17: Axle counter placed on the railway track

4.5 Technical feasibility analysis of the hybrid wind energy system for AALRT electrical auxiliary loads.

While the detailed modeling, simulation and validation of the standalone Savonius VAWT with its FLC-MPPT control strategy (as presented in Chapter 4) demonstrated significant improvements in power extraction and reliability, the inherent intermittency of wind resources and the continuous nature of the AALRT auxiliary electrical loads indicated that the wind energy system might not consistently ensure the required energy reliability. To address this observed energy deficit and comprehensively assess the long term viability and optimal configuration for a reliable power supply, a technical feasibility study was undertaken using the HOMER pro software. This is a computational based software tool that enables the designer to compare different power systems based on technical/economic aspects[135]. It optimises the system through the simulation of the system components as it aims to evaluate the best system basing on the decision variables, it performs many optimizations to examine the sensitivity analysis and the effect of external parameters which include; wind speed data, capacity shortages, fuel cost etc[136]. *Figure 4.18* shows the schematic set up of the system. HOMER was selected for this feasibility study due to its industry wide recognition, robust optimization capabilities and its ability to integrate diverse resources with detailed load profiles and economic parameters. This allows for a comprehensive assessment that goes beyond the instantaneous power output analyzed in Simulink, providing a holistic view of system viability.

4.5.1 System components

While designing any power system, there is need to put into consideration the configuration of the system i.e., types of components to be included, their size, and quantity. In this simulation, we considered a wind turbine which produces an alternating current voltage, this AC is rectified to DC using the converter which ensures that a DC input is fed to the battery which in turn supplies the DC electrical loads i.e., primary load and the deferrable load. The *Figure 4.18* shows the schematic representation of the energy system configuration. The *Table 4.6* outlines the key operational parameters and specifications of the system components providing a comprehensive overview of the energy system configuration.

i. Wind turbine; this is the primary energy converter generating AC electricity from the wind. As detailed in the *Table 4.6* the optimal system incorporated one AWS HC 650W wind turbine rated 0.650kW.

ii. AC/DC rectifier; this converts the alternating current from the wind turbine's generator into stable DC power.

iii. Battery Energy Storage System(BESS); as indicated in *Table 4.6* the lithium ion battery is employed. This acts as an energy buffer while storing excess wind power.

iv. Loads; comprises of both the primary and deferrable electrical demands of the AALRT auxiliary systems.

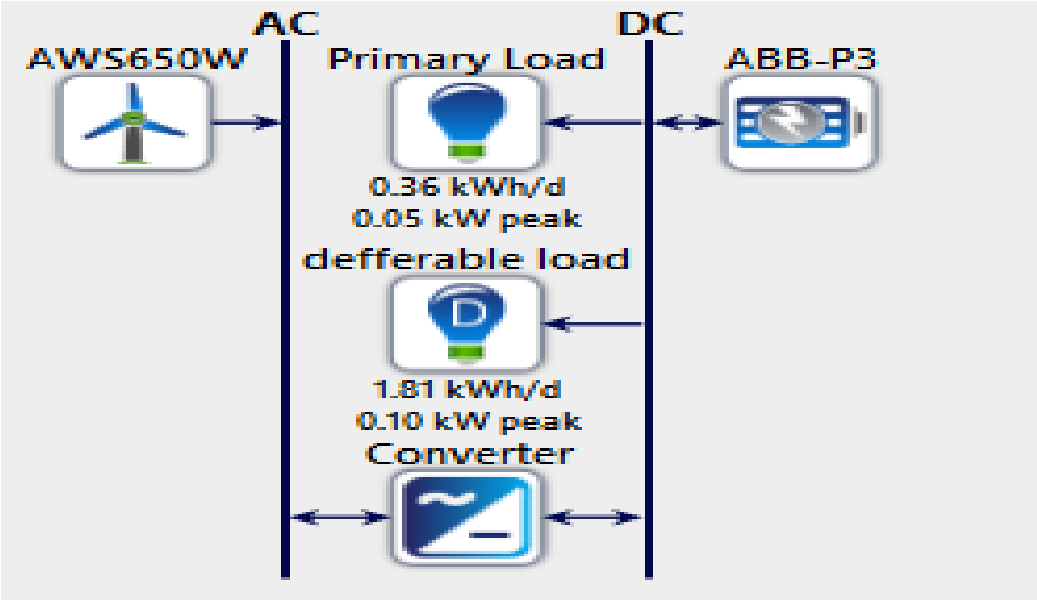

Figure 4.18: Schematic diagram of the electrical components connection by HOMER

4.5.2 **Wind resource**

The small scale wind turbine was selected and configured with the wind profile of the AALRT vicinity as provided by the National Meteorological Agency(NMA) and Global Wind Atlas(GWA)(see *Figure 4.19*). The wind resource data for the AALRT location was imported into HOMER pro. This data was derived from the detailed wind speed analysis which provides hourly wind speed profiles at 10m height.

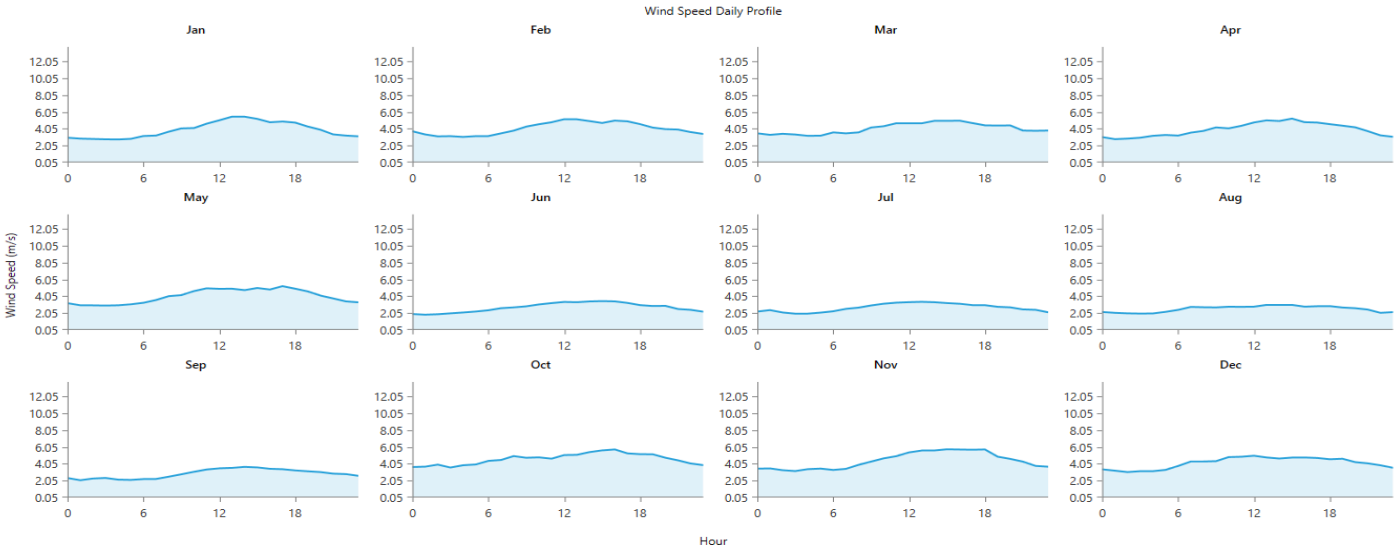

Figure 4.19: Wind speed daily profile from the HOMER analysis

Table 4.6: Specifications of the components used in the HOMER analysis

Wind turbine	Primary load	Deferrable load	Converter	Battery
▪ Type: AWS 650W ▪ Rated power: 650W(0.65 kW) ▪ Mean output power: 0.154kW ▪ Capacity factor: 22.3% ▪ Annual energy production: 1271kWh	▪ Type: LED lights ▪ Rating: 36W(0.036kW) ▪ Operational hours: 10 hours ▪ Peak load: 0.05kW ▪ Daily load: 0.36kWh/d	▪ Type: Non critical loads ▪ Rating:1-1.5kW ▪ Operational times(Feb-Dec) ▪ Peak load: 0.10kW ▪ Daily load: 1.81kW/d	▪ Efficiency:95% ▪ Rated capacity : 100kW ▪ Relative capacity : 100% ▪ Lifetime : 15yrs	▪ Type: Lithium-ion, ABB PS-BatP3 ▪ Nominal capacity : 0.289kWh ▪ Nominal capacity : 78Ah ▪ Operating temp: -25^{0}C to 60^{0}C ▪ Energy density: 295Wh/L

4.5.3 **Electrical loads estimation**

The electrical loads of the AALRT auxiliary systems are classified into primary loads and deferrable load which is also known as the secondary load[135]. A primary load is an electrical load that requires to be served immediately without interruption e.g., critical lighting systems, signaling and communication equipment etc., the primary load consists of the 36W LED bulb(as shown in *Table 3.1*), assumed to operate for 10 hours daily. The hourly load profile was estimated based on the typical energy consumption of lighting systems at the railway stations. For the subsequent system optimization, HOMER scaled this primary load profile to achieve an average daily consumption of 0.36 kWh/day, a peak demand of 0.05 kW(see *Figure 4.20*) and an annual consumption of 125kWh/yr. This scaling ensures that the system design directly addresses the

intended operational load demand. The annual energy consumption is calculated as follows[135];

$$Annual\ Energy\ Consumption(kWh) = (Number\ of\ LED\ lamps\ used\ x\ Power\ rating\ of\ each\ LED\ lamp\ x\ hours\ of\ operation\ x\ number\ of\ days)/1000)/7\ days \quad \textbf{4.1}$$

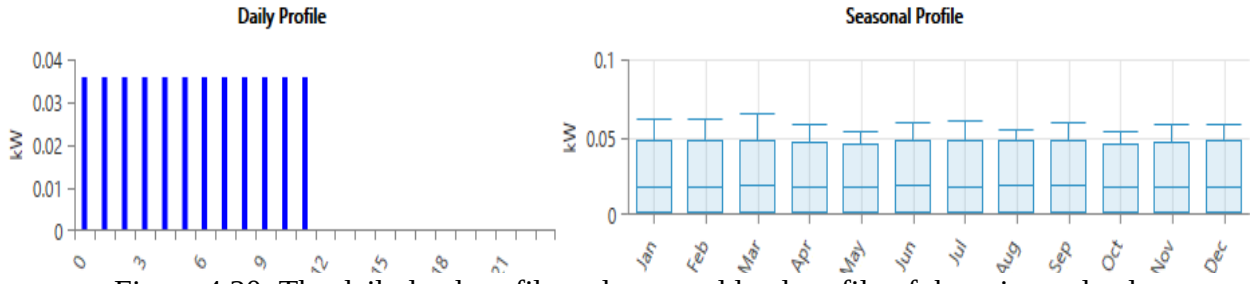

Figure 4.20: The daily load profile and seasonal load profile of the primary load

The deferrable load is an electrical load that is not is not as critical as the primary load i.e., it should be served after the needs of the primary load have been met[135]. In railway systems, some of the deferrable loads include; non urgent station operations(lighting), auxiliary systems like ventilation, heating and cooling in non-critical areas. The deferrable load ranging between 1 – 1.5kWh/d was incorporated to facilitate efficient utilisation of any surplus renewable energy ranging between the months of February and November with the exceptions of January and December. The total consumption of the deferrable load per year is 317kWh/yr. *Figure 4.21* shows the monthly average deferrable electrical load of the AALRT railway. To mitigate the intermittent nature of wind

energy and ensuring the continuous, reliable power supply required by the AALRT auxiliary loads, as clearly stated in *Figure 4.8*, showing the performance of battery technologies conducted in, the Lithium-ion (Li-ion) battery was selected as the preferred storage option for the HOMER feasibility analysis due to its demonstrated superior State of Charge (SOC) gain, stable voltage profile across varying discharge rates, and notably higher charge and discharge efficiencies compared to other batteries(see *Table 4.4)*. The selected Lithium-ion battery bank serves as the critical energy buffer, enabling the hybrid system to effectively manage the fluctuating power output from the wind turbines. It discharges the stored energy to meet the electrical loads (both primary and deferrable) during periods when wind generation is insufficient, thereby ensuring uninterrupted power supply to critical auxiliary AALRT systems.

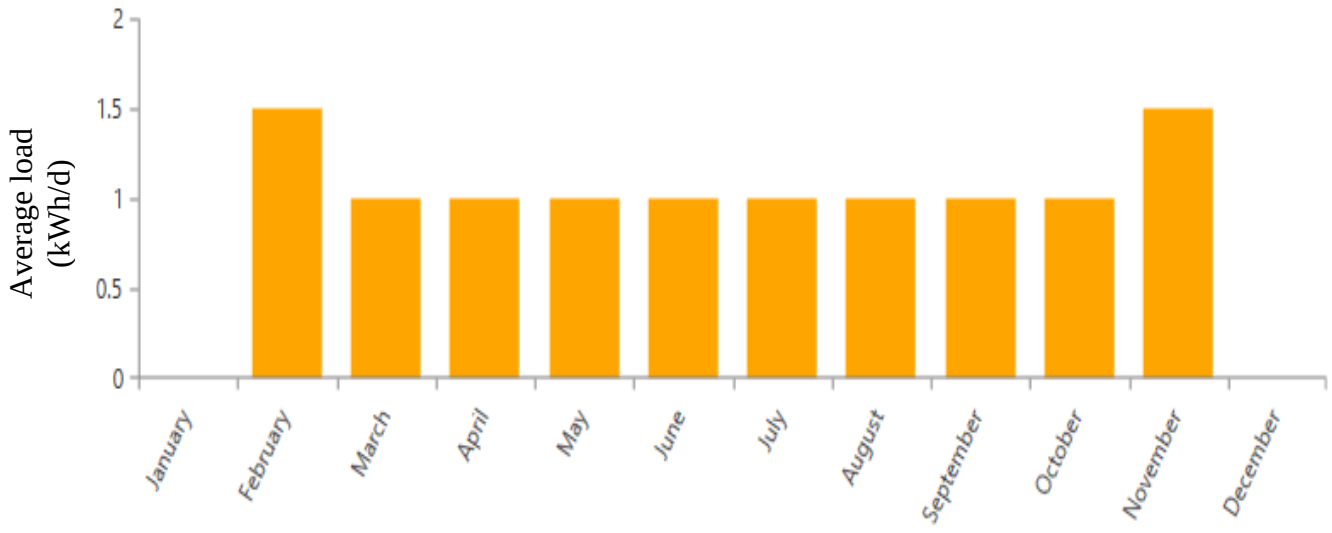

Figure 4.21: The monthly average load profile of the deferrable load

4.5.4 **Power production feasibility and analysis**

The HOMER analysis as shown in *Figure 4.23* for the AWS HC 650W wind turbine indicates an annual production of 648 kWh, effectively meeting the total energy consumption of 442 kWh/year, which includes a significant DC primary load of 125 kWh/year and a deferrable load of 317kWh/year. The system generates a surplus of 18.7% in excess electricity, ensuring all energy demands are satisfied with 4.61% unmet electric load. Overall, the analysis underscores the reliability and feasibility of integrating wind energy into the energy strategy for the case study.

The power curve of the wind turbine in *Figure 4.22* illustrates the relationship between wind speed (m/s) and power output (kW).

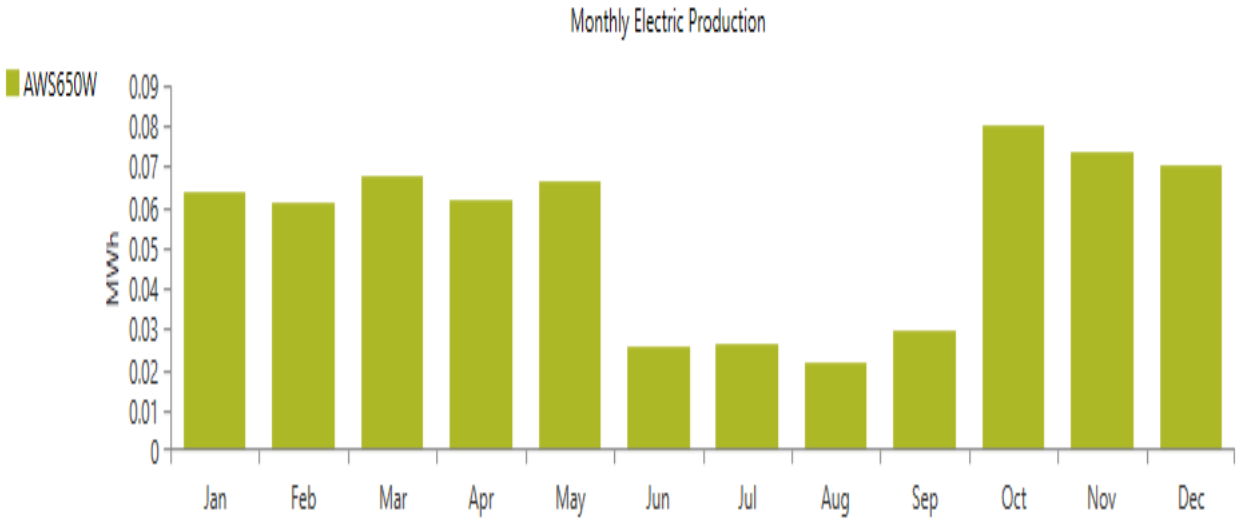

Figure 4.22: Monthly wind turbine power production

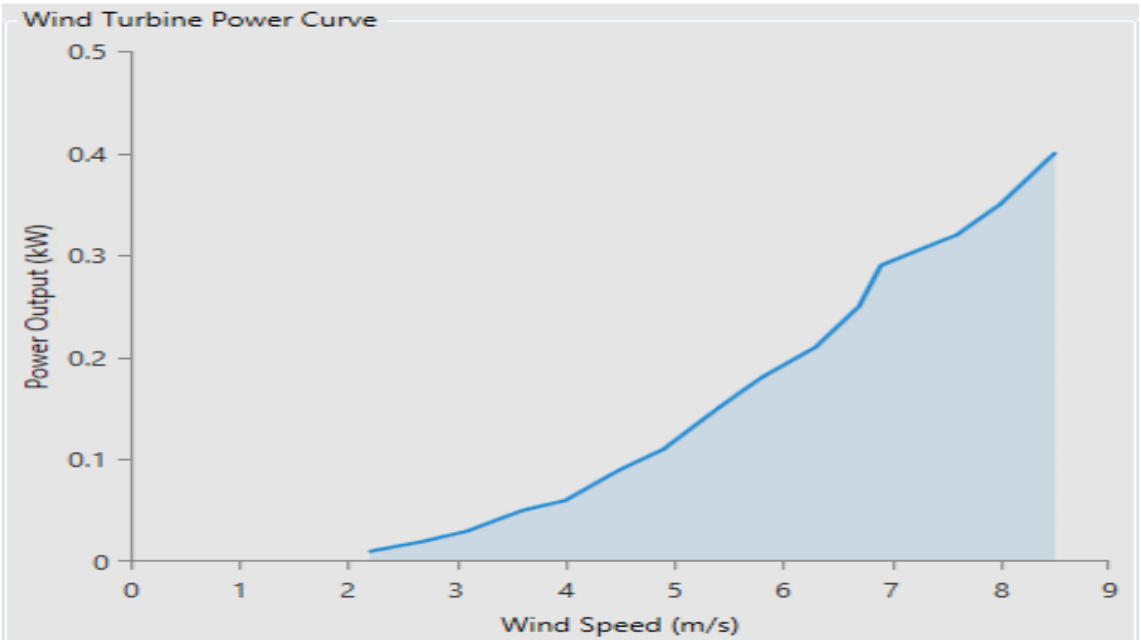

Figure 4.23: Wind turbine power output curve by HOMER

The *Figure 4.24* shows the total renewable power output per month illustrating a relatively stable generation capacity throughout the year with values system ranging between 0.1 kW to 0.3 kW reaching 0.4 kW in higher power output seasons. This reinforces the feasibility of the WEHS system to meet the energy demands of the electrical loads of AALRT ensuring that operational needs can be consistently fulfilled throughout the year.

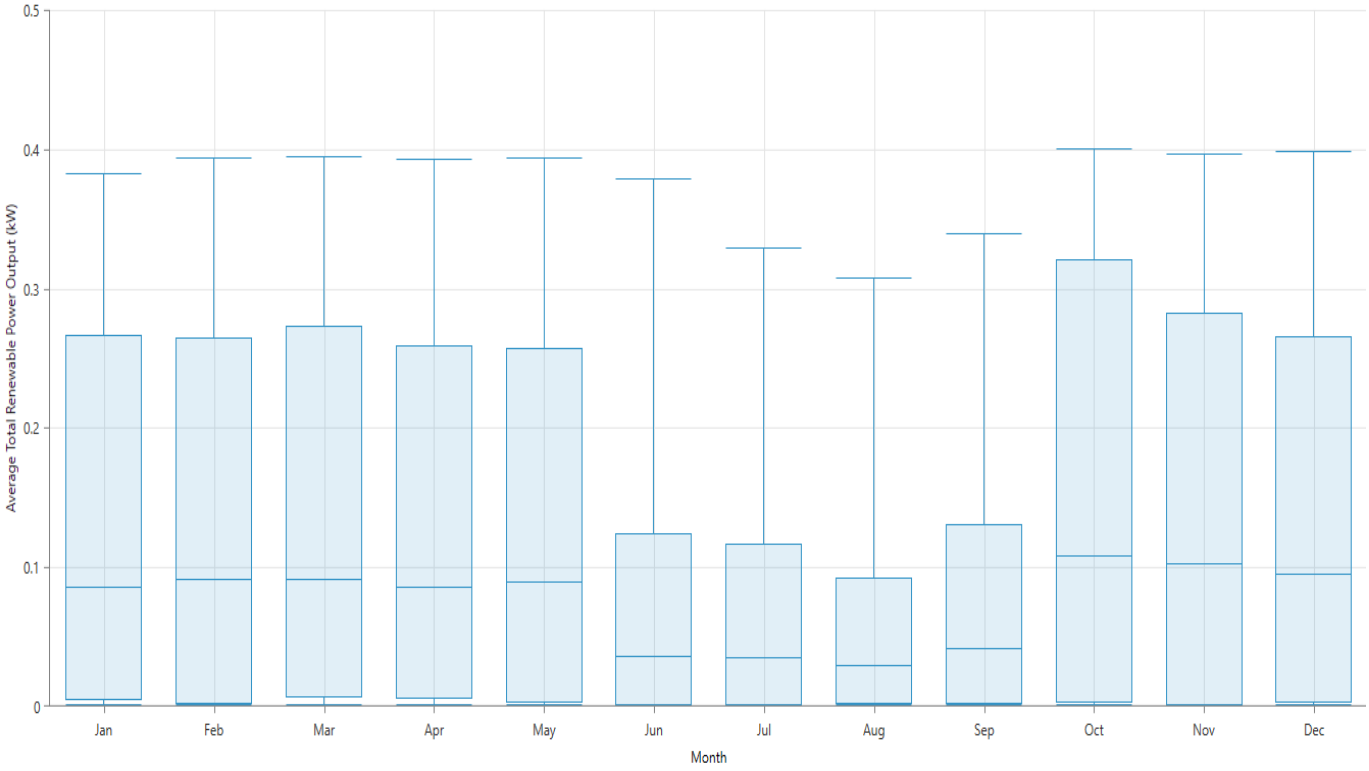

Figure 4.24: Monthly average renewable power output

Figure 4.25 illustrates the monthly distribution of the total electrical load successfully served by the optimized hybrid energy system. The system is consistently capable of serving peak demands ranging between 0.05 kW to 0.15 kW across all months. The overall demand remains steady and the absence of significant peaks in load demands reinforces the reliability of the energy system, indicating that it can consistently meet the operational requirements throughout the year.

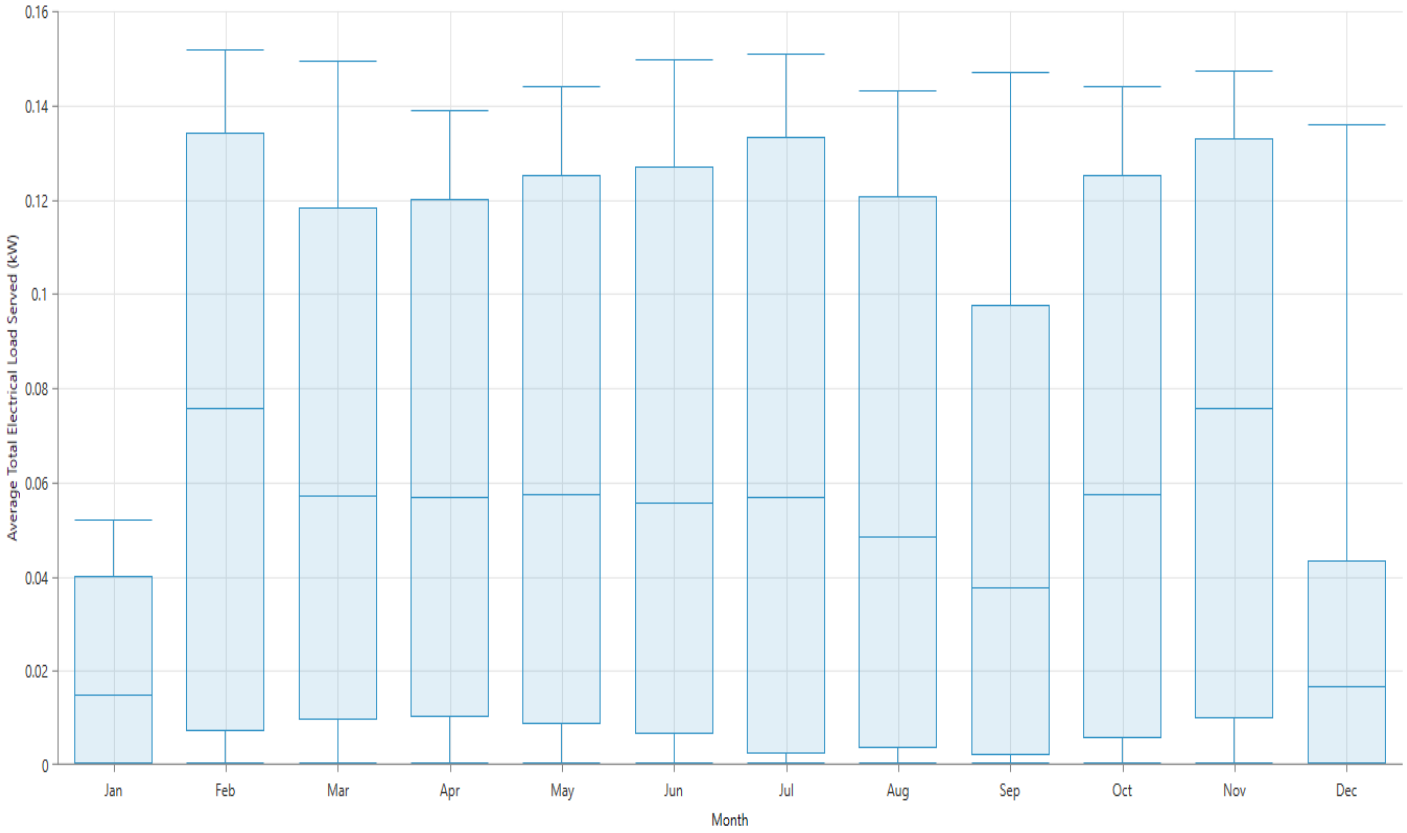

Figure 4.25: Monthly Distribution of Total Electrical Load Served

The overall steady demand and the absence of significant unmet load demands reinforces the reliability and technical feasibility of the wind energy conversion system to consistently meet the operational requirements of the AALRT auxiliary loads throughout the year.

5 CONCLUSION AND RECOMMENDATIONS

5.1 Conclusions

In conclusion, this research has investigated the analytical model design, simulation and performance validation of a small-scale WECS designed to harness wind energy along the AALRT railway corridor, where the feasibility of the system was also put into consideration. This further denotes the great importance of renewable energy technologies in the energy sector. The study focused on integrating Savonius vertical axis wind turbines(S-VAWT) with an FLC-MPPT algorithm to optimise energy extraction during intermittent wind conditions. The results demonstrated that the system proposed is feasible and that it can generate an increased amount of power for auxiliary railway subsystems such as sensors, lighting, signalling and communication devices even under low to moderate wind speeds ranging from 2.66m/s to 7.6m/s.

The FLC-MPPT algorithm proved to be highly effective in handling periodic variation in wind intensity, delivering superior performance than Perturb & Observe(P&O) and other traditional methods. It dynamically adjusted the key control parameters such as Pitch Angle and TSR, ensuring maximum energy delivery. This adaptability is crucial for urban environments where wind profiles are highly variable due to obstacles and turbulence. Furthermore, the validation process confirmed the accuracy of the Simulink model by replicating results from a benchmark study, including average power output.

Crucially, while the optimized WECS in this thesis demonstrated enhanced power output, the technical feasibility analysis conducted using HOMER highlighted that a hybrid energy system is essential to consistently meet the continuous and critical auxiliary electrical loads of the AALRT (such as signaling, lighting, and communication devices). The dedicated primary load of 36W bulbs consumes 125kWh/year while the deferrable load consumes upto 317kWh/year and a total electrical load consumption 442kWh/year. The optimization process resulted in 18.7% of excess electricity and a minimal unmet electric load percentage of 4.61%, indicating a highly efficient system that balances reliability with economic viability This approach efficiently bridges the intermittency of wind power, ensuring uninterrupted supply for the served loads. These findings establish the feasibility of integrating small-scale WECS into urban railway infrastructure,

contributing to Ethiopia's renewable energy goals and enhancing the energy reliability in public transit systems.

5.2 Recommendations

To build upon the findings of this research and facilitate real-world implementation, several recommendations are proposed:

1. Field testing and prototype scaling. While this study relied on simulations, it is essential to conduct long-term field trials along the AALRT corridor to evaluate system performance under actual wind conditions. This includes measuring train-induced airflow and ambient wind profiles over extended periods. A full-scale prototype should be developed to address limitations observed in lab-scale testing, such as scaling effects on turbine performance and structural integrity. Field testing will also provide valuable insights into operational challenges such as maintenance requirements and environmental impacts.
2. Hybrid energy system integration; Wind energy alone may not be sufficient during periods of low wind availability or extended calm conditions. To enhance system reliability, it is recommended to integrate hybrid energy solutions by combining wind turbines with solar photovoltaic (PV) panels or advanced ESS systems like lithium-ion batteries. Hybrid systems ensure a continuous energy supply by leveraging complementary energy sources and storing excess energy for later use. This approach will further improve the practicality of WECS for urban rail applications.
3. Advanced control strategies; the FLC-MPPT algorithm performed well in simulations but can be further refined by incorporating real-time wind forecasting techniques and machine learning algorithms for effective tuning, which posed a great problem during this research. Predictive models can anticipate changes in wind speed and adjust control parameters proactively, improving tracking accuracy and response times. Additionally, integrating adaptive control strategies that account for environmental variations (e.g., temperature, humidity) will enhance overall system efficiency.
4. Component Optimization; to reduce costs and improve scalability, to reduce costs and improve scalability, future research should focus on optimising individual components of the WECS. For instance, lightweight materials such as carbon fibre or composite plastics

can be used for turbine blades to reduce weight and increase durability. High-efficiency Permanent Magnet Synchronous Generator(PMSG) designs can minimize losses during energy conversion, while low-loss DC-DC boost converters can ensure efficient power transfer to the battery or load. These advancements will make the system more economically viable for widespread adoption.

5. Policy support and stakeholder engagement; successful implementation of WECS along AALRT requires collaboration with policymakers, engineers, and stakeholders in Ethiopia's public transit sector. Policies supporting renewable energy integration into urban infrastructure should be developed, including incentives for research funding, subsidies for manufacturing costs, and streamlined regulatory approvals for pilot projects.

By addressing these recommendations, future research can advance the development of the small-scale WECS for urban rail systems, contributing to sustainable energy solutions globally while enhancing the reliability and efficiency of public transportation networks.

REFERENCES

[1] A. Oyilieze Akanwa and N. Joe-Ikechebelu, "The Developing World's Contribution to Global Warming and the Resulting Consequences of Climate Change in These Regions: A Nigerian Case Study," in *Global Warming and Climate Change*, J. P. Tiefenbacher, Ed., IntechOpen, 2020. doi: 10.5772/intechopen.85052.

[2] O. Oñederra, F. J. Asensio, G. Saldaña, J. I. S. Martín, and I. Zamora, "Wind Energy Harnessing in a Railway Infrastructure: Converter Topology and Control Proposal," *Electronics*, vol. 9, no. 11, p. 1943, Nov. 2020, doi: 10.3390/electronics9111943.

[3] S. V. Mitrofanov, N. G. Kiryanova, and A. M. Gorlova, "Stationary Hybrid Renewable Energy Systems for Railway Electrification: A Review," *Energies*, vol. 14, no. 18, Art. no. 18, Jan. 2021, doi: 10.3390/en14185946.

[4] M. Khodaparastan and A. Mohamed, "Modeling and Simulation of Regenerative Braking Energy in DC Electric Rail Systems," in *2018 IEEE Transportation Electrification Conference and Expo (ITEC)*, Long Beach, CA, USA: IEEE, Jun. 2018, pp. 1–6. doi: 10.1109/ITEC.2018.8450133.

[5] A. L. Ruscelli, G. Cecchetti, and P. Castoldi, "Energy harvesting for on-board railway systems," in *2017 5th IEEE International Conference on Models and Technologies for Intelligent Transportation Systems (MT-ITS)*, Naples, Italy: IEEE, Jun. 2017, pp. 397–402. doi: 10.1109/MTITS.2017.8005704.

[6] A. K. Bulbul, A. R. Laskar, W. T. S. Chy, and M. Sahariat, "Energy Harvesting for Electric Train: Application of Multi-Renewable Energy Sources with Sophisticated Technology," 2017.

[7] H. Liu, J. Zhong, C. Lee, S.-W. Lee, and L. Lin, "A comprehensive review on piezoelectric energy harvesting technology: Materials, mechanisms, and applications," *Appl. Phys. Rev.*, vol. 5, no. 4, Dec. 2018, doi: 10.1063/1.5074184.

[8] A. E. Espe, T. S. Haugan, and G. Mathisen, "Magnetic Field Energy Harvesting in Railway," *IEEE Trans. Power Electron.*, vol. 37, no. 7, pp. 8659–8668, Jul. 2022, doi: 10.1109/TPEL.2022.3141437.

[9] J. Zuo, L. Dong, F. Yang, Z. Guo, T. Wang, and L. Zuo, "Energy harvesting solutions for railway transportation: A comprehensive review," *Renew. Energy*, vol. 202, pp. 56–87, Jan. 2023, doi: 10.1016/j.renene.2022.11.008.

[10] S. Jaber, "Environmental Impacts of Wind Energy," *J. Clean Energy Technol.*, pp. 251–254, 2014, doi: 10.7763/JOCET.2013.V1.57.

[11] S. Watson *et al.*, "Future emerging technologies in the wind power sector: A European perspective," *Renew. Sustain. Energy Rev.*, vol. 113, p. 109270, Oct. 2019, doi: 10.1016/j.rser.2019.109270.

[12] "Ministry of New and Renewable Energy organises 'Global Wind Day 2024' event with a central theme of 'Pawan-Urja: Powering the Future of India.'" Accessed: Aug. 27, 2024. [Online]. Available: https://pib.gov.in/pib.gov.in/Pressreleaseshare.aspx?PRID=2025585

[13] L. Gupta, "Opportunities And Roadmap For Harnessing Wind Energy In Rail Sector." Indian Railway Technical Bulletin. [Online]. Available: Https://Www.Researchgate.Net/Profile/Rajesh_Gupta74/Publication/331484930_Opportunities_And_Roadmap_For_Harnessing_Wind_Energy_In_Rail_Sector/Links/5c7c7be1a6fdcc4715aca54a/Opportunities-And-Roadmap-For-Harnessing-Wind-Energy-In-Rail-Sector.Pdf

[14] S. Hameer and N. Ejigu, "A prospective review of renewable energy developments in Ethiopia," *AAS Open Res.*, vol. 3, p. 64, Dec. 2020, doi: 10.12688/aasopenres.13181.1.

[15] F. J. Asensio, J. I. S. Martin, I. Zamora, O. Onederra, G. Saldana, and P. Eguia, "A system approach to harnessing wind energy in a railway infrastructure," in *IECON 2018 - 44th Annual Conference of the IEEE Industrial Electronics Society*, Washington, DC: IEEE, Oct. 2018, pp. 1646–1651. doi: 10.1109/IECON.2018.8591777.

[16] B. Ayalew, "Assessment of improvement areas for increasing the capacity of Ethio-Djibouti railway line".

[17] P. Li, D. Li, L. Wang, W. Cai, and Y. Song, "Maximum power point tracking for wind power systems with an improved control and extremum seeking strategy: NOVEL MPPT SCHEME FOR WT," *Int. Trans. Electr. Energy Syst.*, vol. 24, no. 5, pp. 623–637, May 2014, doi: 10.1002/etep.1718.

[18] Q. Hassan, S. Algburi, A. Z. Sameen, H. M. Salman, and M. Jaszczur, "A review of hybrid renewable energy systems: Solar and wind-powered solutions: Challenges, opportunities, and policy implications," *Results Eng.*, vol. 20, p. 101621, Dec. 2023, doi: 10.1016/j.rineng.2023.101621.

[19] T. Funabashi, "Integration of Distributed Energy Resources in Power Systems.," *Integr. Distrib. Energy Resour. Power Syst.*, pp. 1–14, 2016, doi: 10.1016/B978-0-12-803212-1.00001-5.

[20] S. Roga, V. Kisku, and S. Datta, "Performance of a vertical wind turbine with permanent magnet synchronous generator," *Proc. Inst. Civ. Eng. - Energy*, vol. 175, no. 4, pp. 205–215, Nov. 2022, doi: 10.1680/jener.21.00113.

[21] Y.-G. Baek and J. C. Lee, "Railway Systems Development Based on the Concept of Systems Engineering and Safety: A Case Study of Railway Industry Practices".

[22] K. S. J. Surya, "Generation of electricity by using turbine mounted on train," vol. 03, no. 2016.

[23] H. Lars and B. Frede, "Wind Turbine Systems," in *Control in Power Electronics*, Elsevier, 2002, pp. 483–509. doi: 10.1016/B978-012402772-5/50014-4.

[24] D. Liu, Z. Wu, H. Wang, and T. Wang, "MPPT control strategy for off-grid wind power system," in *The 2nd International Symposium on Power Electronics for Distributed Generation Systems*, Hefei, China: IEEE, Jun. 2010, pp. 759–764. doi: 10.1109/PEDG.2010.5545849.

[25] J. Pande, P. Nasikkar, K. Kotecha, and V. Varadarajan, "A Review of Maximum Power Point Tracking Algorithms for Wind Energy Conversion Systems," *J. Mar. Sci. Eng.*, vol. 9, no. 11, p. 1187, Oct. 2021, doi: 10.3390/jmse9111187.

[26] E. A. D. Kumara and N. K. Hettiarachchi, "Review Paper: Overview of the Vertical Axis Wind Turbines," vol. 4, no. 8, 2017.

[27] H. Wang, M. Yi, X. Zeng, T. Zhang, D. Luo, and Z. Zhang, "A hybrid, self-adapting drag-lift conversion wind energy harvesting system for railway turnout monitoring on the Tibetan Plateau," *Sustain. Energy Technol. Assess.*, vol. 46, p. 101262, Aug. 2021, doi: 10.1016/j.seta.2021.101262.

[28] M. Sathyajith and G. S. Philip, Eds., *Advances in Wind Energy Conversion Technology*. in Environmental Science and Engineering. Berlin, Heidelberg: Springer Berlin Heidelberg, 2011. doi: 10.1007/978-3-540-88258-9.

[29] H. L. Thadani, F. D. Zaaba, M. R. Mohammad Shahrizal, A. S. J. A. Jaspal Singh Jaj, and Y. I. Go, "Design and performance evaluation of vertical axis wind turbine for wind energy

harvesting at railway," *World J. Sci. Technol. Sustain. Dev.*, vol. 18, no. 2, pp. 190–217, May 2021, doi: 10.1108/WJSTSD-11-2020-0088.

[30] A. B. Kebede, G. B. Worku, and A. T. Maru, "A Novel Train Roof-Top Wind Energy Conversion System," *Int. J. Eng. Res. Afr.*, vol. 61, pp. 165–194, Jul. 2022, doi: 10.4028/p-ha82nm.

[31] Y. Raja Sekhar, M. Natarajan, C. Chiranjeevi, R. Sukanta, and P. Yugandhar, "Experimental Study on Vertical Axis Wind Turbine to Harness Wind Power from Rapidly Moving Railway Locomotives," in *Theoretical, Computational, and Experimental Solutions to Thermo-Fluid Systems*, M. Palanisamy, V. Ramalingam, and M. Sivalingam, Eds., in Lecture Notes in Mechanical Engineering. , Singapore: Springer Singapore, 2021, pp. 445–450. doi: 10.1007/978-981-33-4165-4_41.

[32] I. S. Utomo, D. S. Atmaja, and Y. Wicaksana, "The utilization of moving train as an alternative energy sources in railways with savonius wind turbine," *J. Phys. Conf. Ser.*, vol. 1700, no. 1, p. 012051, Dec. 2020, doi: 10.1088/1742-6596/1700/1/012051.

[33] A. K. Gupta, "Efficient Wind Energy Conversion: Evolution to Modern Design," *J. Energy Resour. Technol.*, vol. 137, no. 5, p. 051201, Sep. 2015, doi: 10.1115/1.4030109.

[34] S. M. H. Karimian and A. Abdolahifar, "Performance investigation of a new Darrieus Vertical Axis Wind Turbine," *Energy*, vol. 191, p. 116551, Jan. 2020, doi: 10.1016/j.energy.2019.116551.

[35] H. Pan *et al.*, "A portable renewable wind energy harvesting system integrated S-rotor and H-rotor for self-powered applications in high-speed railway tunnels," *Energy Convers. Manag.*, vol. 196, pp. 56–68, Sep. 2019, doi: 10.1016/j.enconman.2019.05.115.

[36] J. Pan, C. Ferreira, and A. Van Zuijlen, "A numerical study on the blade–vortex interaction of a two-dimensional Darrieus–Savonius combined vertical axis wind turbine," *Phys. Fluids*, vol. 35, no. 12, Dec. 2023, doi: 10.1063/5.0174394.

[37] M. Ahmad, A. Shahzad, and S. I. A. Shah, "Experimental investigation and analysis of proposed hybrid vertical axis wind turbine design," *Energy Environ.*, Jun. 2023, doi: 10.1177/0958305x231181675.

[38] J. D. Tan, C. C. W. Chang, M. A. S. Bhuiyan, K. N. Minhad, and K. Ali, "Advancements of wind energy conversion systems for low-wind urban environments: A review," *Energy Rep.*, vol. 8, pp. 3406–3414, Nov. 2022, doi: 10.1016/j.egyr.2022.02.153.

[39] P. Kozak, "Effects Of Unsteady Aerodynamics On Vertical-Axis Wind Turbine Performance".

[40] M. Hyman and M. H. Ali, "A Novel Model for Wind Turbines on Trains," *Energies*, vol. 15, no. 20, p. 7629, Oct. 2022, doi: 10.3390/en15207629.

[41] V. Nurmanova, M. Bagheri, A. Sultanbek, A. Hekmati, and H. Bevrani, "Feasibility study on wind energy harvesting system implementation in moving trains," in *2017 International Siberian Conference on Control and Communications (SIBCON)*, Astana, Kazakhstan: IEEE, Jun. 2017, pp. 1–6. doi: 10.1109/SIBCON.2017.7998495.

[42] K. He, G. Gao, J. Wang, M. Fu, X. Miao, and J. Zhang, "Performance of a turbine driven by train-induced wind in a tunnel," *Tunn. Undergr. Space Technol.*, vol. 82, pp. 416–427, Dec. 2018, doi: 10.1016/j.tust.2018.08.042.

[43] A. Chaudhuri, R. Datta, M. P. Kumar, J. P. Davim, and S. Pramanik, "Energy Conversion Strategies for Wind Energy System: Electrical, Mechanical and Material Aspects," *Materials*, vol. 15, no. 3, p. 1232, Feb. 2022, doi: 10.3390/ma15031232.

[44] M. A. Hannan *et al.*, "Wind Energy Conversions, Controls, and Applications: A Review for Sustainable Technologies and Directions," *Sustainability*, vol. 15, no. 5, p. 3986, Feb. 2023, doi: 10.3390/su15053986.

[45] M. Cheng and Y. Zhu, "The state of the art of wind energy conversion systems and technologies: A review," *Energy Convers. Manag.*, vol. 88, pp. 332–347, Dec. 2014, doi: 10.1016/j.enconman.2014.08.037.

[46] A. Sachan, Motilal Nehru National Institute of Technology Allahabad, India, A. K. Gupta, Motilal Nehru National Institute of Technology Allahabad, India, P. Samuel, and Motilal Nehru National Institute of Technology Allahabad, India, "A Review of MPPT Algorithms Employedin Wind Energy Conversion Systems," *J. Green Eng.*, vol. 6, no. 4, pp. 385–402, 2017, doi: 10.13052/jge1904-4720.643.

[47] B. Sindhuja, "A proposal for implementation of wind energy harvesting system in trains," in *Proceedings of The 2014 International Conference on Control, Instrumentation, Energy and Communication (CIEC)*, Calcutta, India: IEEE, Jan. 2014, pp. 696–702. doi: 10.1109/CIEC.2014.6959180.

[48] C. V. Govinda, S. V. Udhay, C. Rani, Y. Wang, and K. Busawon, "A Review on Various MPPT Techniques for Wind Energy Conversion System," in *2018 Internat2018 International Conference on Computation of Power, Energy, Information and Communication (ICCPEIC)ional conference on computation of power, energy, Information and Communication (ICCPEIC)*, Chennai, India: IEEE, Mar. 2018, pp. 310–326. doi: 10.1109/ICCPEIC.2018.8525219.

[49] D. Kumar and K. Chatterjee, "A review of conventional and advanced MPPT algorithms for wind energy systems," *Renew. Sustain. Energy Rev.*, vol. 55, pp. 957–970, Mar. 2016, doi: 10.1016/j.rser.2015.11.013.

[50] H. H. H. Mousa, A.-R. Youssef, and E. E. M. Mohamed, "State of the art perturb and observe MPPT algorithms based wind energy conversion systems: A technology review," *Int. J. Electr. Power Energy Syst.*, vol. 126, p. 106598, Mar. 2021, doi: 10.1016/j.ijepes.2020.106598.

[51] B. Rached, M. Elharoussi, and E. Abdelmounim, "Design and investigations of MPPT strategies for a wind energy conversion system based on doubly fed induction generator," *Int. J. Electr. Comput. Eng. IJECE*, vol. 10, no. 5, p. 4770, Oct. 2020, doi: 10.11591/ijece.v10i5.pp4770-4781.

[52] E. Abogrean, E. A. Elhatmi, and J. A. Saad, "Simulation of MPPT with a PMSG-based wind energy conversion system considering variable wind speed," *Sci. J. Univ. Benghazi*, vol. 35, no. 2, Dec. 2022, doi: 10.37376/sjuob.v35i2.3807.

[53] J. Hui, A. Bakhshai, and P. K. Jain, "An adaptive approximation method for maximum power point tracking (MPPT) in wind energy systems," in *2011 IEEE Energy Conversion Congress and Exposition*, Phoenix, AZ, USA: IEEE, Sep. 2011, pp. 2664–2669. doi: 10.1109/ECCE.2011.6064125.

[54] M. A. Abdullah, A. H. M. Yatim, and Chee Wei Tan, "A study of maximum power point tracking algorithms for wind energy system," in *2011 IEEE Conference on Clean Energy and Technology (CET)*, Kuala Lumpur, Malaysia: IEEE, Jun. 2011, pp. 321–326. doi: 10.1109/CET.2011.6041484.

[55] A. Kadri, H. Marzougui, and F. Bacha, "MPPT control methods in wind energy conversion system using DFIG," in *2016 4th International Conference on Control Engineering &*

Information Technology (CEIT), Hammamet, Tunisia: IEEE, Dec. 2016, pp. 1–6. doi: 10.1109/CEIT.2016.7929115.

[56] S. Park and S. R. Salkuti, "Optimal Energy Management of Railroad Electrical Systems with Renewable Energy and Energy Storage Systems," *Sustainability*, vol. 11, no. 22, p. 6293, Nov. 2019, doi: 10.3390/su11226293.

[57] S. K. Bade and V. A. Kulkarni, "Analysis of Railway Traction Power System Using Renewable Energy: A Review," in *2018 Internat2018 International Conference on Computation of Power, Energy, Information and Communication (ICCPEIC)ional conference on computation of power, energy, Information and Communication (ICCPEIC)*, Chennai, India: IEEE, Mar. 2018, pp. 404–408. doi: 10.1109/ICCPEIC.2018.8525206.

[58] K. Cory, "Renewable Energy Feed-in Tariffs: Lessons Learned from the U.S. and Abroad".

[59] M. Shahazad Aziz and S. Ahmed, "Wind-hybrid Power Generation Systems Using Renewable Energy Sources- A Review," *Int. J. Renew. Energy Res.*, no. v7i1, 2017, doi: 10.20508/ijrer.v7i1.5102.g6971.

[60] S. Boudoudouh and M. Maaroufi, "Renewable Energy Sources Integration and Control in Railway Microgrid," *IEEE Trans. Ind. Appl.*, vol. 55, no. 2, pp. 2045–2052, Mar. 2019, doi: 10.1109/TIA.2018.2878143.

[61] "Types of Railway Systems," theconstructor.org. Accessed: Sep. 13, 2024. [Online]. Available: https://theconstructor.org/transportation/types-railway-systems/554358/

[62] P. Jamińska-Gadomska, T. Lipecki, M. Pieńko, and J. Podgórski, "Wind velocity changes along the passage between two angled walls – CFD simulations and full-scale measurements," *Build. Environ.*, vol. 157, pp. 391–401, Jun. 2019, doi: 10.1016/j.buildenv.2019.04.052.

[63] Y. Zou, Z. Fu, X. He, C. Cai, J. Zhou, and S. Zhou, "Wind Load Characteristics of Wind Barriers Induced by High-Speed Trains Based on Field Measurements," *Appl. Sci.*, vol. 9, no. 22, Art. no. 22, Jan. 2019, doi: 10.3390/app9224865.

[64] P. B. Chaitanya and G. Gowtham, "Electricity through Train," *IOSR-JEEE*, vol. Volume 10, no. Issue 1 Ver. I, Feb. 2015.

[65] Z. Guo, T. Liu, K. Xu, J. Wang, W. Li, and Z. Chen, "Parametric analysis and optimization of a simple wind turbine in high speed railway tunnels," *Renew. Energy*, vol. 161, pp. 825–835, Dec. 2020, doi: 10.1016/j.renene.2020.07.099.

[66] P. Laws, R. V. Bethi, P. Kumar, and S. Mitra, "Improved design of Savonius rotor for green energy production from moving Singapore metropolitan rapid transit train inside tunnel," *Proc. Inst. Mech. Eng. Part C J. Mech. Eng. Sci.*, vol. 233, no. 7, pp. 2426–2441, Apr. 2019, doi: 10.1177/0954406218784620.

[67] D. Ticali, G. Acampa, And M. Denaro, "Renewable Energy Efficiency By Railway Transit. Case Study On Rebaudengo Railway Tunnel In Turin," Presented At The International Conference Of Computational Methods In Sciences And Engineering 2018 (Iccmse 2018), Thessaloniki, Greece, 2018, P. 140009. Doi: 10.1063/1.5079198.

[68] Z. Tasneem *et al.*, "An analytical review on the evaluation of wind resource and wind turbine for urban application: Prospect and challenges," *Dev. Built Environ.*, vol. 4, p. 100033, Nov. 2020, doi: 10.1016/j.dibe.2020.100033.

[69] H. Garshasbi and A. Mahmoudi, "A Novel Method for Power Generation Using Trains," in *2019 Iranian Conference on Renewable Energy & Distributed Generation (ICREDG)*, Tehran, Iran: IEEE, Jun. 2019, pp. 1–6. doi: 10.1109/ICREDG47187.2019.9218487.

[70] T. Konstantinou and N. Hatziargyriou, "Complex terrains and wind power: enhancing forecasting accuracy through CNNs and DeepSHAP analysis," *Front. Energy Res.*, vol. 11, p. 1328899, Jan. 2024, doi: 10.3389/fenrg.2023.1328899.

[71] A. Hyvärinen and A. Segalini, "Qualitative analysis of wind-turbine wakes over hilly terrain," *J. Phys. Conf. Ser.*, vol. 854, p. 012023, May 2017, doi: 10.1088/1742-6596/854/1/012023.

[72] D. A. K. Ibrahim, "A Comprehensive Review of Vertical Axis Wind Turbines For Urban Usage," vol. 7, no. 4, 2022.

[73] P. Wang, Y. F. Wang, M. Y. Gao, and Y. Wang, "Energy harvesting of track-borne transducers by train-induced wind," *J. Vibroengineering*, vol. 19, no. 3, pp. 1624–1640, May 2017, doi: 10.21595/jve.2017.17592.

[74] A. M. Eltamaly, A. Y. Abdelaziz, and A. G. Abo-Khalil, Eds., *Control and Operation of Grid-Connected Wind Energy Systems*. in Green Energy and Technology. Cham: Springer International Publishing, 2021. doi: 10.1007/978-3-030-64336-2.

[75] "Wind Turbine Control Methods." Accessed: Aug. 29, 2024. [Online]. Available: https://www.ni.com/en/solutions/energy/condition-monitoring/wind-turbine-control-methods.html

[76] L. Du, G. Ingram, and R. G. Dominy, "A review of H-Darrieus wind turbine aerodynamic research," *Proc. Inst. Mech. Eng. Part C J. Mech. Eng. Sci.*, vol. 233, no. 23–24, pp. 7590–7616, Dec. 2019, doi: 10.1177/0954406219885962.

[77] M. Yamada and T. Murakami, "Individual Pitch Control of Wind Turbine System by Estimating Wind Speed Using Pitching Moment," *IEEJ J. Ind. Appl.*, vol. 12, no. 5, pp. 1008–1014, Sep. 2023, doi: 10.1541/ieejjia.23000261.

[78] S. Apelfröjd, S. Eriksson, and H. Bernhoff, "A Review of Research on Large Scale Modern Vertical Axis Wind Turbines at Uppsala University," *Energies*, vol. 9, no. 7, p. 570, Jul. 2016, doi: 10.3390/en9070570.

[79] O. Apata and D. T. O. Oyedokun, "An overview of control techniques for wind turbine systems," *Sci. Afr.*, vol. 10, p. e00566, Nov. 2020, doi: 10.1016/j.sciaf.2020.e00566.

[80] B. Kumar, K. S. Sandhu, and R. Sharma, "Comparative Analysis of Control Schemes for DFIG-Based Wind Energy System," *J. Inst. Eng. India Ser. B*, vol. 103, no. 2, pp. 649–668, Apr. 2022, doi: 10.1007/s40031-021-00660-z.

[81] C. Wei, Z. Zhang, W. Qiao, and L. Qu, "An Adaptive Network-Based Reinforcement Learning Method for MPPT Control of PMSG Wind Energy Conversion Systems," *IEEE Trans. Power Electron.*, vol. 31, no. 11, pp. 7837–7848, Nov. 2016, doi: 10.1109/TPEL.2016.2514370.

[82] Saibal Manna, Deepak Kumar Singh, and Ashok Kumar Akella, "A Review of Control Techniques for Wind Energy Conversion System," *Int. J. Eng. Technol. Innov.*, vol. 13, no. 1, pp. 40–69, Jan. 2023, doi: 10.46604/ijeti.2023.9051.

[83] Y. K. Teklehaimanot, F. K. Akingbade, B. C. Ubochi, and T. O. Ale, "A review and comparative analysis of maximum power point tracking control algorithms for wind energy conversion systems," *Int. J. Dyn. Control*, May 2024, doi: 10.1007/s40435-024-01434-3.

[84] O. Zebraoui and M. Bouzi, "Comparative study of different MPPT methods for wind energy conversion system," *IOP Conf. Ser. Earth Environ. Sci.*, vol. 161, p. 012023, Jun. 2018, doi: 10.1088/1755-1315/161/1/012023.

[85] M. A. Abdullah, A. H. M. Yatim, C. W. Tan, and R. Saidur, "A review of maximum power point tracking algorithms for wind energy systems," *Renew. Sustain. Energy Rev.*, vol. 16, no. 5, pp. 3220–3227, Jun. 2012, doi: 10.1016/j.rser.2012.02.016.

[86] Y. Sun, Y. Liu, and L. Li, "Fuzzy Adaptive Control for Fractional Nonlinear Systems with External Disturbances and Unknown Control Directions," *J. Math.*, vol. 2020, pp. 1–9, Dec. 2020, doi: 10.1155/2020/6677704.

[87] R. Doshi, V. Jotangiya, M. Bhatt, and S. Andipara, "Meticulous analysis and optimization of maximum power point tracking techniques for standalone wind energy conversion system," in *2016 IEEE 1st International Conference on Power Electronics, Intelligent Control and Energy Systems (ICPEICES)*, Delhi, India: IEEE, Jul. 2016, pp. 1–5. doi: 10.1109/ICPEICES.2016.7853447.

[88] P. Sathish Babu, C. K. Sundarabalan, C. Balasundar, and T. Santhana Krishnan, "Fuzzy logic based optimal tip speed ratio MPPT controller for grid connected WECS," *Mater. Today Proc.*, vol. 45, pp. 2544–2550, 2021, doi: 10.1016/j.matpr.2020.11.259.

[89] H. Amimeur And F. Hamoudi, "Fuzzy Logic Control Of A Dual-Stator Induction Generator For Wind Energy Conversion Systems".

[90] B. N. Phung, Y.-K. Wu, and M.-H. Pham, "Novel Fuzzy Logic Controls to Enhance Dynamic Frequency Control and Pitch Angle Regulation in Variable-Speed Wind Turbines," *Energies*, vol. 17, no. 11, p. 2617, May 2024, doi: 10.3390/en17112617.

[91] D. M. Teferra, L. M. H. Ngoo, and G. N. Nyakoe, "A Fuzzy Controlled Pitch Angle in a Permanent Magnet Synchronous Generator Type Wind Energy Conversion System," in *2022 IEEE 21st Mediterranean Electrotechnical Conference (MELECON)*, Palermo, Italy: IEEE, Jun. 2022, pp. 324–329. doi: 10.1109/MELECON53508.2022.9843136.

[92] P. Nagwanshi, M. Y. Zargar, and Mairaj-ud-Din-Mufti, "Fuzzy logic based battery storage system for a standalone wind energy conversion system," in *2017 International Conference on Computing, Communication and Automation (ICCCA)*, Greater Noida: IEEE, May 2017, pp. 1512–1517. doi: 10.1109/CCAA.2017.8230041.

[93] R. Tiwari and N. R. Babu, "Fuzzy Logic Based MPPT for Permanent Magnet Synchronous Generator in wind Energy Conversion System," *IFAC-Pap.*, vol. 49, no. 1, pp. 462–467, 2016, doi: 10.1016/j.ifacol.2016.03.097.

[94] K. Chaicharoenaudomrung, K. Areerak, K. Areerak, S. Bozhko, and C. I. Hill, "Maximum Power Point Tracking for STAND-ALONE Wind Energy Conversion System Using FLC -P&O Method," *IEEJ Trans. Electr. Electron. Eng.*, vol. 15, no. 12, pp. 1723–1733, Dec. 2020, doi: 10.1002/tee.23246.

[95] H. Gaied *et al.*, "Comparative analysis of MPPT techniques for enhancing a wind energy conversion system," *Front. Energy Res.*, vol. 10, p. 975134, Aug. 2022, doi: 10.3389/fenrg.2022.975134.

[96] G. B. A. Kumar and Shivashankar, "Optimal power point tracking of solar and wind energy in a hybrid wind solar energy system," *Int. J. Energy Environ. Eng.*, vol. 13, no. 1, pp. 77–103, Mar. 2022, doi: 10.1007/s40095-021-00399-9.

[97] L. Cristaldi, M. Faifer, M. Rossi, and S. Toscani, "MPPT definition and validation: A new model-based approach," in *2012 IEEE International Instrumentation and Measurement Technology Conference Proceedings*, Graz, Austria: IEEE, May 2012, pp. 594–599. doi: 10.1109/I2MTC.2012.6229673.

[98] D. Chinnakullay Reddy, S. Satyanarayana, and V. Ganesh, "Design of Hybrid Solar Wind Energy System in a Microgrid with MPPT Techiques," *Int. J. Electr. Comput. Eng. IJECE*, vol. 8, no. 2, p. 730, Apr. 2018, doi: 10.11591/ijece.v8i2.pp730-740.

[99] S. A. Nasef, A. A. Hassan, H. T. Elsayed, M. B. Zahran, M. K. El-Shaer, and A. Y. Abdelaziz, "Optimal Tuning of a New Multi-input Multi-output Fuzzy Controller for Doubly Fed Induction Generator-Based Wind Energy Conversion System," *Arab. J. Sci. Eng.*, vol. 47, no. 3, pp. 3001–3021, Mar. 2022, doi: 10.1007/s13369-021-05946-4.

[100] A. M. Eltamaly, M. A. Mohamed, and A. G. Abo-Khalil, "Maximum Power Point Tracking Strategies of Grid-Connected Wind Energy Conversion Systems," in *Control and Operation of Grid-Connected Wind Energy Systems*, A. M. Eltamaly, A. Y. Abdelaziz, and A. G. Abo-Khalil, Eds., in Green Energy and Technology. , Cham: Springer International Publishing, 2021, pp. 193–225. doi: 10.1007/978-3-030-64336-2_8.

[101] T. George, J. P, T. Francis, and C. E. S. Sreedharan, "Wind Energy Conversion System Based PMSG for Maximum Power Tracking and Grid Synchronization Using Adaptive Fuzzy Logic Control," *J. Appl. Res. Technol.*, vol. 20, no. 6, pp. 703–717, Dec. 2022, doi: 10.22201/icat.24486736e.2022.20.6.1256.

[102] E. Chavero-Navarrete, M. Trejo-Perea, J. C. Jáuregui-Correa, R. V. Carrillo-Serrano, G. Ronquillo-Lomeli, and J. G. Ríos-Moreno, "Hierarchical Pitch Control for Small Wind Turbines Based on Fuzzy Logic and Anticipated Wind Speed Measurement," *Appl. Sci.*, vol. 10, no. 13, p. 4592, Jul. 2020, doi: 10.3390/app10134592.

[103] B. Rached, M. Bensaid, M. Elharoussi, and E. Abdelmounim, "DSP in the loop Implementation of the Control of a DFIG Used in Wind Power System," in *2020 1st International Conference on Innovative Research in Applied Science, Engineering and Technology (IRASET)*, Meknes, Morocco: IEEE, Apr. 2020, pp. 1–6. doi: 10.1109/IRASET48871.2020.9092165.

[104] E. Lotfi, B. Rached, M. Elhaissouf, M. Elharoussi, and E. Abdelmounim, "DSP Implementation in the Loop of the Vector Control Drive of a Permanent Magnet Synchronous Machine," in *Proceedings of the 2nd International Conference on Computing and Wireless Communication Systems*, Larache Morocco: ACM, Nov. 2017, pp. 1–7. doi: 10.1145/3167486.3167542.

[105] K. R. Prajapati, "Application of fuzzy logic for MPPT control in stand-alone wind energy conversion system with a battery storage system," in *2019 IEEE International Conference on Intelligent Techniques in Control, Optimization and Signal Processing (INCOS)*, Tamilnadu, India: IEEE, Apr. 2019, pp. 1–6. doi: 10.1109/INCOS45849.2019.8951386.

[106] B. Rached, M. Elharoussi, and E. Abdelmounim, "Fuzzy Logic Control for Wind Energy Conversion System based on DFIG," in *2019 International Conference on Wireless Technologies, Embedded and Intelligent Systems (WITS)*, Fez, Morocco: IEEE, Apr. 2019, pp. 1–6. doi: 10.1109/WITS.2019.8723722.

[107] J. Azevedo, F. Mendonça, and Centre for Exact Science and Engineering, University of Madeira, Funchal, Portugal, "Small scale wind energy harvesting with maximum power tracking," *AIMS Energy*, vol. 3, no. 3, pp. 297–315, 2015, doi: 10.3934/energy.2015.3.297.

[108] H. Ibadi, A. Sangidzun, D. S. Wijayanto, H. Saputro, Soenarto, and M. B. Triyono, "Effect of Adding of Pitch on the Darrieus Blade Against the Cut In Speed of the Savonius Type S - Darrieus Type H Hybrid Turbine," *J. Phys. Conf. Ser.*, vol. 1808, no. 1, p. 012003, Mar. 2021, doi: 10.1088/1742-6596/1808/1/012003.

[109] S. A. Al-Shammari, A. H. Karamallah, and S. Aljabair, "Blade Shape Optimization of Savonius Wind Turbine at Low Wind Energy by Artificial Neural network," *IOP Conf. Ser. Mater. Sci. Eng.*, vol. 881, no. 1, p. 012154, Jul. 2020, doi: 10.1088/1757-899X/881/1/012154.

[110] A. Belay And G. Biru, "Addis Ababa Light Rail Transit System Energy Flow Analysis".

[111] F. Akello, "Determining the Optimum Parameters of an Energy harvesting System using Simulation," Addis Ababa University, 2019. Accessed: Apr. 24, 2025. [Online]. Available: http://etd.aau.edu.et/handle/123456789/21012

[112] M. B. Tadie Fogaing, H. Gordon, C. F. Lange, D. H. Wood, and B. A. Fleck, "A Review of Wind Energy Resource Assessment in the Urban Environment," in *Advances in Sustainable Energy*, vol. 70, A. Vasel and D. S.-K. Ting, Eds., in Lecture Notes in Energy, vol. 70. , Cham: Springer International Publishing, 2019, pp. 7–36. doi: 10.1007/978-3-030-05636-0_2.

[113] N. Rezaei, K. Mehran, and C. Cossar, "A model-based implementation of an MPPT technique and a control system for a variable speed wind turbine PMSG," *Int. J. Model. Identif. Control*, vol. 31, no. 1, p. 3, 2019, doi: 10.1504/IJMIC.2019.096833.

[114] H. L. Thadani, F. D. Zaaba, M. R. Mohammad Shahrizal, A. S. J. A. Jaspal Singh Jaj, and Y. I. Go, "Design and performance evaluation of vertical axis wind turbine for wind energy harvesting at railway," *World J. Sci. Technol. Sustain. Dev.*, vol. 18, no. 2, pp. 190–217, May 2021, doi: 10.1108/WJSTSD-11-2020-0088.

[115] "Ebcs-1 5 | PDF | Wound | Wind Speed." Accessed: Dec. 21, 2024. [Online]. Available: https://www.scribd.com/document/142990216/EBCS-1-5

[116] D. Rocchi, G. Tomasini, P. Schito, and C. Somaschini, "Wind effects induced by high speed train pass-by in open air," *J. Wind Eng. Ind. Aerodyn.*, vol. 173, pp. 279–288, Feb. 2018, doi: 10.1016/j.jweia.2017.10.020.

[117] D. Guo, K. Shang, Y. Zhang, G. Yang, and Z. Sun, "Influences of affiliated components and train length on the train wind," *Acta Mech. Sin.*, vol. 32, no. 2, pp. 191–205, Apr. 2016, doi: 10.1007/s10409-015-0553-z.

[118] Federal Railroad and Administration, "Assessment of potential aerodynamic effects on personnel and equipment in proximity to High Speed Train operations." Office of Research and Development Washington, D.C. 20590. [Online]. Available: https://railroads.fra.dot.gov/sites/fra.dot.gov/files/fra_net/3982/DOT-FRA-ORD-99-11.pdf

[119] H.-J. Yoon *et al.*, "Effect of High-Speed Train-Induced Wind on Trackside UAV Thrust Near Railway Bridge," *Appl. Sci.*, vol. 10, no. 10, p. 3495, May 2020, doi: 10.3390/app10103495.

[120] Y. Zou, Z. Fu, X. He, C. Cai, J. Zhou, and S. Zhou, "Wind Load Characteristics of Wind Barriers Induced by High-Speed Trains Based on Field Measurements," *Appl. Sci.*, vol. 9, no. 22, p. 4865, Nov. 2019, doi: 10.3390/app9224865.

[121] Page | D-8. Burbank to Los Angeles Section Administrative Draft EIR/EIS. 5, "Potential impact from induced winds." California High-Speed Rail Project Environmental Document, Mar. 2017.

[122] H. Zong and F. Porté-Agel, "A momentum-conserving wake superposition method for wind farm power prediction," *J. Fluid Mech.*, vol. 889, p. A8, Apr. 2020, doi: 10.1017/jfm.2020.77.

[123] J. He, H. Xiang, Y. Li, and B. Han, "Aerodynamic performance of traveling road vehicles on a single-level rail-cum-road bridge under crosswind and aerodynamic impact of traveling trains," *Eng. Appl. Comput. Fluid Mech.*, vol. 16, no. 1, pp. 335–358, Dec. 2022, doi: 10.1080/19942060.2021.2012516.

[124] "Global Wind Atlas." Accessed: Apr. 29, 2025. [Online]. Available: https://globalwindatlas.info

[125] Department of Electrical Engineering, EINA, University of Zaragoza, Spain, V. Ballestín-Bernad, J. S. Artal-Sevil, J. A. Domínguez-Navarro, and J. L. Bernal-Agustín, "Low-cost variable-speed wind turbines design by recycling small electrical machines. Arrangement of permanent magnets in the rotor," *Renew. Energy Power Qual. J.*, vol. 20, pp. 833–838, Sep. 2022, doi: 10.24084/repqj20.450.

[126] S. F. Pamungkas, D. S. Wijayanto, H. Saputro, and I. Widiastuti, "Performance 'S' Type Savonius Wind Turbine with Variation of Fin Addition on Blade," *IOP Conf. Ser. Mater. Sci. Eng.*, vol. 288, p. 012132, Jan. 2018, doi: 10.1088/1757-899X/288/1/012132.

[127] M. Zemamou, M. Aggour, and A. Toumi, "Review of savonius wind turbine design and performance," *Energy Procedia*, vol. 141, pp. 383–388, Dec. 2017, doi: 10.1016/j.egypro.2017.11.047.

[128] A. Gupta, U. Ali, H. A. Abderrahmane, and I. Janajreh, "Blade pitching in vertical axis wind turbines: A double multiple stream tube theoretical approach to performance enhancement," *Heliyon*, vol. 11, no. 3, p. e42101, Feb. 2025, doi: 10.1016/j.heliyon.2025.e42101.

[129] "NiMH Battery vs Li-Ion Battery vs NiCad Battery." Accessed: Apr. 14, 2025. [Online]. Available: https://www.ufinebattery.com/blog/nimh-battery-vs-li-ion-battery-vs-nicad-battery-how-are-they-different/

[130] M. Effendy, N. Mardiyah, and K. Hidayat, "Efficiency improvement of photovolatic by using maximum power point tracking based on a new fuzzy logic controller," *J. Mechatron. Electr. Power Veh. Technol.*, vol. 9, no. 2, pp. 57–64, Dec. 2018, doi: 10.14203/j.mev.2018.v9.57-64.

[131] S. M. Muyeen, Ed., *Wind Energy Conversion Systems*. in Green Energy and Technology. London: Springer London, 2012. doi: 10.1007/978-1-4471-2201-2.

[132] T. Zhang, "A Novel Wind Energy Gathering Structure for the Savonius Wind Turbine and Its Parameter Optimization Based on Taguchi's Method." Energies 2024, 17, 5348., Oct. 28, 2024. [Online]. Available: https://doi.org/10.3390/en17215348

[133] I. Marinić-Kragić, D. Vučina, and Z. Milas, "Global optimization of Savonius-type vertical axis wind turbine with multiple circular-arc blades using validated 3D CFD model," *Energy*, vol. 241, p. 122841, Feb. 2022, doi: 10.1016/j.energy.2021.122841.

[134] A.-S. Sarah Ali, K. Abdul Hassan, and A. Sattar, "Blade Shape Optimization of Savonius Wind Turbine at Low Wind Energy by Artificial Neural network." 3rd International Conference on Sustainable Engineering Techniques (ICSET 2020) IOP Conf. Series: Materials Science and Engineering 881 (2020) 012154, Aug. 21, 2022. [Online]. Available: doi:10.1088/1757-899X/881/1/012154

[135] S. T. Bahta, "Design and Analyzing of an Off-Grid Hybrid Renewable Energy System to Supply Electricity for Rural Areas".

[136] T. K. Roy, Md. A. Mahmud, and A. M. T. Oo, "Techno-economic feasibility of stand-alone hybrid energy systems for a remote Australian community: Optimization and sensitivity analysis," *Renew. Energy*, vol. 241, p. 122286, Mar. 2025, doi: 10.1016/j.renene.2024.122286.

APPENDICES

Appendix 1: Wind speed around AALRT at 10m height from the ground

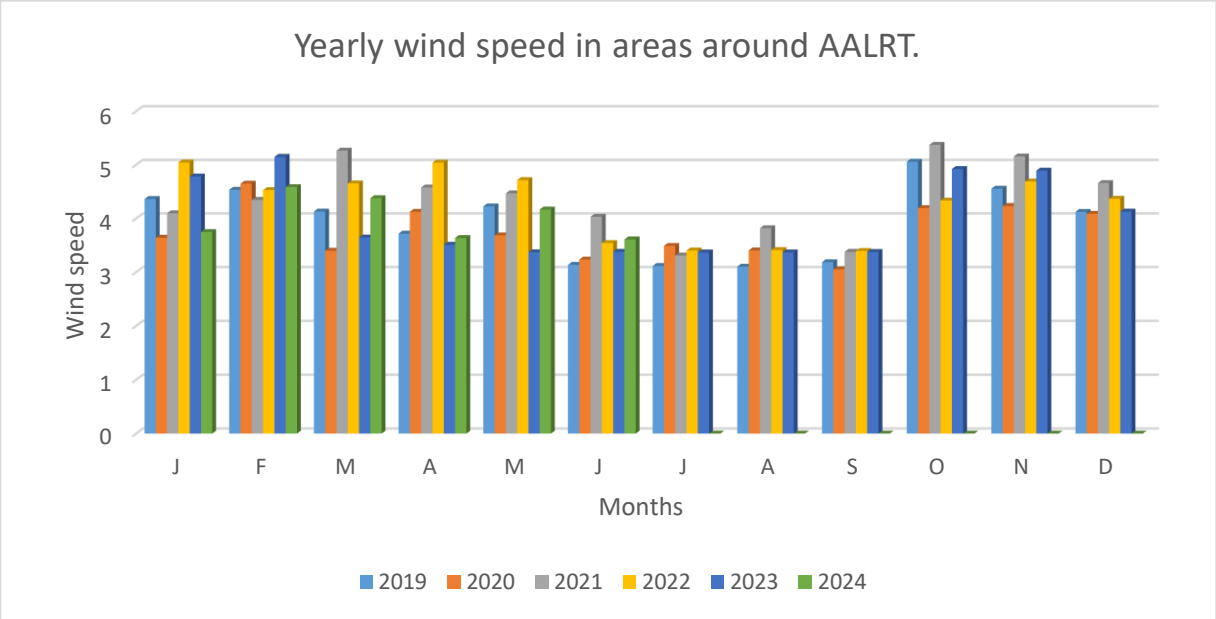

Appendix 2: Fuzzy Inference System (FIS) and the Rule base

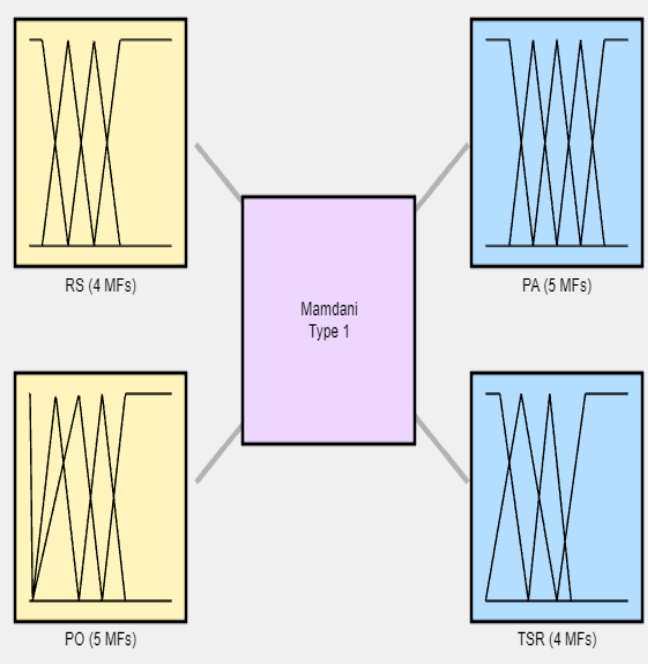

	Rule	Weight	Name
1	If RS is VL and PO is VL then PA is VH, TSR is VL	1	rule1
2	If RS is L and PO is VL then PA is VH, TSR is VL	1	rule2
3	If RS is M and PO is VL then PA is VH, TSR is VL	1	rule3
4	If RS is VL and PO is L then PA is VH, TSR is VL	1	rule4
5	If RS is L and PO is H then PA is VH, TSR is VL	1	rule5
6	If RS is M and PO is H then PA is VH, TSR is VL	1	rule6
7	If RS is H and PO is VL then PA is VH, TSR is VL	1	rule7
8	If RS is M and PO is H then PA is VH, TSR is VL	1	rule8
9	If PO is VL then PA is VH, TSR is VL	1	rule9
10	If PO is L then PA is VH, TSR is VL	1	rule10
11	If RS is VL and PO is H then PA is VH, TSR is VL	1	rule11
12	If RS is L and PO is H then PA is VH, TSR is VL	1	rule12
13	If RS is M and PO is H then PA is VH, TSR is VL	1	rule13
14	If RS is H and PO is H then PA is VH, TSR is VL	1	rule14
15	If RS is VL and PO is VH then PA is VH, TSR is VL	1	rule15
16	If RS is L and PO is VH then PA is VH, TSR is VL	1	rule16
17	If RS is M and PO is VH then PA is VH, TSR is VL	1	rule17
18	If RS is H and PO is VH then PA is VH, TSR is VL	1	rule18
19	If PO is H then PA is VH, TSR is VL	1	rule19

Appendix 3: Membership function(MF)

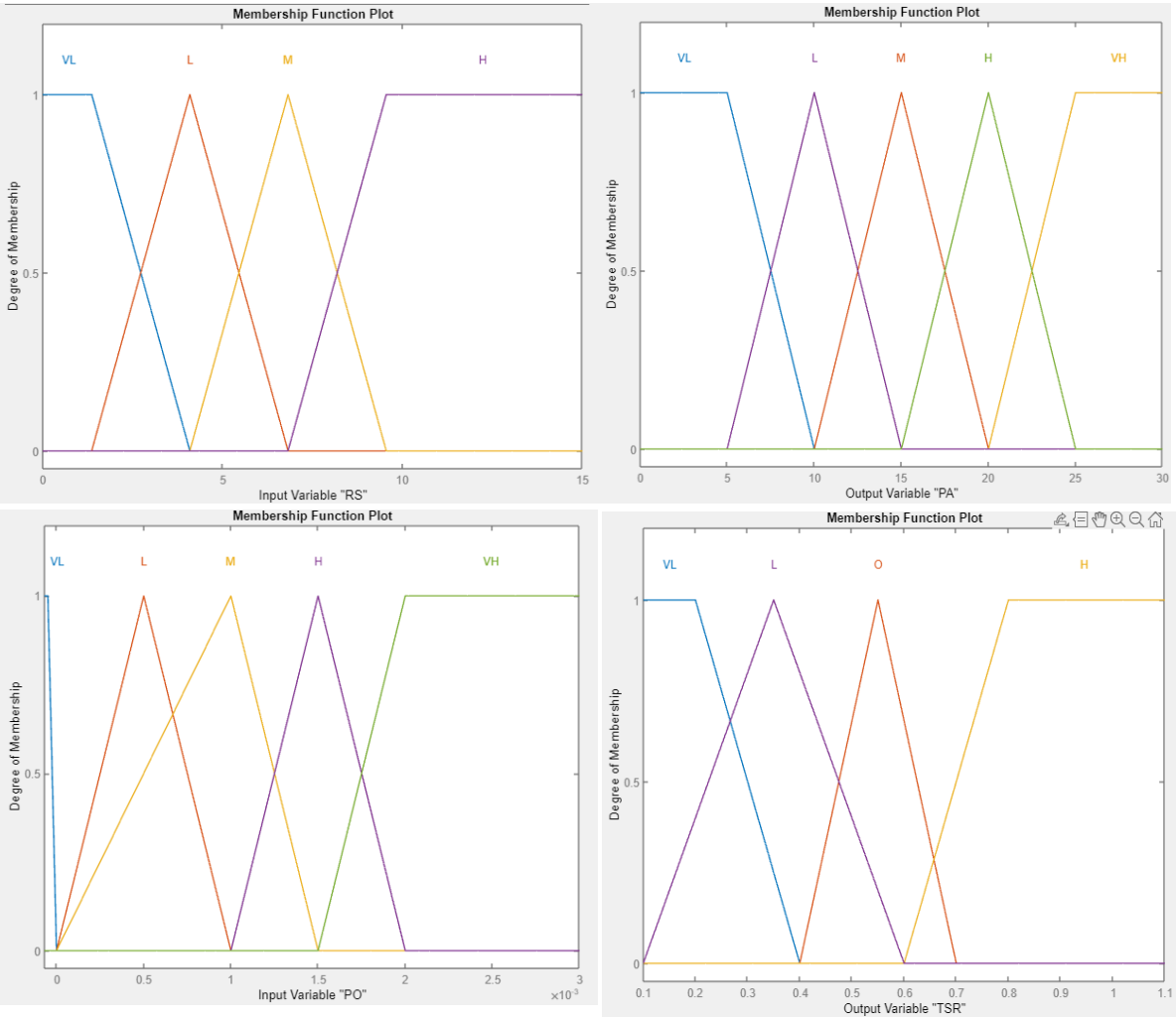

Appendix 4: Code for the boost converter calculation

```
Vinmin=0; % minimum output voltage present at rectifier output
Vout=5;  % DC-DC converters output
Po=250;  % The power rating of the DC-DC converter(Watts)
% The switching frequency (fs)
fs=10000;
% The efficiency(n) of the DC-DC converter
n=0.95;


D=(1-(Vinmin*n)/Vout); % D is the dutycycle of the DC-DC boost converter
Io=Po/Vout;
% input current ripple (dI)
```

```
Ioriple=0.2; % 20%-40% of the output current
dI=Ioriple*Io*(Vout/Vinmin);
% Output voltage ripple(dV)
% I am considering 0.5% voltage variations in output voltage,
% standard is 0.5%-1%.


dV= Vout*0.5/100;
% the inductance value (L)
L=((Vinmin)*(Vout-Vinmin))/(dI*fs*Vout);
% the capacitance value(C)
C=(Io*D)/(fs*dV);


% Minimum load to be applied more then of
RL=(Vout/Io);
```

Appendix 5: Wind speed daily profile from the HOMER analysis

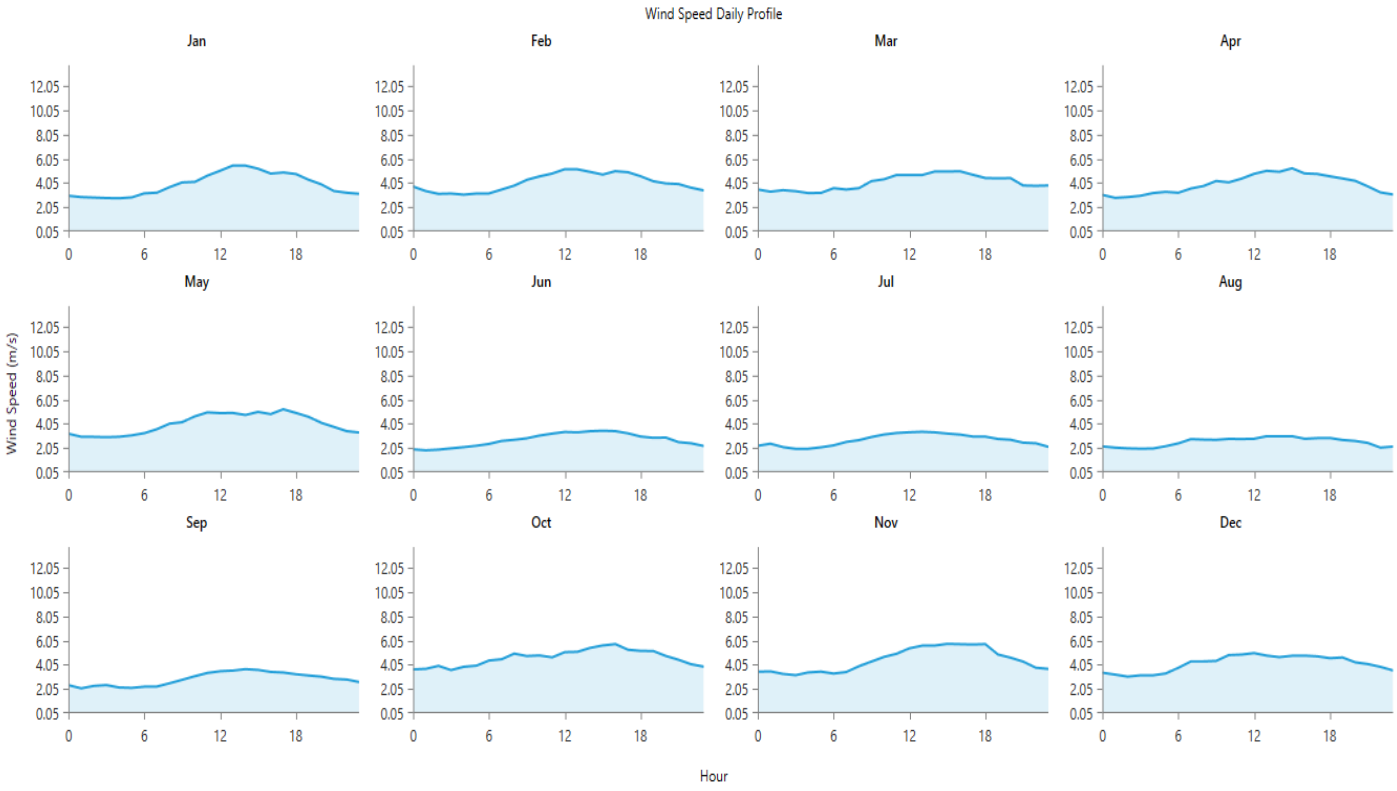

Appendix 6: Daily profile of the wind turbine power output of the HOMER analysis

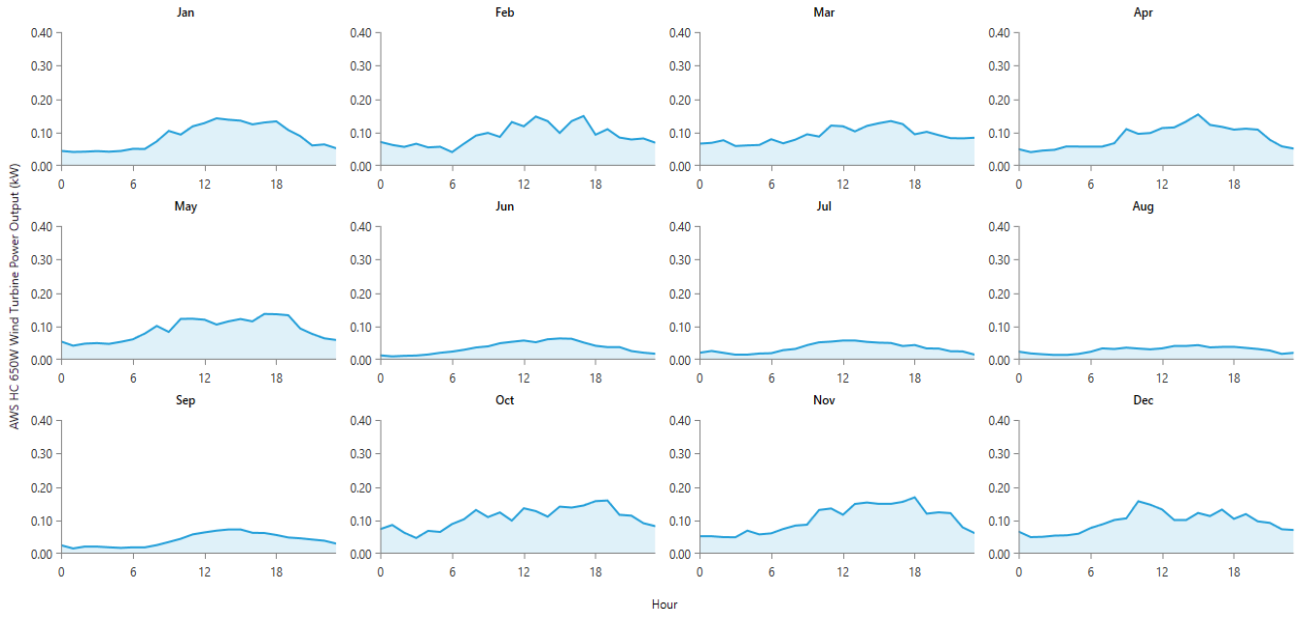

Appendix 7: Daily profile of the total electrical load served of the HOMER analysis

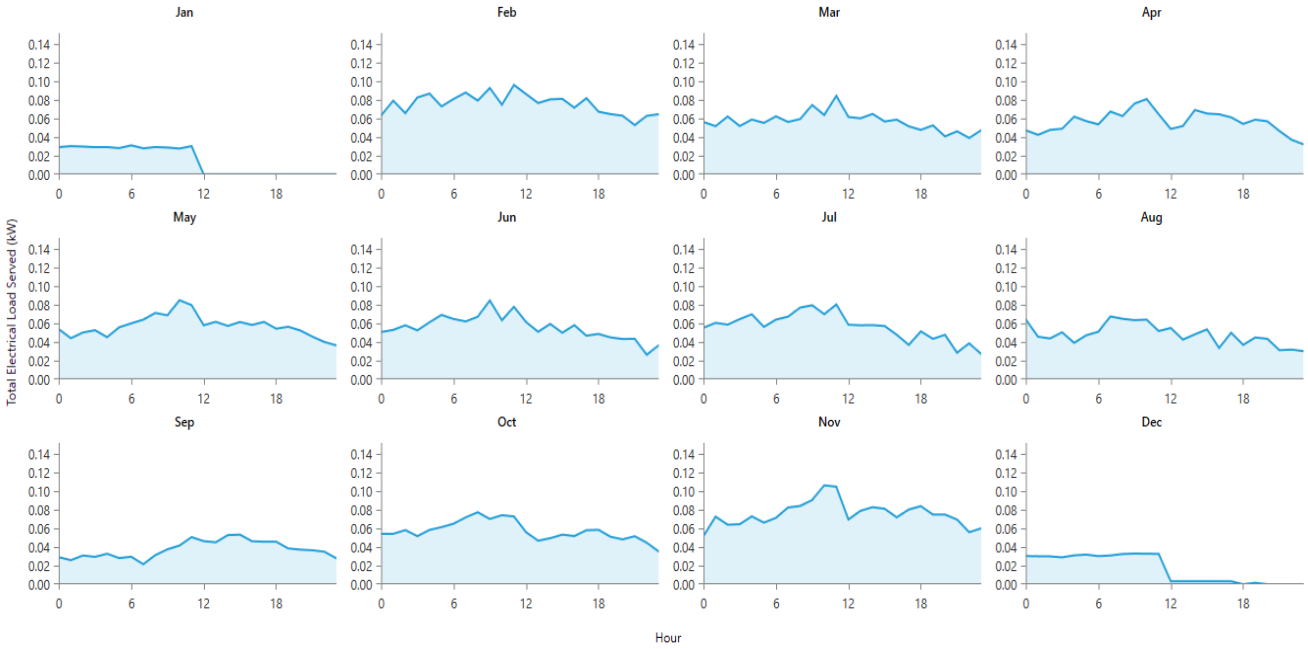

Appendix 8: The daily profile of the excess electrical production of the HOMER analysis

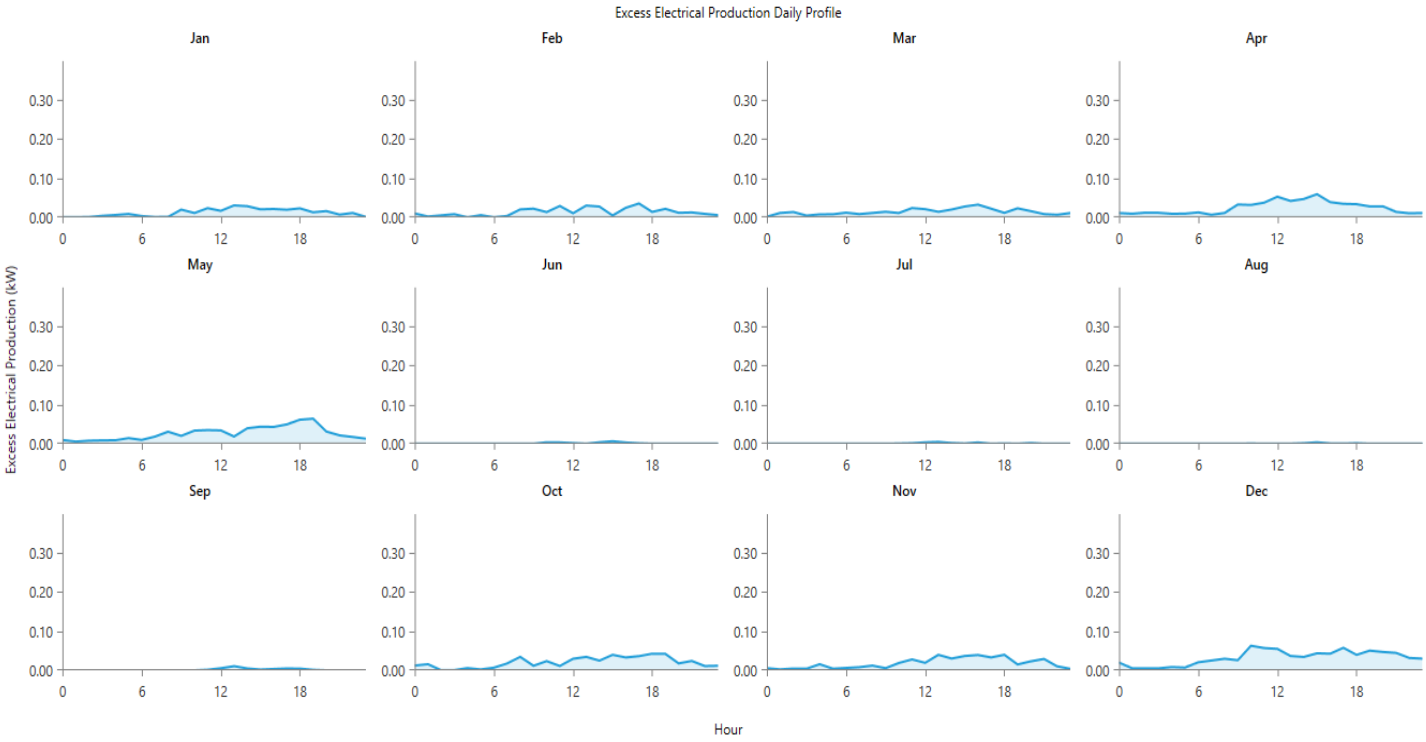

Appendix 9: The daily profile of the unmet electrical load of the HOMER analysis